HASAN KALYONCU UNIVERSITY
GRADUATE SCHOOL OF
NATURAL & APPLIED SCIENCES

NUMERICAL MODELING AND EXPERIMENTAL EVALUATION OF SHRINKAGE OF CONCRETES INCORPORATING FLY ASH AND SILICA FUME

M. Sc. THESIS
IN
CIVIL ENGINEERING

BY
MOHAMED MOAFAK AZIZ ARBILI
DECEMBER 2014

Numerical modeling and experimental evaluation of shrinkage of concretes incorporating fly ash and silica fume
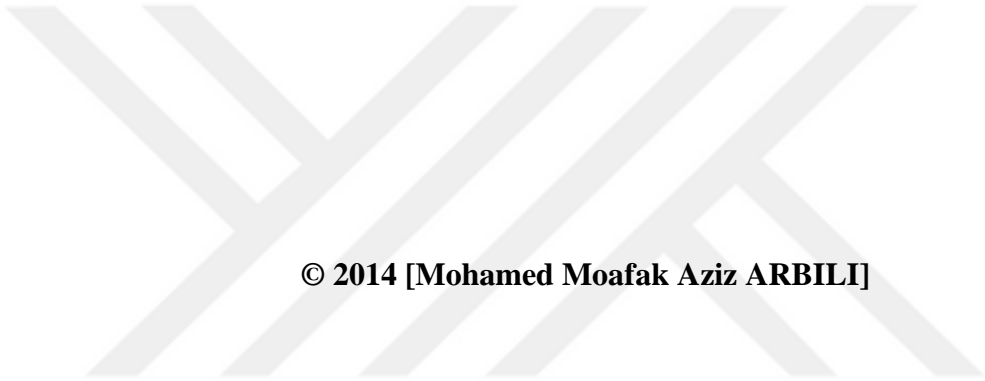
M.Sc. Thesis

In

Civil Engineering

Hasan Kalyoncu University

Supervisor

Assist. Prof. Dr. Kasım MERMERDAŞ

By

Mohamed Moafak Aziz ARBILI

December 2014

Name of the thesis: Numerical modeling and experimental evaluation of shrinkage of concretes incorporating fly ash and silica fume

Name of the student: Mohamed Moafak Aziz ARBILI
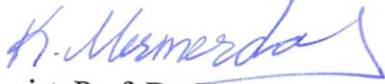
Exam date: 16.12.2014

Approval of the Graduate School of Natural and Applied Sciences

Prof. Dr. Mehmet KARPUZCU
Director

I certify that this thesis satisfies all the requirements as a thesis for the degree of Master of Science.

Assist. Prof. Dr. Kasım MERMERDAŞ
Head of Civil Engineering Department

This is to certify that we have read this thesis and that in our opinion it is fully adequate, in scope and quality, as a thesis for the degree of Master of Science.

Assist. Prof. Dr. Kasım MERMERDAŞ
Supervisor

Examining Committee Members   Signature

Assoc. Prof. Dr. Erhan GÜNEYİSİ

Assoc. Prof. Dr. Mehmet GESOĞLU

Assist. Prof. Dr. Kasım MERMERDAŞ
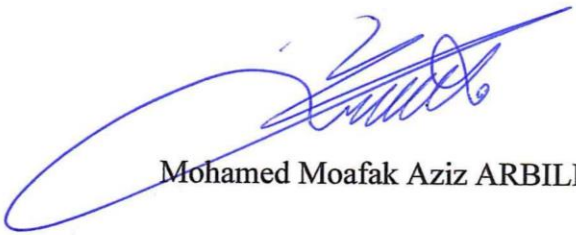
I hereby declare that all information in this document has been obtained and presented in accordance with academic rules and ethical conduct. I also declare that, as required by these rules and conduct, I have fully cited and referenced all material and results that are not original to this work.

Mohamed Moafak Aziz ARBILI

ABSTRACT

NUMERICAL MODELING AND EXPERIMENTAL EVALUATION OF SHRINKAGE OF CONCRETES INCORPORATING FLY ASH AND SILICA FUME

ARBILI, Mohamed Moafak Aziz

M.Sc. in Civil Engineering

Supervisor: Assist. Prof. Dr. Kasım MERMERDAŞ

December 2014, 108 pages

Shrinkage is generally considered as an important hardened concrete property. During the drying process, free and absorbed water is lost from the concrete. When the drying shrinkage is restrained, cracks can occur, depending on the internal stresses in the concrete. The ingress of deleterious materials through these cracks can cause decrease in the compressive strength and the durability of concrete. In the first stage of the study, prediction models through gene expression programming (GEP) and neural network (NN) were derived. The data set used for training and testing covers the experimental data presented in the literature. In the second stage of the study presented herein, the findings of an experimental study on drying shrinkage behavior of concretes incorporated with silica fume (SF) and fly ash (FA) were reported. Free shrinkage strain measurements as well as corresponding weight loss were measured over 40 days of drying. The obtained experimental results were also used for the validation of the proposed prediction models. The highest amount of mineral admixture resulted in high shrinkage strain development. Moreover, the proposed NN model also accurately predicted the values obtained from experimental study. The errors obtained from GEP model were very high, especially for SF incorporated concrete

Keywords: Shrinkage, modeling, Prediction, Experimental validation, Mineral admixtures

ÖZET

UÇUCU KÜL VE SİLİS DUMANI İÇEREN BETONLARİN RÖTESİNİN SAYISAL MODELLENMESİ VE DENEYSEL İNCELEMESİ

ARBILI, Mohamed Moafak Aziz

Yüksek Lisans Tezi, İnşaat Mühendisliği Bölümü

Tez Yöneticisi: Yrd.Doç.Dr. Kasım Mermerdaş

December 2014, 108 sayfa

Rötre genellikle sertleşmiş betonun önemli bir özelliği olarak ele alınır. Kuruma sürecinde boşluk yapısında bulunan serbest ve emilmiş su kaybedilir. Betonun rötresi kısıtlandığı zaman betonda olşan gerilmelere bağlı olarak çatlak oluşumu gözlenir. Bu çatlaklardan zararlı maddelerin geçmesiyle betonun dayanım ve dayanıklılığında azalma olur. Bu çalışman ilk aşamasinde genetik programlama ve yapay sinir ağları yöntemleri kullanılarak rötre tahmin modelleri geliştirilmiştir. Modellerin eğitimi ve test edilmesi için literatürden veri toplanmıştır. Çalışmanın ikinci aşamasında ise uçucu kül ve silis dumanı içeren betonlar hazırlanarak kırk günlük kuruma sürecinde rötreleri ölçülmüştür. En yüksek rötre değerleri en çok mineral katkı içeren betonlarda gözlenmiştir. Bunların yanı sıra deneysel çalışmada elde edilen sonuçlar tahmin modellerinin verdikleriyle karşılaştırılmışlardır. YSA ile elde edilen değerlerin GP ile elde edilenlere göre gerçeğe daha yakın oldukları görülmüştür.

Anahtar kelimeler: Rötre, Modelleme, Tahmin deneysel doğrulama, Mineral katkılar

To my parents

ACKNOWLEDGEMENT

TABLE OF CONTENTS

LIST OF FIGURES

LIST OF TABLES

LIST OF SYMBOLS/ABBREVIATIONS

ACI   American Concrete Institute

Agg/b   Aggregate-to binder ratio

AI   artificial intelligence

ANN   Artificial Neural Network

ASTM   American Society for Testing and Materials

C   Cement

ET   Expression Tree

FA   Fly Ash

f_c Mpc   Compressive strength

GEP   Genetic Expression Programming

GP   Gene Programming

HPC   High Performance Concrete

NN   Neural network

OPC   Ordinary Portland cement

PC   Portland Cement

S   Shrinkage

SCMs   Supplementary cementitious materials

SF   Silica Fume

SP   Superplasticizer

W/B   Water-to Binder ratio

W/C   Water-to Cement ratio

CHAPTER 1

INTRODUCTION

1. General

Concrete is the most widely used construction material all over the world. However, shrinkage is of concern when it relates to durability of concrete structure. Excessive shrinkage may cause concrete cracking, even structural failure. Thus, cracking may lead to increased corrosion rate of steel reinforcement in concrete structure, (Tia M. et al., 2005). In the view of global sustainable development. Therefore, researchers start to make use of blending of two or three SCMs to optimize durability and cost for the benefit of engineers, owners, contractors and material suppliers. The industrial by-products used as SCMs, such as fly ash and silica fume, have become more efficient admixtures to diminish the shrinkage effects and increase the durability of concrete, and usage of SCMs could substantially reduce the final cost of concrete mixtures since these materials are quite heaper in comparison to Portland cement. (Yang et al., 2007; Wang and Li, 2007).

The problems encountered in the field of engineering are generally unstructured and imprecise influenced by intuitions and past experiences of a designer. (Chandwani et al., 2013). Complexity to mathematically model real world problems has compelled the human civilization to search for nature inspired computing tools. The evolution of such computing tools revolves around the information processing characteristics of biological systems. In contrast to conventional computing, these tools are rather "soft" as they lack the exactness and therefore placed under the umbrella of a multidisciplinary field called soft computing. Soft Computing is an emerging collection of methodologies, which aim to exploit tolerance for imprecision, uncertainty and partial truth to achieve robustness, tractability and total low cost (Chaturvedi, 2008).

Soft Computing tools exploit the reasoning, intuition, consciousness, wisdom and adaptability to changing environments possessed by human beings for developing

computing paradigms like Fuzzy Logic (FL), Neural Networks (NN) and Genetic Algorithms (GA). The integration of these techniques into the computing environment has given impetus to the development of intelligent and wiser machines possessing logical and intuitive information processing capabilities equivalent to human beings. These techniques whether complementing each other or working on their own, are able to model complex or unknown relationships which are either nonlinear or noisy. Soft computing techniques have a self-adapting characteristic paving a way for development of automated design systems. A synergistic partnership exploiting the strengths of these individual techniques can be harnessed for developing hybrid-computing tools (Chaturvedi, 2013).

Civil engineers have very well accepted soft computing tools such as fuzzy computing, neuro-computing, evolutionary computing, and probabilistic computing. This special session is a perfect platform to discuss the various soft computing applications in civil engineering domain.

For example, some applications of soft computing are invited in the following fields on

- Structural Engineering: Vanluchene and Sun (1990) presented an introduction to neural network by using back-propagation algorithm to solve three different structural engineering problems related to pattern recognition, decision making and problems that have numerically complex solutions.
- Concrete Strength Modeling: in the study of Ozcan et al (2009), compressive strength prediction was done by using ANN and Fuzzy logic.
- Geotechnical Engineering: Shahin et al. (2002) used neural networks for predicting settlement of shallow foundations on cohesion less soils. The predictive ability of ANN is compared with three of the most commonly used traditional methods.
- Water Resources: Tokar and Johnson (1999) used ANN to forecast daily runoff as a function of daily precipitation, temperature and snowmelt.
- Earthquake Engineering: Lee and Han (2002) developed efficient neural network models for generation of artificial earthquakes and response spectra.

1.2 The aim of the study

The main objective of the thesis is to investigate can be listed as follows:

- In order to handle complex nonlinear relationships between various inputs and outputs, soft computing techniques are used, to derive mathematical models obtained from neural network and genetic programming. For this, experimental data were utilized from the available test results presented in the previous studies. The prediction parameters were selected from mixture constituents of concrete and drying period.

- Second stage of the thesis is to evaluate the model by experimental validation.

The purpose of this thesis is to perform a comprehensive study of how supplementary cementitious materials (SCMs), fly ash (FA), and silica fume (SF), can be used to improve the performance of concrete mixtures. In this thesis, SF and FA were used as a replacement for Portland cement (PC), ranging from 0% to 15% by weight, to evaluate its efficiency upon the concrete properties. For this purpose, four different concrete mixtures with w/b ratio of 0.45 were designed. The focus of the study is to evaluate the effectiveness of FA and SF on strength and durability properties of the concretes, which are subjected to different curing regimes. Drying shrinkage and weight loss due to the corresponding drying were also monitored. Furthermore, in order to examine the main effect of FA and SF on the performance properties of the concretes. Based on the test results, the effects of replacement level of FA, SF, w/b ratio, age, and curing procedure upon strength and particularly durability properties of the concrete were discussed.

1.3 Thesis organization

The thesis is divided into five chapters. Chapter 1 provides an introduction, background, thesis objectives and thesis organization, Chapter 2 gives a brief literature review of the concrete drying shrinkage phenomenon, factors affecting concrete drying shrinkage. The review aims to provide background and general information about concrete shrinkage behaviors, Chapter 3 provides analytical modeling, models based on soft-computing techniques and proposed models,

Chapter 4 covers the experimental program conducted throughout this study. Properties of cement, aggregates, mineral and chemical admixtures used in the concrete production as well as the tests on hardened properties of concrete are included. Chapter 5 summarizes the major findings of the study, reference and appendix

CHAPTER 2

LITERATURE REVIEW

2.1 Introduction

This chapter provides a review of past researches in the field of concrete. There are several published papers that investigated the shrinkage, types of shrinkage, mechanism of shrinkage, shrinkage-reducing admixtures. Moreover, the chapter also includes utilization of artificial intelligence in civil engineering applications, and using binary and ternary blend cement system.

2.2 Shrinkage

Water movement and moisture losses within the concrete mixtures are the major factors causing shrinkage. Chemical reactions induce water movements within the concrete elements leading to chemical and autogenous shrinkage, although water movement outside the concrete elements, which are water losses, causes drying shrinkage (Mehta and Monterio, 2006). Tazawa et al. (1999) defined concrete shrinkage as a reduction in volume through time, and is mainly due to water movement within a concrete's porous structure and to chemical reactions. The emptying of pores due to water movement generates tensile stresses that pull the cement paste closer causing shrinkage, while chemical reactions generate products whose volume is less than the volume of the initial ingredients.

Shrinkage is divided into two phases; the early age shrinkage, which occurs in the first 24 hours and the long-term shrinkage, which occurs after 24 hours (Holt, 2001). This division was put toward to distinguish between the driving mechanisms for each phase (Holt, 2001). For a concrete mixture with water-to-cement ratio greater than 0.42, the shrinkage at early age is mainly due to the chemical hydration reactions, while the long term shrinkage is attributed to water exchange and evaporation. Traditionally, the early age shrinkage was not a concern since its

magnitude was considered to be negligible in comparison to the long term drying shrinkage (Holt, 2001). The shrinkage types are mapped in Figure 2.1
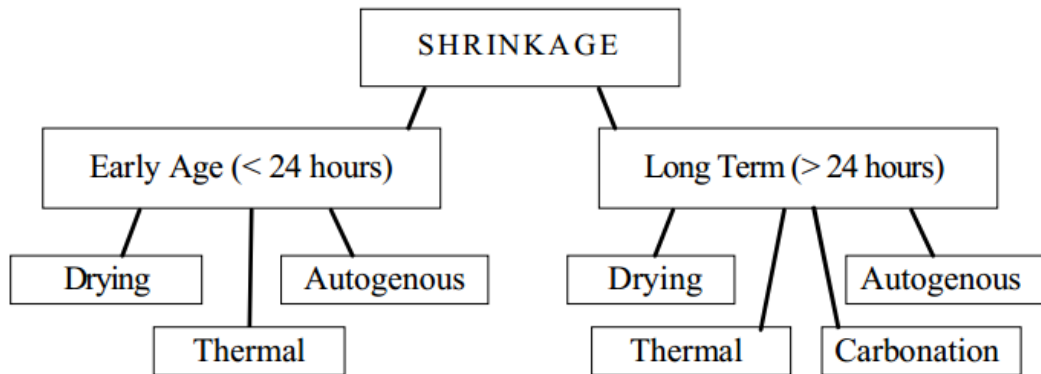
Figure 2.1 Diagram of shrinkage stages and types (Holt, 2001)

In the literature review, shrinkage has been divided into six types reflecting the different mechanisms. They are plastic shrinkage, dry shrinkage, carbonation shrinkage, thermal shrinkage, chemical shrinkage and autogenous shrinkage.

2.2.1 Plastic Shrinkage

Plastic shrinkage is idiom for freshly poured concrete. Plastic shrinkage occurs when water is allowed to evaporate from the fresh concrete surface. Environmental considerations including solar effects, wind speed, high temperature and low relative humidity drastically influence the potential of plastic shrinkage cracking (Schaels and Hover, 1988). In general, plastic shrinkage cracking can be averted by limiting early-age evaporation through the use of plastic sheeting, mono-molecular films, water fogging, or wind breaks in conjunction with properly designed concrete mixtures.

In the Figure 2.2 demonstrated the process of plastic shrinkage cracking in initiation and final state.

Evaporation

Tension

Bleeding

(a) Initiation

Cracks

(b) After a few hours
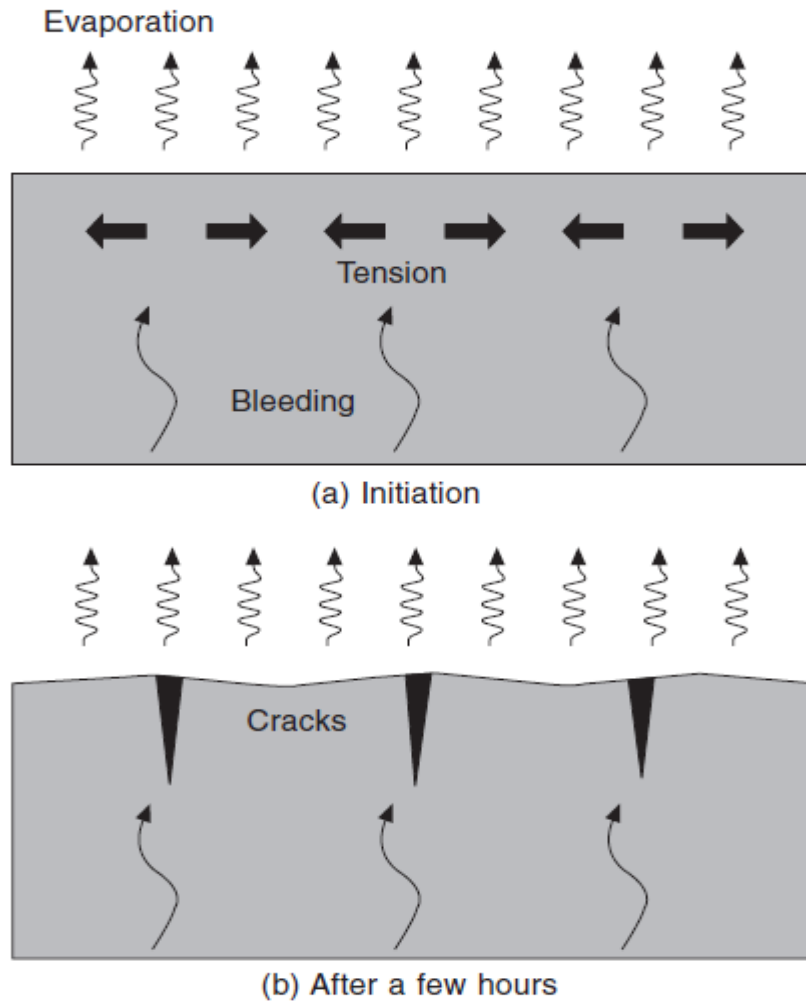
Figure 2.2 Process of plastic shrinkage cracking (initiation and final state).

(Newman and Choo, 2003)

2.2.2 Drying Shrinkage

Drying shrinkage is due to the loss of the water from the concrete pores. As the water evaporates to the outside, concrete shrinks. Drying shrinkage is similar to the autogenous shrinkage where both occur due to loss of water. For drying shrinkage, the water is transferred to the outside, whereas for autogenous shrinkage the water is transferred within the pore structure.

When the concrete is in contact with the exterior environment and in conditions of low humidity or high temperature, water begins to evaporate from the exposed surface. During the first stages of drying shrinkage, the free water exits from the concrete mass to the surface as a bleed water (Holt, 2001).

Figure 2.3 shows that as the water evaporation proceeds, the surface tension responsible for the drying shrinkage increases
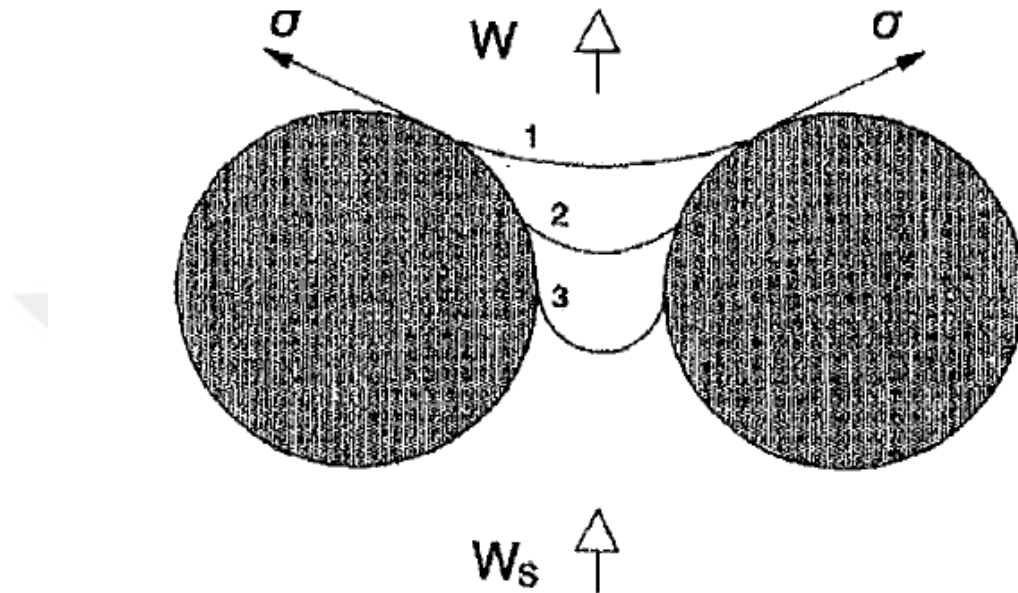
Figure 2.3 Drying shrinkage mechanism according to Power's theory – Stresses pushing water meniscus down between two cement particles (Radocea, 1992)

Other internal factors affecting the drying shrinkage are mineral admixtures, namely silica fume, ground granulated blast furnace slag, GGBFS, and fly ash (Omar et al. 2008). Silica fume and GGBFS, when added within certain proportion, play a major role in reducing the drying shrinkage due to the additional pozzolanic reactions that lead to stronger concrete pore structure and elevated resistance to deformations (Li and Yao, 2001). The use of fly ash in a mixture reduces the water requirement, therefore reduces drying shrinkage (Tangtermsirikul, 1995)

Guneyisi et al (2012) investigated the effectiveness of metakaolin (MK) and silica fume (SF) on the mechanical properties, shrinkage, and permeability related to durability of high performance concretes. Shrinkage behavior of the concretes with and without mineral admixtures were dealt through measurements of free shrinkage strains and weight loss of the specimens due to drying. In addition, test results

revealed that replacement level of MK and SF had significant effects on the mechanical and especially durability characteristics of high performance concretes.

2.2.3 Carbonation Shrinkage

Carbonation occurs be caused by a reaction that occurs between hydrated cement and carbon dioxide in the atmosphere which causes the concrete to shrink. Carbonation shrinkage occurs along the surface of concrete and as such, it is usually not a main cause for concern in structural concrete

2.2.4 Thermal Shrinkage

Solid materials such as concrete undergo contraction on cooling and expansion on heating. The rate of strain associated with these temperature changes are related to the rate of temperature changes and to the materials properties such as the coefficient of thermal expansion. These volume changes due to temperature changes are referred to as thermal shrinkage or swelling. Thermal shrinkage is a concern with the concrete at early age when the tensile strength is low and in massive concrete structure where the heat of hydration produced is very high (Khairallah, 2009).

2.2.5 Chemical Shrinkage

Chemical shrinkage is defined as "the phenomenon in which the absolute volume of hydration products is less than the total volume of unhydrated cement and water before hydration." (Tazawa et al., 1999). This type of shrinkage is due mainly to chemical reactions in the concrete. At the early stage, when the concrete is still plastic, in the liquid phase, the chemical shrinkage results in overall reduction of the specimen volume. The stage where the concrete begins to be stiffer, chemical shrinkage tends to create pores within the mix structure (Lura et al, 2003).

2.2.6 Autogenous Shrinkage

The Japan Concrete Institute, JCI, (Tazawa et al. 1999) has defined autogenous shrinkage as "the macroscopic volume reduction of cementitious materials when cement hydrates after initial setting. Autogenous shrinkage does not include the volume change due to loss or ingress of substances, temperature variation, application of an external force and restraint". As long as, the autogenous shrinkage is a volume reduction of the concrete with no moisture transfer with the outer

environment. The autogenous shrinkage is a concern where concrete has a water-to-cement ratio less than 0.42 (Holt, 2001). According to Justnes et al. (1996), autogenous shrinkage has been given many labels such as bulk shrinkage, Le Chatelier shrinkage, indigenous shrinkage, self-desiccation shrinkage, and autogenous volume change.

The effects of mineral admixtures and water-to-cement ratio, w/c on autogenous shrinkage very important. Zhang et al. (2003) presented an experimental study on the autogenous shrinkage of Portland cement concrete (OPC) and concrete incorporating silica fume (SF). The water-to cementitious materials (w/c) ratio of the concrete studied was in the range of 0.26 to 0.35 and the SF content was in the range of 0% to 10% by weight of cement, the results confirmed that the autogenous shrinkage increased with decreasing w/c ratio, and with increasing SF content. The results confirmed that the autogenous shrinkage increased with decreasing w/c ratio, and with increasing SF content. The results showed that the autogenous shrinkage strains of the concrete with low w/c ratio and SF developed rapidly even at early ages. The results singled that most of the total shrinkage of the concrete specimens with very low w/c ratio and SF exposed to 65% relative humidity after an initial moist curing of 7 days did not seem to be due to the drying shrinkage but due to the autogenous shrinkage

Maruyama and Teramoto (2013) presented the temperature dependence of autogenous shrinkage of cement pastes made with silica fume premixed cement with a water–binder ratio of 0.15 extensively. The result showed development of autogenous shrinkage different behaviors before and after the inflection point, and dependence on the temperature after mixing and subsequent temperature histories.

2.2.7 Mechanism of shrinkage

In a drying environment where a relative humidity gradient exists between the concrete and surrounding air, moisture (free water) is initially lost from the larger capillaries and little or no change in volume or shrinkage occurs. However, this creates an internal humidity gradient so that to maintain hygral equilibrium adsorbed water is transferred from the gel pores and, in turn, interlayer water, may be transferred to the larger capillaries. (Newman and Choo, 2003)

The process results in a reduction in volume of the C–S–H caused by induced balancing compression in the C–S–H solid skeleton by the capillary tension set up by the increasing curvature of the capillary menisci. This is known as the capillary tension theory. At lower relative humidity, the change in surface energy of the C–S–H as firmly held adsorbed water molecules are removed is thought to be responsible for the reduction in volume or shrinkage. Another theory is that of disjoining pressure, which occurs in areas of hindered adsorption (interlayer water); removal of this water causes a reduction in pressure and, hence, a reduction in volume (Newman and Choo, 2003).

The foregoing theories apply to reversible behavior and shrinkage is not fully reversible, probably because aditional bonds are formed during the process of drying. Moreover, carbonation shrinkage can occur, which prevents ingress of water on re-wetting (Newman and Choo, 2003).

It was concerned with drying shrinkage, namely, shrinkage resulting from the loss of water from the concrete to the outside environment. It should be mentioned that plastic shrinkage occurs before setting and can be prevented by eliminating evaporation after casting the concrete. Like drying shrinkage, autogenous shrinkage occurs after setting. It is determined in sealed concrete and is caused by the internal consumption of water by hydration of cement, the products of which occupy less volume than the sum of the original water and unhydrated cement. In normal strength concrete, autogenous shrinkage is small ($<100 \times 10–6$) and is included with drying shrinkage. On the other hand, in high performance or high strength concrete made with a low water/cementitious materials ratio, autogenous shrinkage can exceed drying shrinkage. Design guidelines do not provide methods of estimating autogenous shrinkage (Newman and Choo, 2003).

2.2.8 Shrinkage-reducing admixtures

Shrinkage-reducing admixtures can significantly reduce both the early and long-term drying shrinkage of hardened concrete. This is achieved by treating the 'cause' of drying shrinkage within the capillaries and pores of the cement paste, as water is lost. This type of admixture should not be confused with shrinkage-compensating materials which are normally added at above 5% on cement and function by creating

an expansive reaction within the cement paste to treat the 'effects' of drying shrinkage.

Shrinkage-reducing admixtures are mainly based on glycol ether derivatives. These organic liquids are totally different from most other admixtures, which are water-based solutions. Shrinkage reducing admixtures are normally 100% active liquids and are water-soluble (Newman and Choo, 2003).

They have a characteristic odour and a specific gravity of less than 1.00. The dosage is largely independent of the cement content of the concrete and is typically in the range 5–7 liters/m3 (Newman and Choo, 2003).

When excess water begins to evaporate from the concrete's surface after placing, compacting, finishing and curing, an air/water interface or 'meniscus' is set up within the capillaries of the cement paste. Because water has a very high surface tension, this causes a stress to be exerted on the internal walls of the capillaries where the meniscus has formed. This stress is in the form of an inward-pulling force that tends to close up the capillary. Thus the volume of the capillary is reduced, leading to shrinkage of the cement paste around the aggregates and an overall reduction in volume of the concrete.

The shrinkage-reducing admixtures operate by interfering with the surface chemistry of the air/water interface within the capillary, reducing surface tension effects and consequently reducing the shrinkage as water evaporates from within the concrete. They may also change the microstructure of the hydrated cement in a way that increases the mechanical stability of the capillaries.

2.3 Artificial Intelligence

Artificial intelligence is the getting of computers to do things that seem to be intelligent. The hope is that more intelligent computers can be more helpful to us better able to respond to our needs and wants, and more clever about satisfying them. Nevertheless, "intelligence" is a vague word. Therefore, artificial intelligence is not a well-defined field. One thing it often means is advanced software engineering, sophisticated software techniques for hard problems that cannot be solved in any easy way. Another thing it often means is nonnumeric ways of solving

problems, since people cannot handle numbers well. Nonnumeric ways are often "common sense" ways, not necessarily the best ones. Therefore, artificial-intelligence programs like people--are usually not perfect, and even make mistakes. (Rowe, 1988)

According to (Rowe, 1988) Artificial intelligence includes:

- Getting computers to communicate with us in human languages like English, either by printing on a computer terminal, understanding things we type on a computer terminal, generating speech, or understanding our speech (natural language);
- Getting computers to remember complicated interrelated facts, and draw conclusions from them (inference);
- Getting computers to plan sequences of actions to accomplish goals (planning);
- Getting computers to offer us advice based on complicated rules for various situations (expert systems);
- Getting computers to look through cameras and see what's there (vision);
- Getting computers to move themselves and objects around in the real world (robotics).

Artificial intelligence is a branch of computer science, involved in the research, design, and application of intelligent computer. Traditional methods for modeling and optimizing complex structure systems require huge amounts of computing resources, and artificial-intelligence-based solutions can often provide valuable alternatives for efficiently solving problems in the civil engineering (Lu et al., 2012).

The aim of the study of Artificial Intelligence is no longer to create a robot as intelligent as a human, but rather to use algorithms, heuristics, and methodologies based on the ways in which the human brain solves problems (Coppin, 2004).

In the study by Sgambi (2008) demonstrated the A.I. are divided in two fields:

- The first, called Strong Artificial Intelligence, sustained by functionalists, retain that a computer correctly programmed can be capable of pure

intelligence, non-distinguished in any significant way from human intelligence. The basic idea of such theory springs from the concept expressed by English empiric philosopher Thomas Hobbes, whom affirmed that reasoning is nothing else but a calculation: Hence, the human mind should be the result of complexes calculations performed by the brains.

- The second, so called Weak Artificial Intelligence, sustain that a computer couldn't ever be capable to equal human mind, but can only level up to simulate some human cognitive processes but never reproducing then in their total complexity

2.3.1 Origin

Philosophers in the past (going back to Plato in 400 B.C.) made possible the very concept of artificial intelligence, considering the idea of the mind as somehow a machine that operates on the knowledge codificated by some internal language processes. Nevertheless only with the genesis of computers in the beginning of the fifties, transformed the wise philosophic reflections in a articulated theory and experimental discipline (Sgambi, 2008).

In 1950, in an article a clue is given about how to create a program to abilitate a computer in order to function in an intelligent manner (Sgambi, 2008).

In 1956, John McCarthy first used the term artificial intelligence at a conference in Dartmouth College, in Hanover, New Hampshire. In 1957, Newell and Simon invented the idea of the GPS, whose purpose was, as the name suggests, solving almost any logical problem. The program used a methodology known as means ends analysis, which is based on the idea of determining what needs to be done and then working out a way to do it. This works well enough for simple problems, but AI researchers soon realized that this kind of method could not be applied in such a general way the GPS could solve some fairly specific problems for which it was ideally suited, but its name was really a misnomer.

In 1958, McCarthy invented the LISP programming language, which is still widely used today in Artificial Intelligence research (Coppin, 2004).

2.3.2 Current studies

Recently many authors suggested various definitions that can be collected in the following four categories (Russel, 1995):

- Systems that think like human beings (Haugeland, 1985).
- Systems that operate like human beings (Rich, 1991).
- Systems that rationally think (Charniak, 1985).
- Systems that rationally perform (Luger, 1993).

The AI as currently is being studied; focus on the individuation of models (proper description of a problem to solve) and algorithms (effective procedure to solve the model). Each one of the two aspects (modelization or algorithm) has major or minor importance and variation along a wide spectrum. The activities and capacities of I.A. comprehend:

- Automatic learning (machine learning).
- The representation of knowledge and automatic reasoning in the same level to the human mind.
- Planning.
- The collaboration between intelligent agents, in software as hardware (robot).
- The elaboration of natural language (Natural Language Processing).
- The simulation of the vision and interpretation of images, as in OCR case.

At this time, there was a great deal of optimism about Artificial Intelligence. Predictions that with hindsight appear rash were widespread. Many commentators were predicting that it would be only a few years before computers could be designed that would be at least as intelligent as real human beings and able to perform such tasks as beating the world champion at chess, translating from Russian into English, and navigating a car through a busy street. Some success has been made in the past 50 years with these problems and other similar ones, but no one has yet designed a computer that anyone would describe reasonably as being intelligent.

2.4 Soft computing techniques

Soft computing is a collection of methodologies that aim to exploit the tolerance for imprecision and uncertainty to achieve tractability, robustness, and low solution cost. Its principal constituents are fizzy logic, neurocomputing, and probabilistic reasoning.

Soft computing is likely to play an increasingly important role in many application areas, including sof2ware engineering. The role model for soft computing is the human mind (Zade, 1994).

According to Konar (2000) Soft computing an emerging approach to computing, which parallels the remarkable ability of the human mind to reason and learn in an environment of uncertainty and imprecision. It, in general, is a collection of computing tools and techniques, shared by closely related disciplines that include fuzzy logic, artificial neural nets, genetic algorithms, belief calculus, and some aspects of machine learning like inductive logic programming. These tools are used independently as well as jointly depending on the type of the domain of applications. The scope of the first three tools in the broad spectrum of AI is outlined below.

2.4.1 Artificial neural network

artificial neural networks (ANNs) technology, a family of massively parallel architectures that solve difficult problems via the cooperation of highly interconnected but simple computing elements (or artificial neurons), is being used to solve a wide variety of problems in civil engineering applications (Ozcan et al., 2009).

''The basic strategy for developing ANNs systems based models for material behavior is to train (ANNs) systems on the results of a series of experiments using the material in question. If the experimental results contain the relevant information about the material behavior, then the trained ANNs systems will contain sufficient information on the material's behavior to qualify as a material model. Such trained ANN systems not only would be able to reproduce the experimental results, but they would be able to approximate the results in other experiments trough their generalization capability'' (Topcu and Sarıdemir, 2008).

Their network topology and learning or training algorithms commonly classify ANNs. For example, a multilayer feed forward neural network with back propagation indicates the architecture and learning algorithm of the neural network Figure 2.4 (Özbay, 2007).
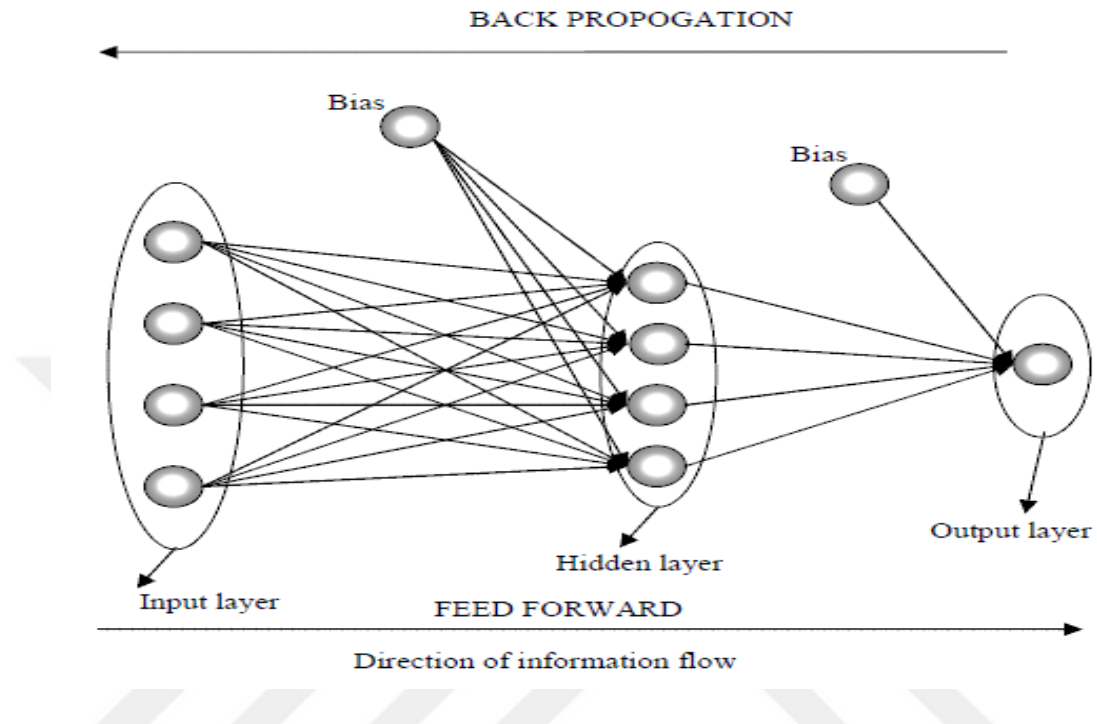
Figure 2.4 Multilayered artificial neural network (Özbay, 2007)

2.4.2 Genetic programming

GP creates computer programs to solve a problem by simulating the biological evolution of living organisms (Koza, 1992). The genetic operators of genetic algorithm (GA) and GP are almost the same. The difference between GA and GP is that the former gives the solution as a string of numbers, while the solution generated by the latter is computer programs represented as tree structures.

2.4.3 Fuzzy logic

Fuzzy logic is the method of common sense decision support approach based on natural language (gulley, 1995). Fuzzy logic is raised from the concepts of fuzzy sets, which are the sets without clearly defined boundaries. It should be noted that there is a real distinction between fuzzy set theory (FST) and probability theory (PT) because they are based on models of different semantic concepts. (Zarandi et al., 2008)

Fuzzy logic concept provides a natural way of dealing with problems in which the source of imprecision is valid rather than the presence of random variables. The key elements in human thinking are not numbers but levels of fuzzy sets through linguistic words. In consequence, linguistic variables are introduced as parameter descriptions in a natural and logical linguistic statements or propositions (Abbas et al., 2013).

Zarandi et al. (2008) develop fuzzy polynomial neural networks FPNN to predict the compressive strength of concrete. The results show that FPNN-Type1 has strong potential as a feasible tool for prediction of the compressive strength of concrete mix-design.

Pedrycz and Aliev (2009) demonstrated how the logic blueprint of the networks is supported by the use of various constructs of fuzzy sets including logic operators, logic neurons, referential operators and fuzzy relational constructs, through concentrating on the fundamentals and essential development issues of logic-driven constructs of fuzzy neural networks. These networks, referred to as logic-oriented neural networks, constitute an interesting conceptual and computational framework that greatly benefits from the establishment of highly synergistic links between the technology of fuzzy sets and neural networks. This proposal concluded two major advantages. First, the transparency of neural architectures becomes highly relevant when dealing with the mechanisms of efficient learning. Second, the network can be easily interpreted and thus it directly translates into a series of truth- quantifiable logic expressions formed over a collection of information granules, regarding that the training had completed.

Guler et al. (2012) presented a fuzzy approach for modelling of high strength concrete under uniaxial loading. The fuzzy logic approach, which was applied to test data of concrete cylinder test, was available in previous studies. In his paper, the stress–strain behavior of high strength concrete was subjected to axial load which was obtained by using the fuzzy logic model. It was shown that the current model could predict the stress–strain behavior of concrete accurately by taking into account the parameters of the problem. The outcomes were compared with the analytical models given in various studies concerning cylinder tests. The new approach

showed that there is no need to obtain different expressions for ascending and descending branches of the stress–strain behavior.

Nedushan (2012) proposed an adaptive network-based fuzzy inference system (ANFIS) model and three optimized nonlinear regression models to predict the elastic modulus of normal and high strength concrete. The optimal values of parameters for nonlinear regression models were determined with differential evolution (DE) algorithm. The elastic modulus predicted by ANFIS and nonlinear regression models were compared with the experimental data and those from other empirical models. Results showed that the ANFIS model outperforms the nonlinear regression models and most of other predictive models proposed in the previous studies and therefore could be used as a reliable model for prediction of elastic modulus of normal and high strength concrete.

Silva and Stemberk (2012) developed an experimental based on fuzzy logic model to predicting self-compacting concrete shrinkage. The fuzzy logic model decision-making was optimized despite an evolutionary computing method, to improve computational effectiveness. The obtained results were compared to the B3 shrinkage prediction model and statistical analysis, indicating the reliability of the proposed model, are presented. The optimized group of fuzzy sets led to a proper prediction of the shrinkage curves with a reduced number of rules, making the modelling process more effective.

2.5 Utilizations of artificial intelligence on civil engineering applications

Artificial intelligence is a science on the research and application of the law of the activities of human intelligence. Nowadays, this technology is applied in many fields such as expert system, knowledge base system, intelligent database system, and intelligent robot system. Expert system is the earliest and most extensive, the most active and most fruitful area, which was named as "the knowledge management and decision-making technology of the 21 century." In the field of civil engineering, many problems, especially in engineering design, construction management, and program decision-making, were influenced by many uncertainties which could be solved not only in need of mathematics, physics, and mechanics calculations but also depend on the experience of practitioners. This knowledge and experience are illogically incomplete and imprecise, and they cannot be handled by

traditional procedures. However, artificial intelligence has its own superiority. It can solve complex problems to the levels of experts by means of imitate experts. Overall, artificial intelligence has a broad application prospects in the practice of civil engineering (Lu et al., 2012).

2.5.1 Use of Neural networks for concrete properties

Karthikeyan et al. (2007) used Artificial Neural Network (ANN) model for predicting creep and shrinkage. While concrete undergoes time-dependent deformations that must be considered in the design of reinforced/ prestressed high performance concrete (HPC) bridge girders. They researches experiments on the creep and shrinkage properties of a HPC mix were conducted for 500 days. The results indicated from research were compared to different models to determine which model was the better one. The CEB-90 model was found better in prediction time-dependent strains and deformations for the above HPC mix. In addition, the experimental database was used along with the CEB-90 model database to train the neural network because in a far zone, some deviation was observed. The developed Artificial Neural Network (ANN) model will serve as a more rational as well as computationally efficient model in predicating creep coefficient and shrinkage strain.

Sarıdemir (2009) developed models in artificial neural networks (ANN) for predicting compressive strength of concretes containing metakaolin and silica fume. The data used in the multilayer feed forward neural networks models are arranged in a format of eight input parameters that cover the age of specimen, cement, metakaolin (MK), silica fume (SF), water, sand, aggregate and superplasticizer. According to these input parameters, the compressive strength values of concretes containing metakaolin and silica fume were predicted. The training and testing results in the neural network models showed that neural networks have a stronger possibility for predicting 1, 3, 7, 28, 56, 90 and 180 days compressive strength values of concretes containing metakaolin and silica fume.

A study carried out by Baykasoglu et al. (2009) utilized soft computing approaches for Prediction and multi-objective optimization of high-strength concrete parameters, they study presented multi-objective optimization (MOO) of high-strength concretes (HSCs). One of the main problems in the optimization of HSCs is

to obtain mathematical equations that represents concrete characteristic in terms of its constitutions. During the study, two-step approach used to find effective solutions and mathematical equations. Step one consist predation of HSCs parameters by using regression analysis, neural networks and Gene Expression Programming (GEP). In second step, the equations developed in the first step were used. The outcome of MOO model is solved by using a Genetic Algorithm (GA).

According to Ozcan (2009) utilized an artificial neural network (ANN) and fuzzy logic (FL) study were developed to predict the compressive strength of silica fume concrete. A data set of a laboratory work, in which 48 concretes were produced, was used in the ANNs and FL study. The concrete mixture parameters were four different water–cement ratios, three different cement dosages and three partial silica fume replacement levels. Compressive strength of moist cured specimens was measured at five different ages. The achieved results with the experimental methods were compared with ANN and FL results. The results indicated that ANN and FL can be alternative approaches for the predicting of compressive strength of silica fume concrete.

Cevik et al. (2009) presented the application of soft computing techniques for strength prediction of heat treated extruded aluminum alloy columns failing by flexural buckling, using Neural networks (NN) and genetic programming (GP) as soft computing techniques, and gene expression programming (GEP) which is an extension to GP. The training and test sets for soft computing models were obtained from experimental results are available in literature. An algorithm is also developed for the optimal NN model selection process. The proposed NN and GEP models were presented in explicit form to be used in practical applications. The accuracy of the proposed soft computing models were compared with existing codes and were found to be more accurate.

Deng and Wang (2010) conducted a study about probabilistic neural networks (PNN) to predict shrinkage of thermal insulation mortar. Probabilistic results were obtained from the PNN model with the aid of Parzen non-parametric estimator of the probability density functions (PDF). Five variables, water-cementitious materials ratio, content of cement, fly ash, aggregate and plasticizer, were employed for input variables, while a category of 56-d shrinkage of mortar was used for the output

variable. A total of 192 groups of experimental data from 64 mixtures designed using JMP7.0 software were collected, of which 120 groups of data were used for training the model and the other 72 groups of data for testing. They concluded that the PNN model with an optimal smoothing parameter determined by the curves of the mean square error (MSE) and the number of unrecognized probability densities (UPDs) exhibited a promising capability of predicting shrinkage of mortar.

Tsai and Lin (2011) proposed a modular neural network MNN that is designed to accomplish both artificial intelligent prediction and programming. Each modular element adopted a high-order neural network to create a formula that considers both weights and exponents, while MNN represented practical problems in mathematical terms using modular functions, weight coefficients and exponents. Genetic algorithms was used to optimize MNN parameters and designed a target function to avoid over-fitting. Input parameters were identified and modular function influences were addressed in manner that significantly improved previous practices. A reference study on high strength concrete was adopted to compare the effectiveness of results, which had been previously studied using a genetic programming (GP) approach. On the other hand MNN calculations were more accurate than GP, used more concise programmed formulas, and allowed the potential to conduct parameter studies. The proposal "MNN" concluded that using artificial neural networks is a valid alternative approach to prediction and programming.

Uysal and Tanyildizi (2012) utilized artificial neural network model for compressive strength of self-compacting concretes (SCCs) containing mineral additives and polypropylene (PP) fiber exposed to elevated temperature were devised. Tests were conducted to determine loss in compressive strength. The results showed that a severe strength loss was observed for all of the concretes after exposure to 600 C, especially the concretes that containing polypropylene fibers though they reduce and eliminate the risk of the explosive spalling. Additionally, according to the experimental results, an artificial neural network (ANN) model-based explicit formulation was proposed to predict the loss in compressive strength of SCC, which is expressed in terms of amount of cement, amount of mineral additives, amount of aggregates, heating degree and with or without PP fibers. Besides, it was found that the empirical model developed by using ANN seemed to have had a high prediction

capability of the loss in compressive strength after had been exposed to elevated temperature.

Figs. 2.5–2.10 present the measured compressive strengths versus predicted compressive strengths by ANN model with R^2 coefficients. Figs. 6 show that the best algorithm for compressive strength of SCC exposed to high temperature is the BFGS quasi-Newton back propagation algorithm with R^2 of 0.9757 (Uysal and Tanyildizi; 2012).
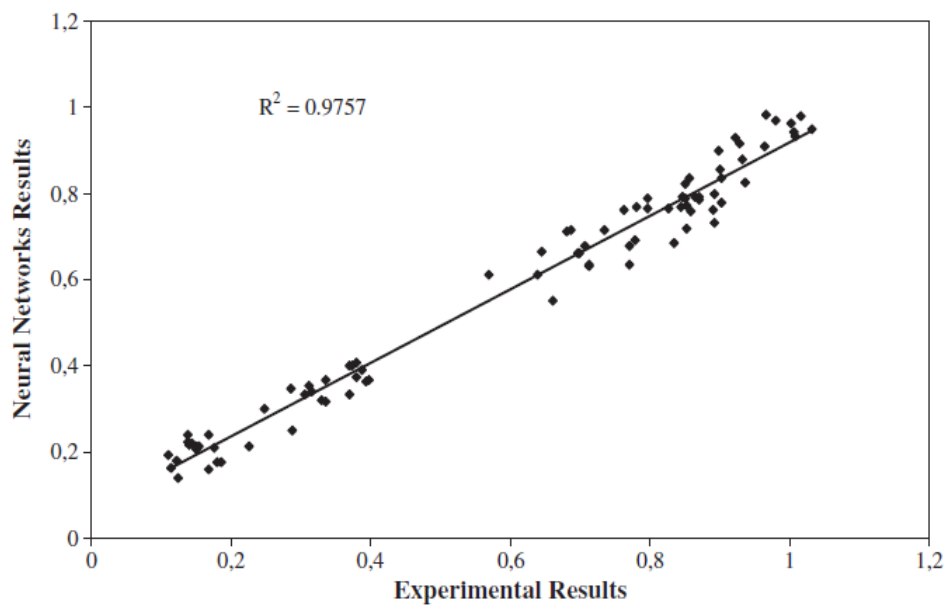
Figure 2.5 Linear relationship between measured and predicted compressive strengths (the Levenberg–Marquardt backpropagation algorithm). (Uysal and Tanyildizi, 2012)
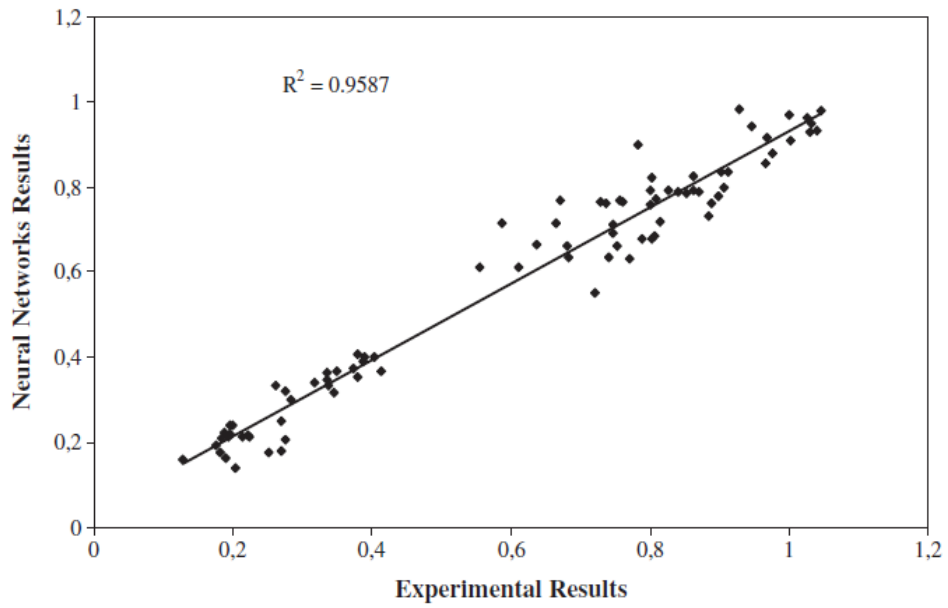
Figure 2.6 Linear relationship between measured and predicted compressive strengths (the BFGS quasi-Newton backpropagation algorithm). (Uysal and Tanyildizi, 2012)
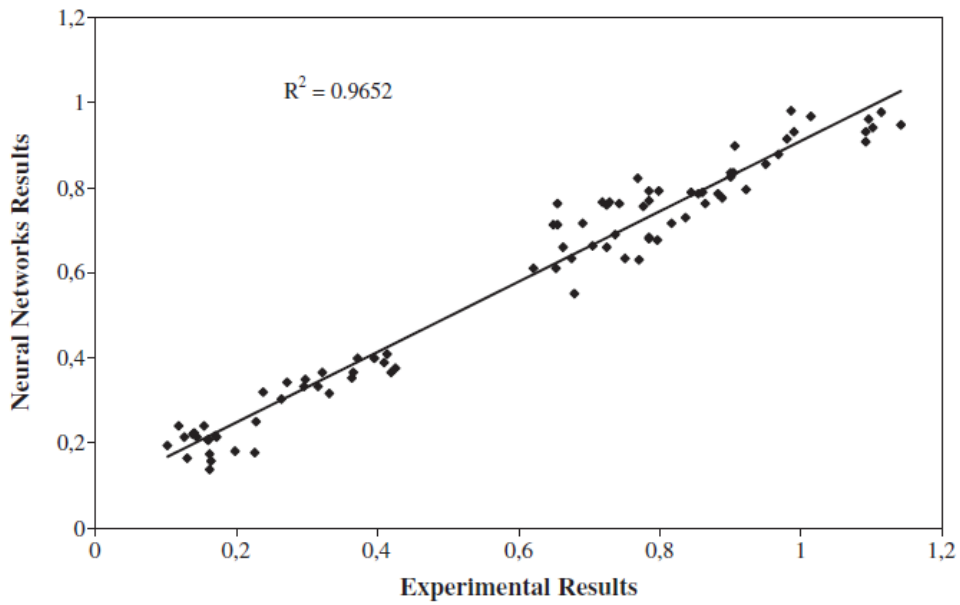
Figure 2.7 Linear relationship between measured and predicted compressive strengths (the Powell–Beale conjugate gradient backpropagation algorithm). (Uysal and Tanyildizi, 2012)
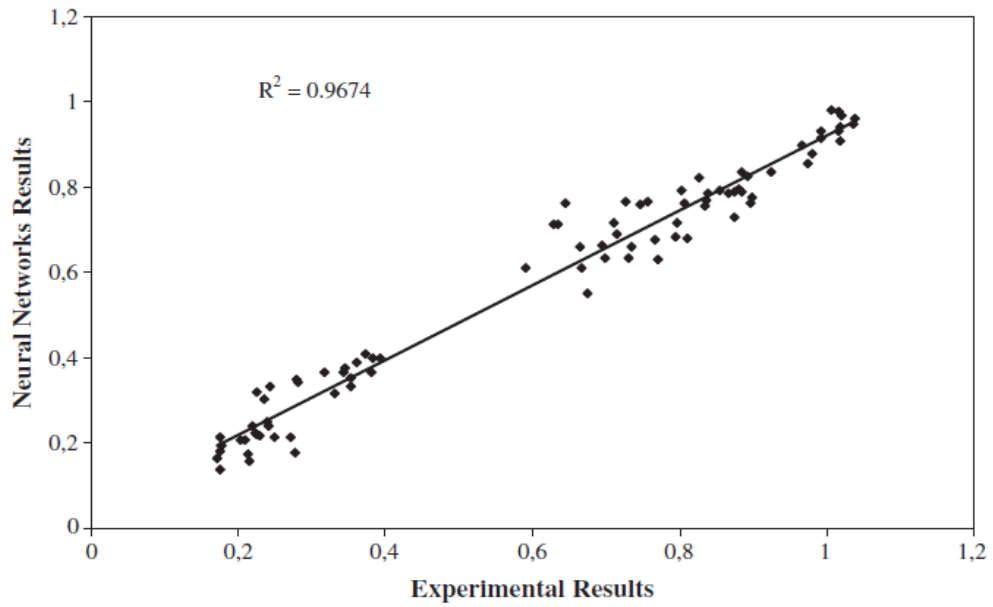
Figure 2.8 Linear relationship between measured and predicted compressive strengths (the Fletcher–Powell conjugate gradient backpropagation algorithm). (Uysal and Tanyildizi, 2012)
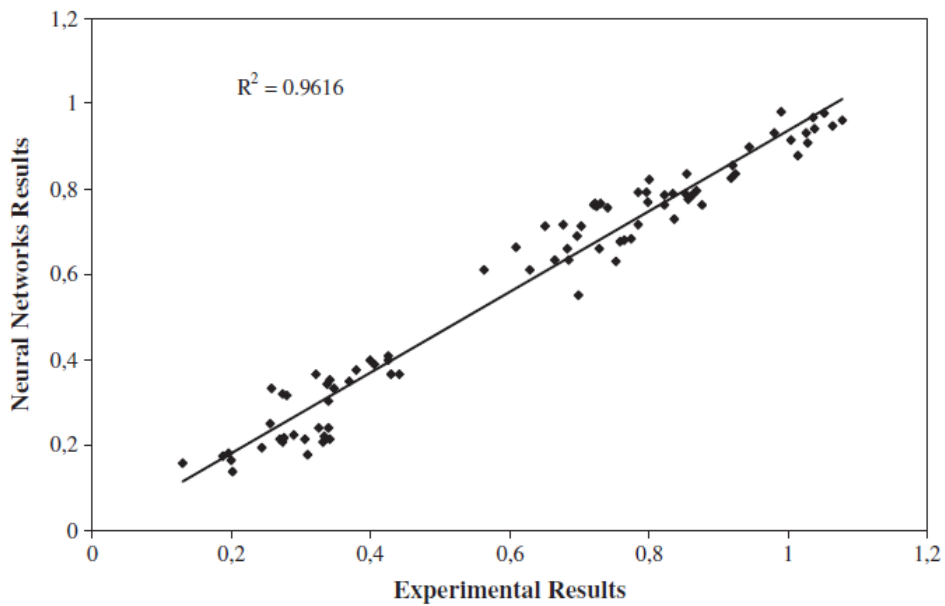
Figure 2.9 Linear relationship between measured and predicted compressive strengths (the Polak–Ribiere conjugate gradient backpropagation algorithm). (Uysal and Tanyildizi, 2012)
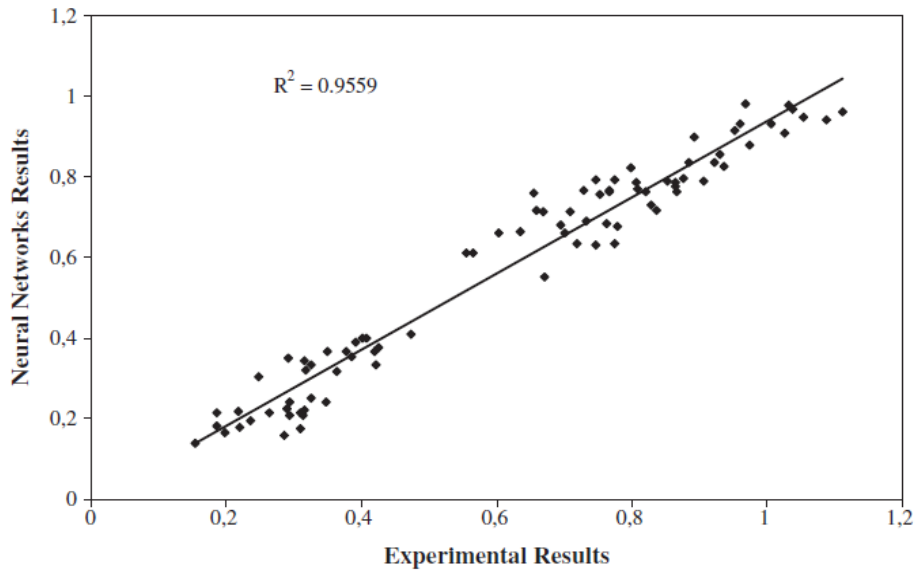
Figure 2.10 Linear relationship between measured and predicted compressive strengths (the one-step secant backpropagation algorithm). (Uysal and Tanyildizi, 2012)

Nazari and Torgal (2013) developed six different models based on artificial neural networks to predict the compressive strength of different types of geopolymers. The differences between the models were in the number of neurons in hidden layers and in the method of finalizing the models; a compressive strength of geopolymers was obtained for each variable input. Furthermore, validated and tested network showed a strong potential for predicting the compressive strength of geopolymers with a reasonable performance in the considered range.

Dantas et al. (2013) applied Artificial Neural Networks (ANNs) models, which were developed for predicting the compressive strength of 3, 7, 28 and 91 days, of concretes containing Construction and Demolition Waste (CDW). The experimental results used to construct the models were gathered from literature .They used data in two phases, the training and testing phases, The results of (ANNs) models indicated in both, the training and testing phases strongly showed the potential use of ANN to predict 3, 7, 28 and 91 days compressive strength of concretes containing CDW.

Bal and Bodin (2013) utilized Artificial Neural Network (ANN) to predict effectively dimensional variations due to drying shrinkage. They depend on a very large database of experimental result to develop models for predicting shrinkage.

They used different parameters of concrete preservation and making, which affect drying shrinkage of concrete. To validate these models, they were compared with parametric models as: B3, ACI 209, CEB and GL2000, it was clear that ANN approach described correctly the evolution with time of drying shrinkage. In addition, a parametric study was also conducted to quantify the degree of influence of some the different parameters used in the developed neural network model.

The most basic system presents three layers, the first layer with input neurons sending via synapses data to the second layer of neurons, and then via other synapses to the third layer of output neurons. The architecture of this network is presented in Fig. 2.11
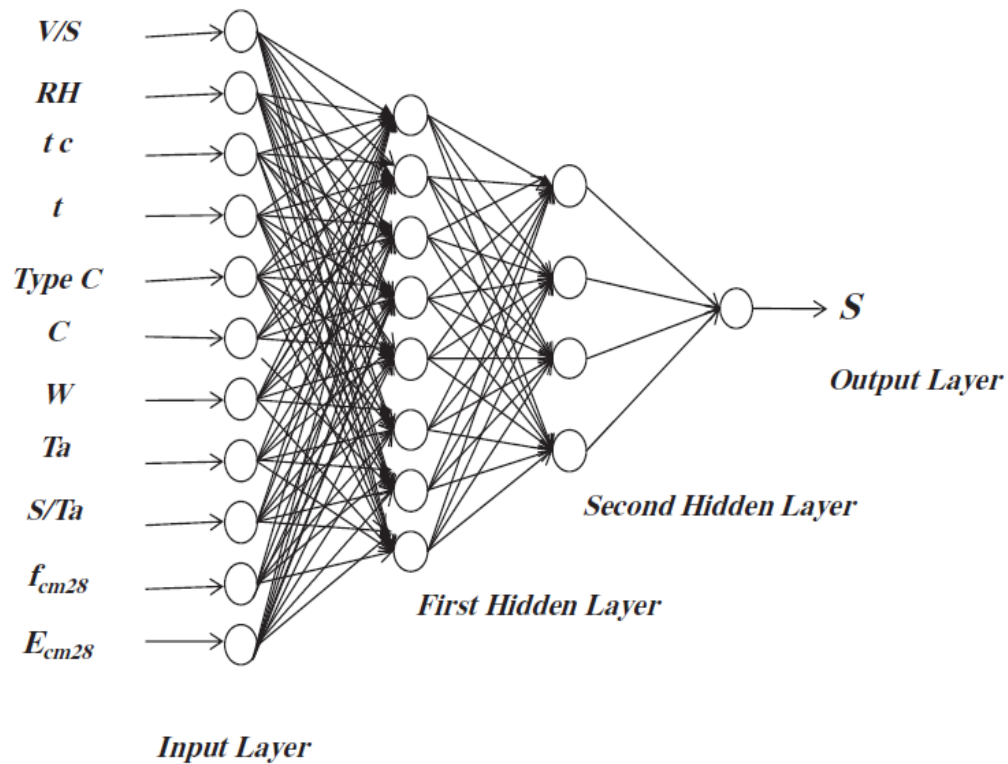
Figure 2.11 Selected architecture for prediction of drying shrinkage. (Bal and Bodin, 2013)

2.5.2 Use of Genetic programming on concrete properties

In a study by Kose and Kayadelen (2010) of the efficiency of neuro-fuzzy inference system (ANFIS) and genetic expression programming (GEP) in predicting the transfer length of prestressing strands in prestressed concrete beams was

investigated. Many suggested models for the transfer length of prestressing strands usually consider one or two parameters and do not provide consistent accurate prediction. Six basic parameters were selected as inputs. Results showed that the ANFIS and GEP models were capable of accurately predicting the transfer lengths used in the training and testing phase of the study, and the GEP model indicate better prediction compared to ANFIS model.

Castelli et al (2013) proposed intelligent system based on Genetic Programming for the prediction of high-performance concrete strength called "Geometric Semantic Genetic Programming", it was based on recently defined geometric semantic genetic operators for Genetic Programming. .The experimental results showed the suitability of the suggested system for the prediction of concrete strength. What is worth stating that, the suggested method outperformed the standard Genetic Programming and returns results were significantly better to the ones produced by other well-known machine learning techniques.

Sarıdemir (2014) utilized genetic programming for predicting the compressive strength values. The training, testing and validation set results of the explicit formulations obtained by the genetic programming models showed that artificial intelligent methods have strong potential and can be applied for the prediction of the compressive strength of concrete containing fly ash with different specimen size and shape.

The flowchart of a gene expression algorithm is shown in Fig. 2.12 (Sarıdemir, 2014)
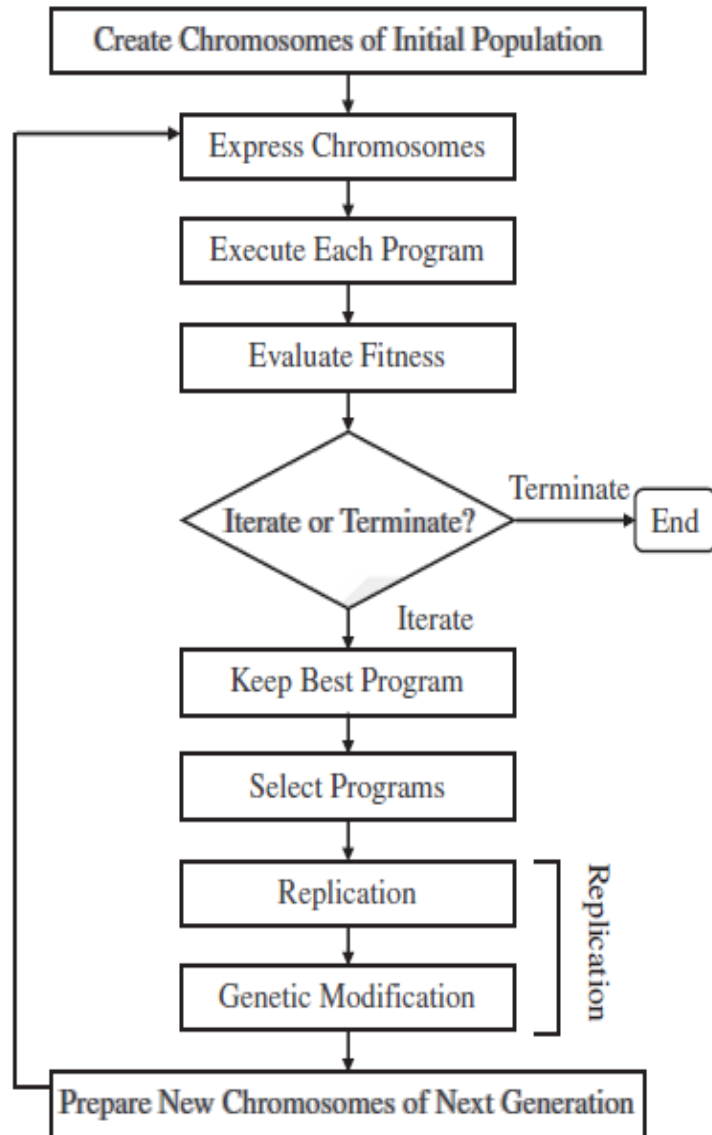
Figure 2.12 The flowchart of a gene expression algorithm. (Sarıdemir, 2014)

The expression tree ETs of the GEP-I for predicting the fc concrete containing fly ash FA at different proportions are given in Fig.2.13 (Sarıdemir, 2014)
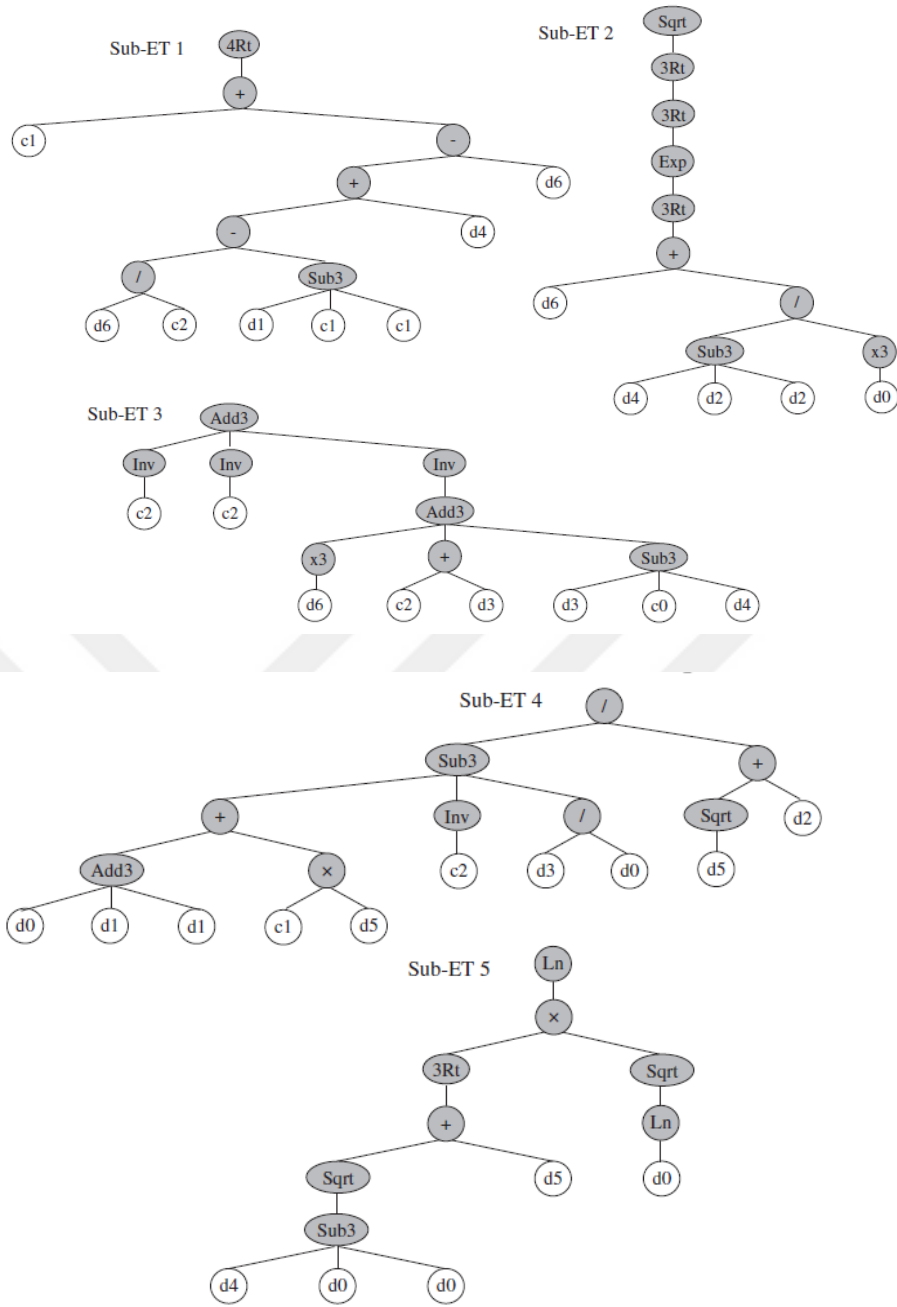
The linear least square fit line and the R^2 values are shown in this figure for the training, testing and validation sets of the models. As can be clearly seen in Fig.2.14 (Sarıdemir, 2014)
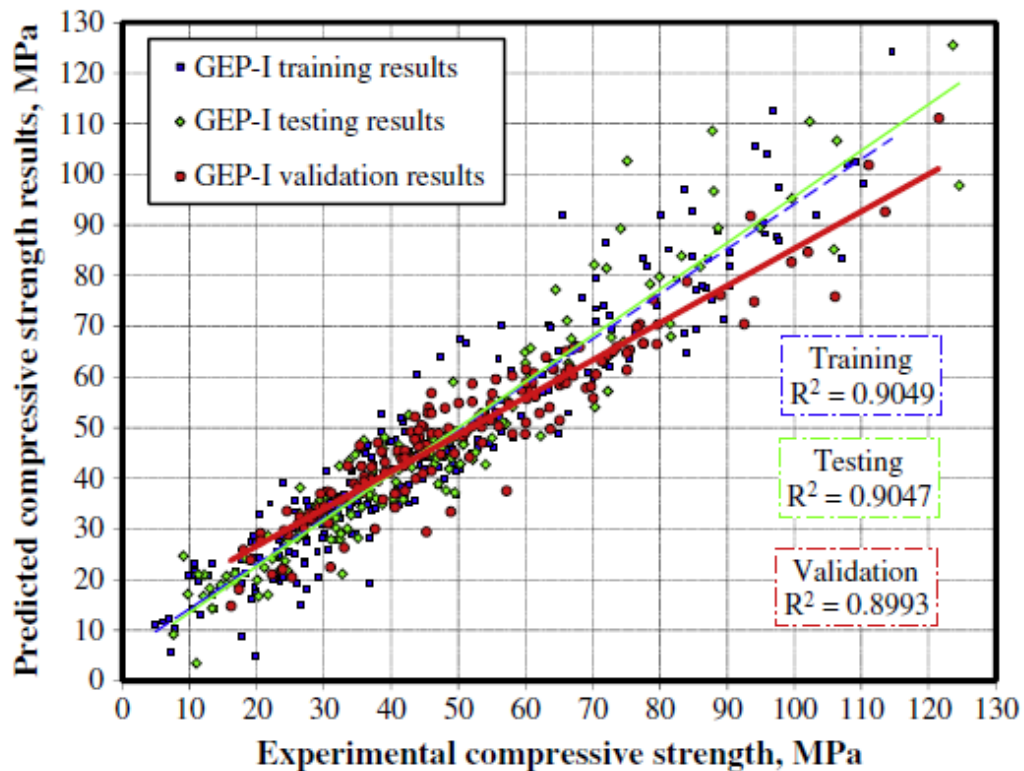
Figure 2.14 Comparison of the experimental results of fc with GEP-I. (Saridemir, 2014)

2.6 Binary and Ternary blending systems of mineral admixture

Using mineral admixtures as cement replacement substance in concrete has a tendency to increase by the future in order to provide greater sustainability in construction industry (Guneyisi et al., 2012). In binary blend, cement system, ordinary Portland cement OPC is partially replaced with only a single type of mineral admixture, and in ternary blend cement system, OPC is partially replaced with double type of mineral admixture. The advantages of using cement additions in concrete are, mainly, the improved concrete properties in fresh and hardened states, and economical and ecological benefits. The achievement of these advantages becomes more important for high strength concrete HSC proportioning since HSC requires high amounts of cementitious materials. However, the selection of additions needs more attention due to their different (Erdem and Kırca, 2008).

Previous literature focuses on investigating how binary systems effect on properties concrete compressive strength, drying shrinkage.

31

Thomas et al. (1999) reported the results from laboratory studies on the durability of concrete that contains ternary blends of Portland cement, silica fume, and a wide range of fly ashes. Concrete made with these proportions generally show excellent fresh and hardened properties since the combination of silica fume and fly ash is somewhat synergistic. For example, fly ash appears to compensate for some of the workability problems often associated with the use of higher levels of silica fume, whereas the silica fume appears to compensate for the relatively low early strength of fly ash concrete. The result testing showed that concrete produced with ternary cementitious blends had a very high resistance to the penetration of chloride ions. Additionally, these data indicated that the diffusivity of the concrete that contains ternary blends continues to decrease with age.

Bouzoubaa et al. (2002) developed ternary blends with optimum amounts of fly ash and silica fume to be used in high-performance concrete. Two sets of air-entrained concrete mixtures were investigated during the study: first set included concretes with a total cementitious materials content (CM) of 350 kg/m3, and a water-to-cementitious materials ratio (W/CM) of 0.40, and second set 2 included concretes with a total CM of 450 kg/m3 and a W/CM of 0.34. In each set, one silica fume and three fly ashes were used; these consisted of two ASTM Class F and one ASTM Class C fly ashes. Properties of the fresh and hardened concrete such as slump, air content, bleeding, setting time, autogenous temperature rise, plastic shrinkage, compressive strength, drying shrinkage and the resistance to chloride-ion penetration were determined. The study concluded that the combined use of fly ash and silica fume in concrete were more advantageous in terms of the following parameters: the dosage of superplasticizer, plastic shrinkage, chloride-ion penetrability and the drying shrinkage.

Erdem and Kırca (2008) produced 80 high strength concrete, containing several types and amounts of supplements. Silica fume content in binary blends that give the highest strengths were decided for different binder contents. This was followed by a third binder (Class F or Class C fly ash or ground granulated blast furnace slag) introduction to the concrete, that already had contained Portland cement and silica fume in the amounts found in the first stage. Results indicated that ternary blends almost always made it possible to obtain higher strengths than Portland cement +

silica fume binary mixtures, only if the replacement level by the supplements was chosen properly. In addition, the performance of slag in the ternary blends was better than Class F fly ash but worse than Class C fly ash. As shown in Fig.2.15, for PC + SF + FA/C mixtures with 600 kg/m3 binder, the highest strength at 3 days occurred at 20% but the highest strength at 7 and 28 days was observed at 30% replacement level. Similarly, in the case of 650 kg/m3 and PC + SF + S mixtures, the optimum replacement level was 20% at 3 days while it was 40% at 7 and 28 days.
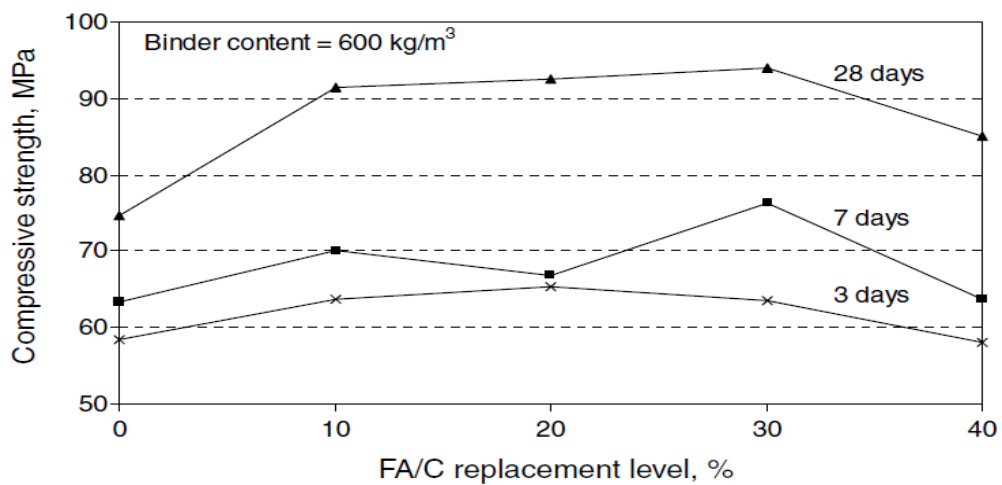
Figure 2.15 Compressive strength of PC + SF + FA/C concretes having 600 kg/m3 binder content. (Erdem and Kırca, 2008)

Guneyisi et al. (2010) investigated compressive strength and particularly drying shrinkage properties of self-compacting concretes containing binary, ternary, and quaternary blends of Portland cement, fly ash (FA), ground granulated blast furnace slag (GGBFS), silica fume (SF), and metakaolin (MK). Therefore, a total of 65 self-compacting concrete (SCC) mixtures were prepared at two different water to binder ratios. The result showed that drying shrinkage decrease with the use of FA, GGBFS, and MK while incorporation of SF increased the drying shrinkage.as show with figures: 2.16-2.21
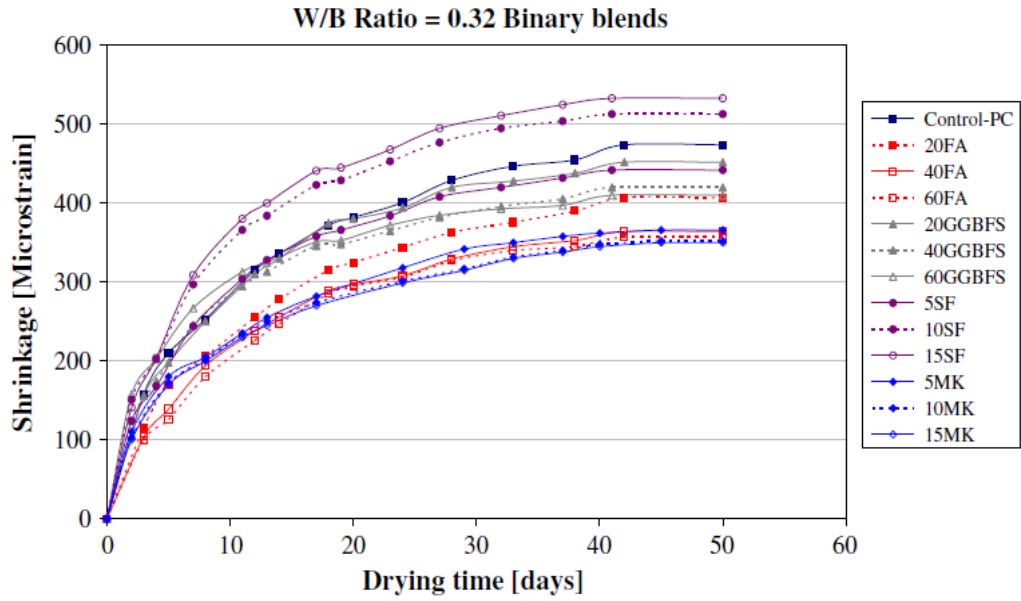
Figure 2.16 Binary effect of mineral admixtures on the free shrinkage of SCCs at w/b ratio of 0.32 (Guneyisi et al., 2010)
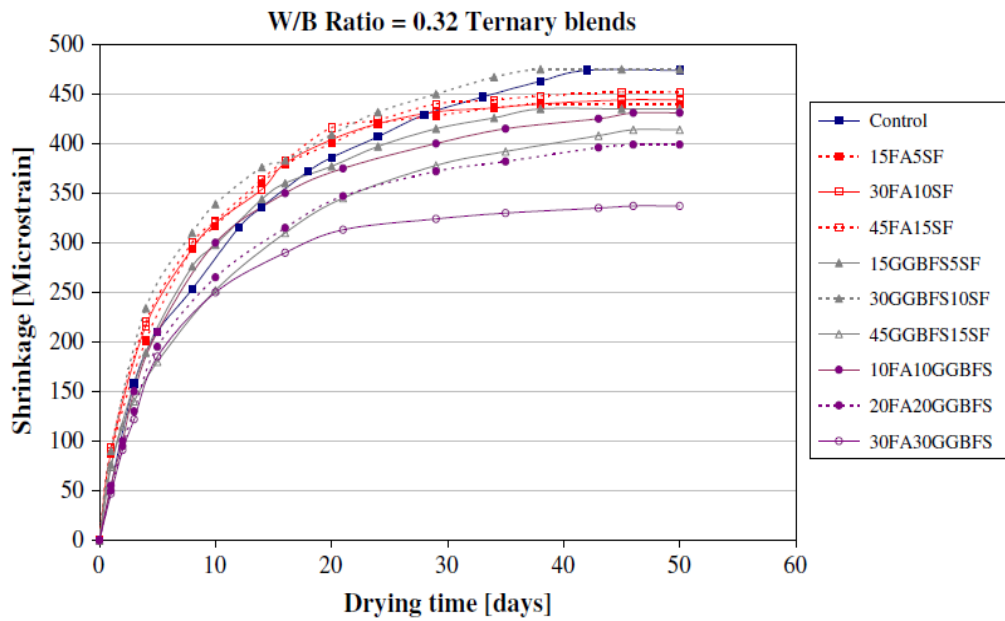
Figure 2.17 Ternary effects of mineral admixtures (PC + FA + SF; PC + GGBFS + SF; PC + FA + GGBFS) on the free shrinkage of SCCs at w/b ratio of 0.32. (Guneyisi et al., 2010)
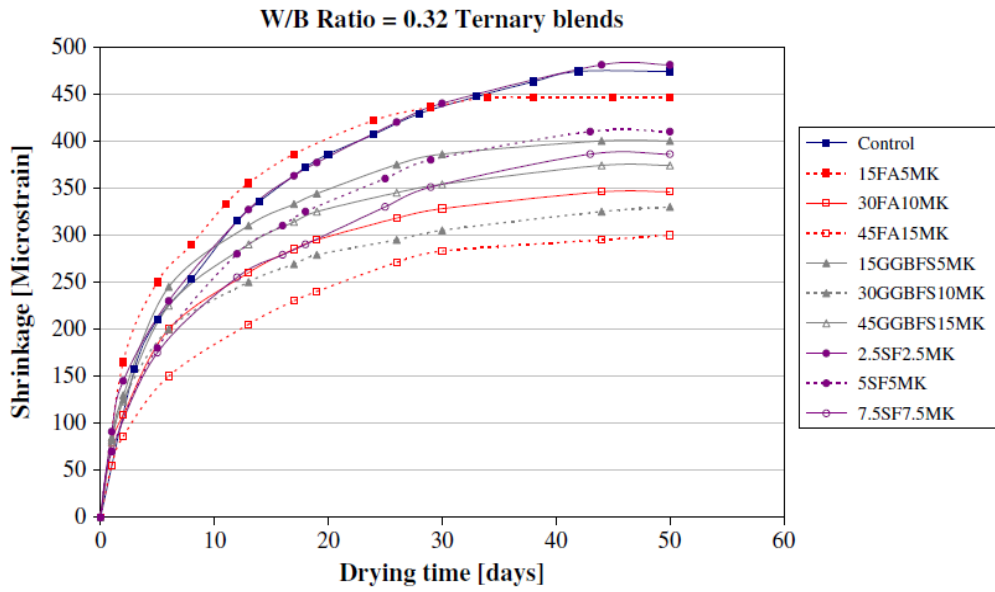
Figure 2.18 Ternary effects of mineral admixtures (PC + FA + MK; PC + GGBFS + MK; PC + SF + MK) on the free shrinkage of SCCs at w/b ratio of 0.32. (Guneyisi et al., 2010)
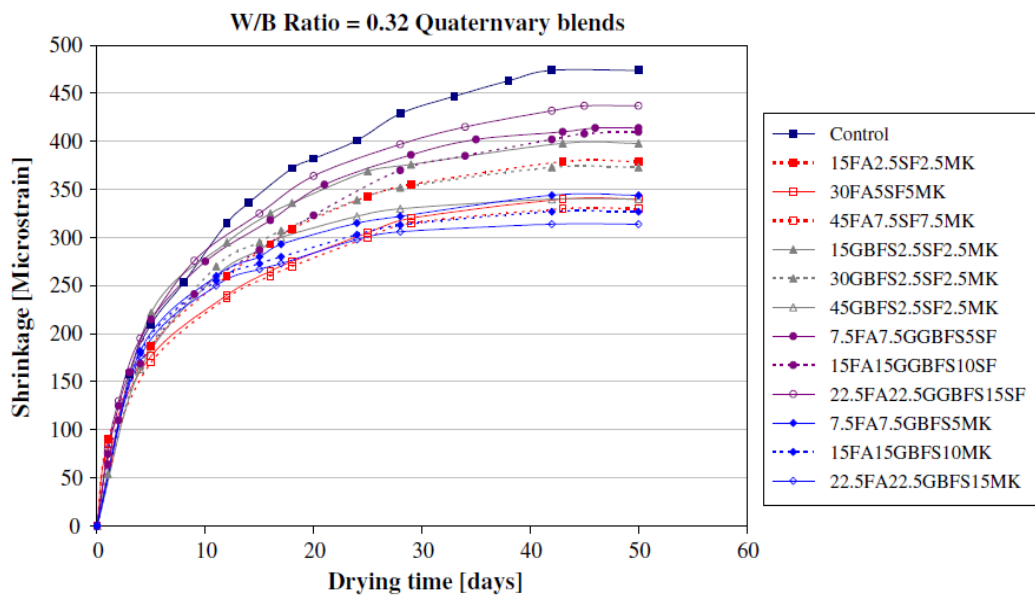
Figure 2.19 Quaternary effects of mineral admixtures on the free shrinkage of SCCs at w/b ratio of 0.32. (Guneyisi et al., 2010)
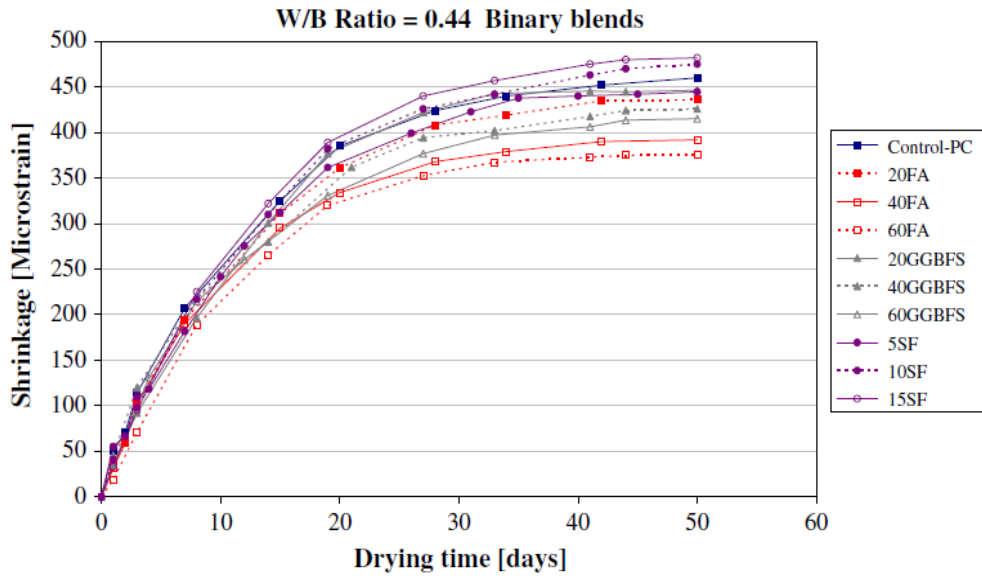
Figure 2.20 Binary effects of mineral admixtures on the free shrinkage of SCCs at w/b ratio of 0.44. (Guneyisi et al., 2010)
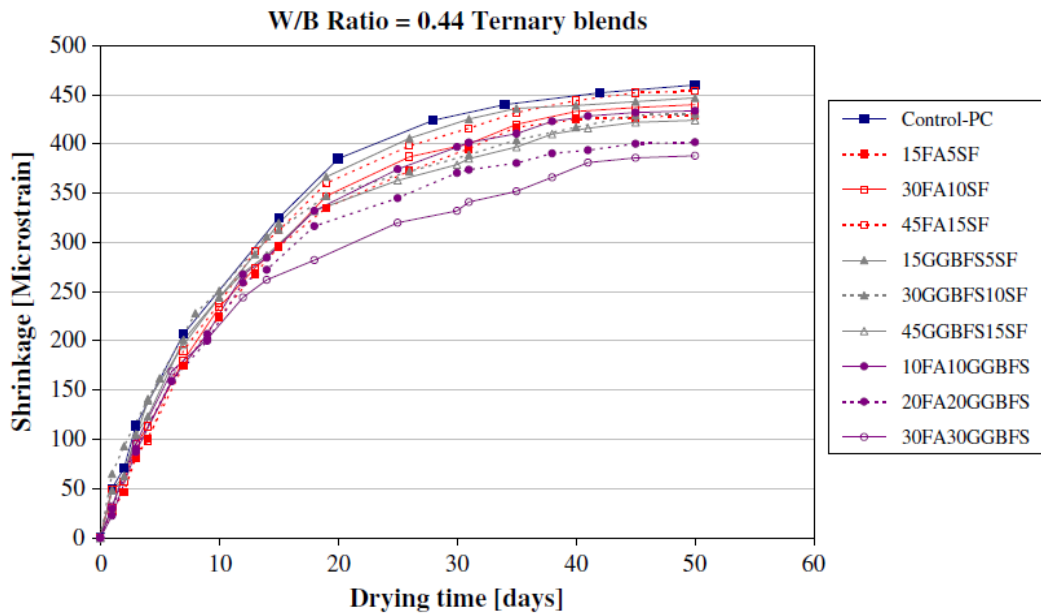
Figure 2.21 Ternary effects of mineral admixtures on the free shrinkage of SCCs at w/b ratio of 0.44. Guneyisi et al., 2010)

In the study Wang et al. (2011), discussed the behavior drying shrinkage of mortar mixtures made with various ternary blends, while considering ternary blends consisting of different combinations of Portland or blended cement, slag, fly ash and silica fume. Free shrinkage of the bars was assessed at 56 days of age after 28 days of drying. A response surface analysis was done to examine the effects of blend proportions on shrinkage behavior of the mortars. The results indicated that among the three supplementary cementitious materials in the ternary blends studied, slag showed a dominant effect on increasing mortar shrinkage. Contribution of class C fly ash to the shrinkage was slightly less than that of slag. Increasing silica fume content slightly increased free shrinkage, and similarly an increase in class F fly ash content slightly increased free shrinkage. There was a close correlation between the measured shrinkage strain and the strain predicted from the shrinkage model developed from the response surface analysis.

Wongkeo et al. (2011) investigated the use of fly ash and silica fume as a cement replacement in binary and ternary blended cements on compressive strength and physical properties of mortar. The results showed that the compressive strength of binary blended cement mortar with FA tends to decreased with increased FA replacement and showed compressive strength lower than PC control. However, compressive strength of binary blended cement mortar with SF was improved and showed compressive strength higher than that of PC control. On the other hand, the compressive strength of ternary blended cement mortar was higher than binary blended cement at the same level replacement and it increased with increased SF replacement.

According to Farzadnia et al. (2011) reviewed the incorporation of mineral admixtures in binary, ternary and quaternary blended mortars in concrete, each mineral such as silica fume, fly ash, rice husk ash, metakaolin, blast furnace slag, palm oil fuel ash, etc. could be improve the performance of concrete. While each mineral has one or two useful characteristics in binder blends, incorporations of two or three supplementary cementitious materials had been explored by different experts, and different properties such as early age or late hardening, compressive strength, tensile strength, dry shrinkage, creep, etc.

Guneyisi et al. (2012) investigated the effectiveness of metakaolin (MK) and silica fume (SF) on the mechanical properties, shrinkage, and permeability related to durability of high performance concretes. Shrinkage behavior of the concretes with and without mineral admixtures were dealt through measurements of free shrinkage strains and weight loss of the specimens due to drying. Moreover, crack formation and propagation of the restrained specimens were observed to better understanding the effect of MK or SF incorporation on the restrained shrinkage properties. The results revealed that replacement level of MK and SF had significant effects on the mechanical and especially durability characteristics of high performance concretes. The Effect mineral admixtures on the compressive strength and are presented in Figs 2.22 - 2.23.
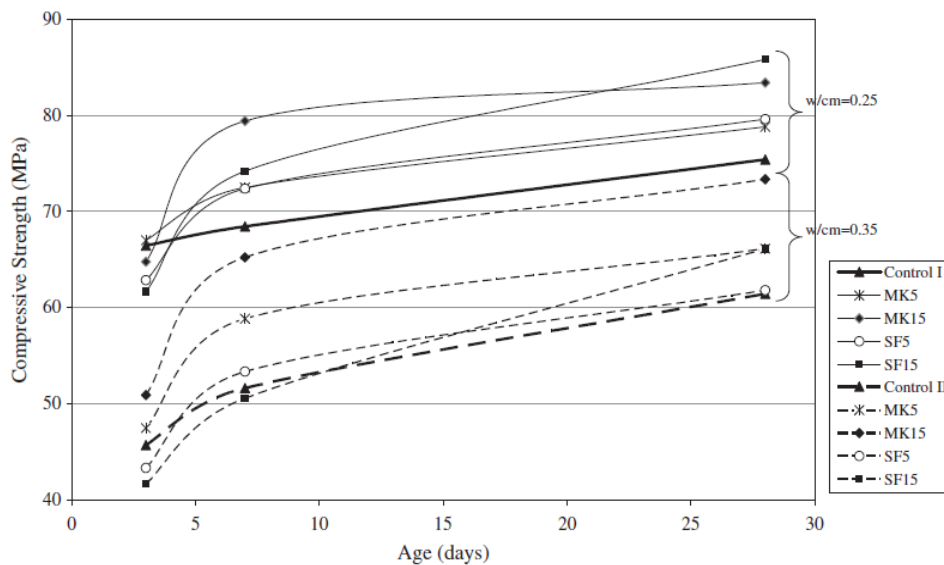
Figure 2.22 Effect of silica fume and metakaolin on compressive strength development of concretes (Guneyisi et al., 2012)
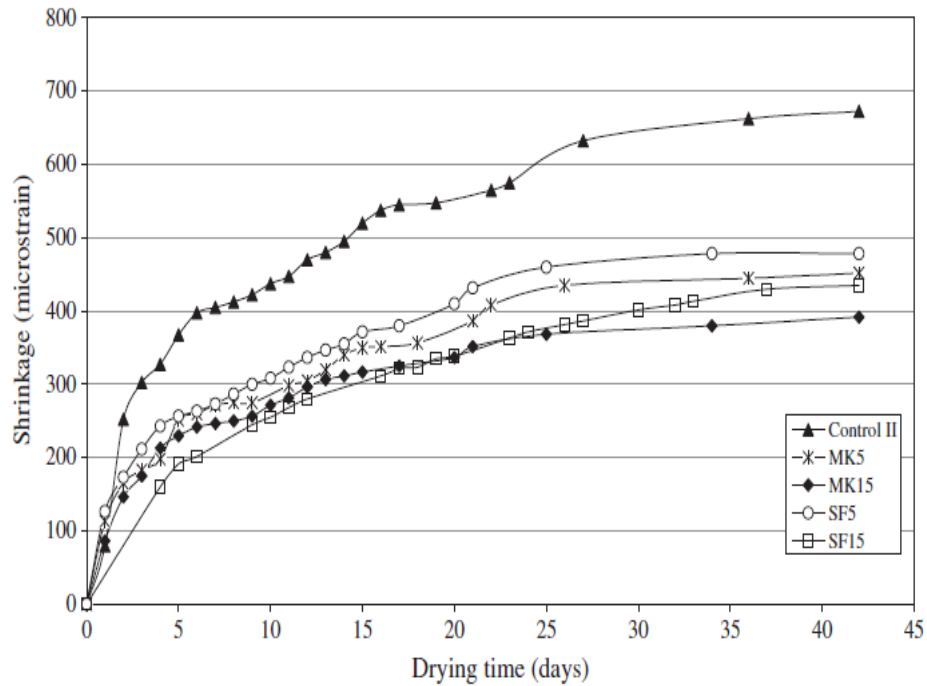
Figure 2.23 Effect of silica fume and metakaolin on drying shrinkage of concretes having a w/cm ratio of 0.35. (Guneyisi et al., 2012)

Mala et al. (2013) proposed a new approach to find the efficiency factor of SF and FA individually in ternary blend cement system, based on principle of modified Bolomey's equation for predicting compressive strength of concrete using binary blend cement system. The results indicated that, as the total replacement level of OPC in concrete using ternary blend of OPC + FA + SF increased, the strength with respect to control mix increased up to certain replacement level and thereafter decreased. If the cement content of control mixes at each w/b ratio kept constant, then as w/b ratio decreased, higher percentage of OPC could be replaced with FA + SF to get 28 days strength comparable to the control mix. Efficiency factor for SF and FA were always higher in ternary blend cement system than their respective binary blend cement system. Split tensile strength of concrete using binary and ternary cement system were higher than OPC for a given compressive strength level. The Effect mineral admixtures on the compressive strength and are presented in Figs. 2.24 - 2.26
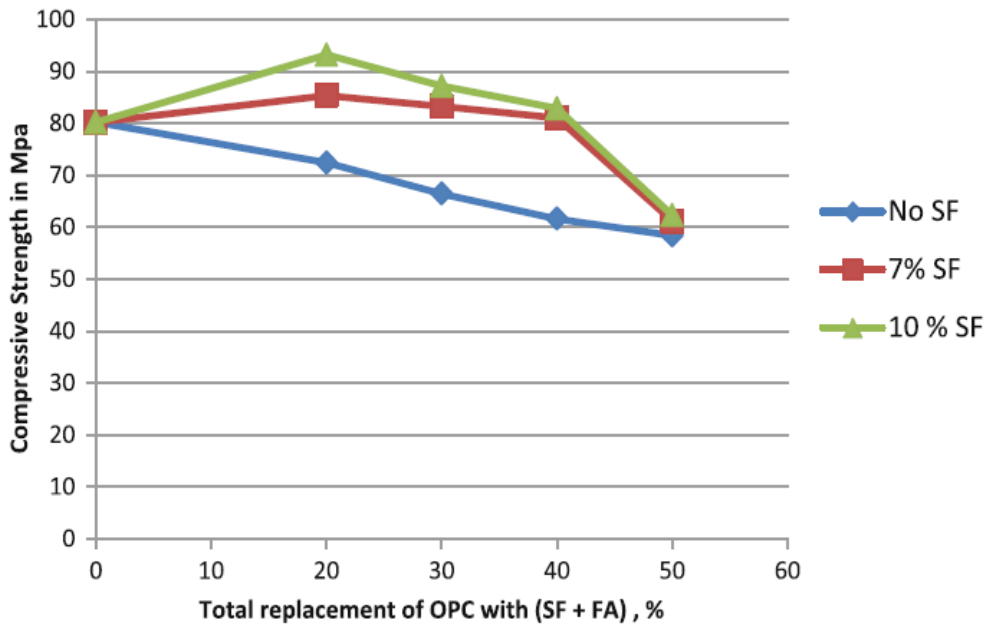
Figure 2.24 (28) days compressive strength of binary and ternary mixes at w/b = 0.3.
(Mala et al., 2013)
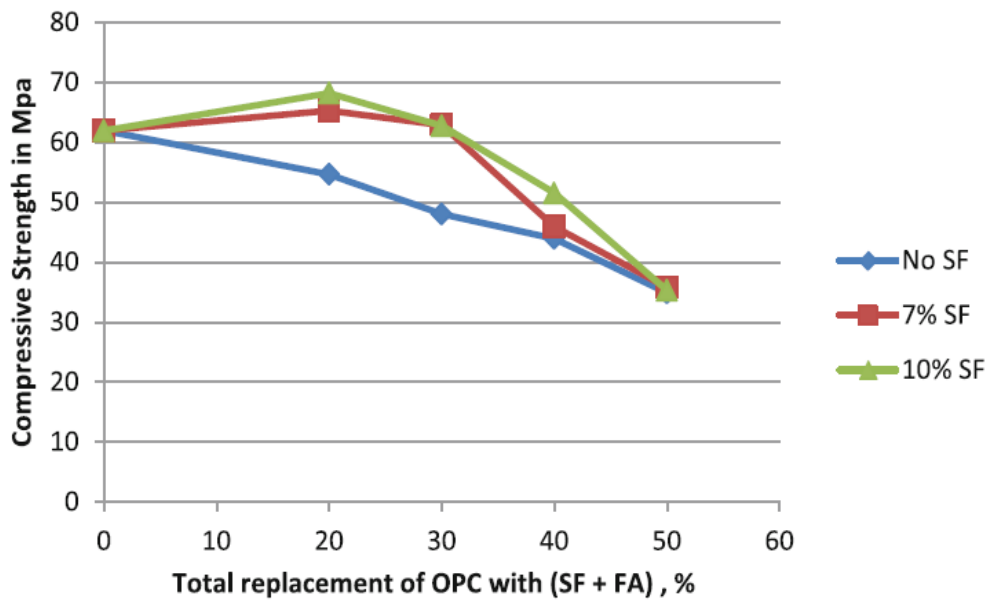
Figure 2.25 (28) days compressive strength of binary and ternary mixes at w/b = 0.4.
. (Mala et al., 2013)
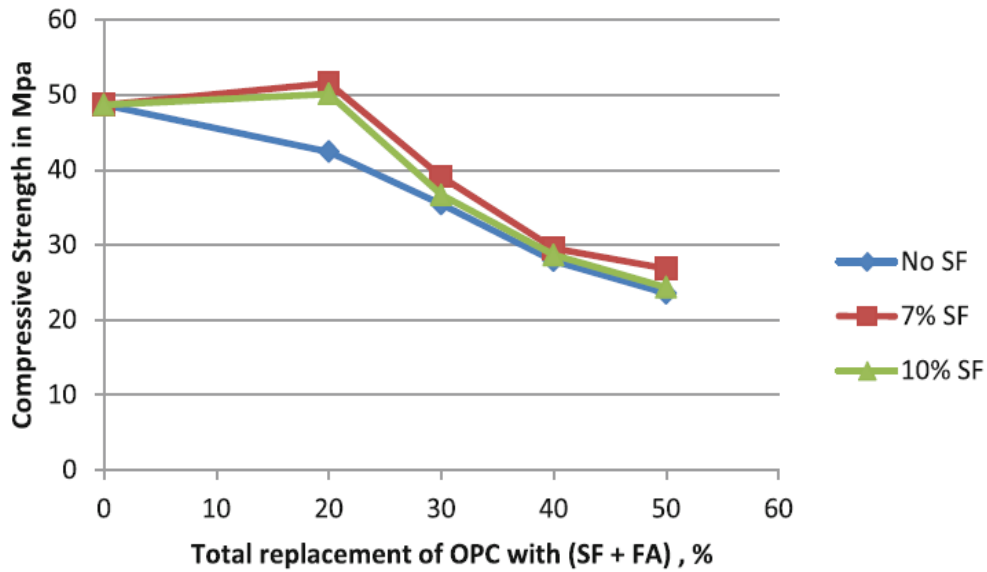
Figure 2.26 (28) days compressive strength of binary and ternary mixes at w/b = 0.45. (Mala et al., 2013)

Meddah et al. (2014) studied on Possibility use of binary and composite limestone cements in concrete production, performance properties of 50 concrete mixes designed with binary, ternary and quaternary cementitious systems, including the use of various proportions of slag (S), fly ash (FA), limestone (LS), silica fume (SF) and metakaolin (MK) as a partial replacement by weight of PC. It has been observed that the use of composite cements improves concrete workability and reduces the amount of superplasticizer required to reach the same slump value compared with LS and PC cements. The strength results indicate that LS could lead to significant strength loss compared with PC and composite cement concretes. The results showed that the mechanical and durability performance of both binary and composite cement concretes are strongly linked to the chemical composition, fineness, particle size distribution and potential reactivity of the cementing materials used.
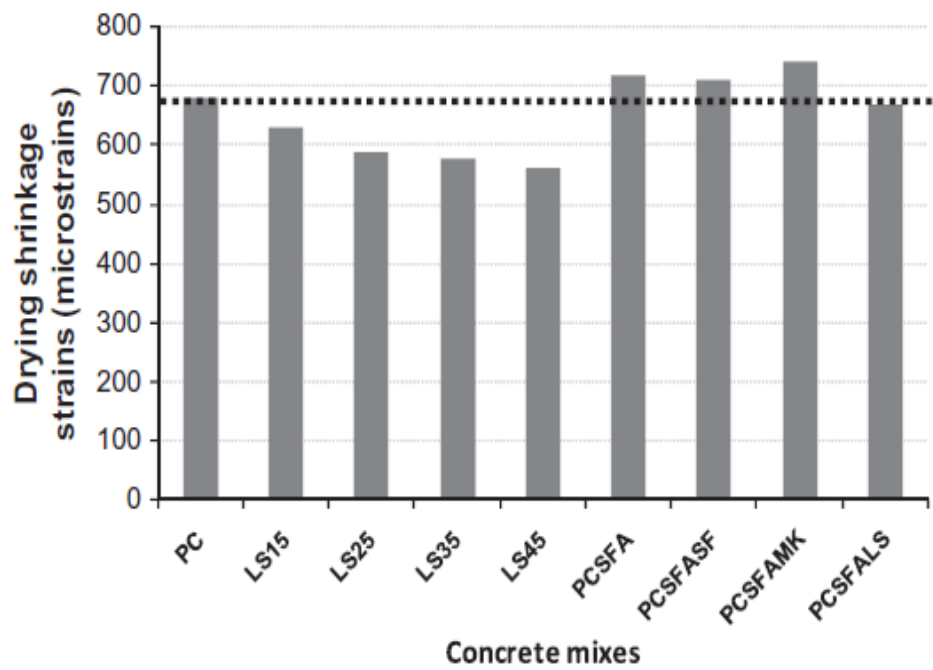
Figure 2.27 Drying shrinkage of Portland and blended cement concretes investigated. (Meddah et al., 2014)

CHAPTER 3

ANALYTICAL MODELS

3. Introduction

Analytical models are constructed and used by capacity planners to predict computing resource requirements related to workload behavior, content, and volume changes, and to measure effects of hardware and software changes. Developing the analytical model provides the capacity planner with an opportunity to study and understand the various behavior patterns of work and hardware that currently exist. Certain factors must be taken into consideration to avoid common errors in model construction, analysis, and predictions.

In most instances, the capacity planner constructs the model using activity measurement information generated and collected during one or more time intervals. It is critical that an interval or series of intervals be used that contain significant volumes of business-critical activity. Units of work are then characterized by type and grouped into workloads. The capacity analyst can then translate future business requirements into measurable units of computing resource consumption, and calculate capacity and performance projections for workloads

3.1 Models based on soft-computing techniques

3.1.1 Generality

(Zadeh, 1994) defines soft computing as a collection of methodologies that aim to exploit the tolerance for imprecision and uncertainty to achieve tractability, robustness, and low solution cost. Its main components are fuzzy logic, neurocomputing, and probabilistic reasoning. Soft computing is likely to play an important role in wide variety of fields of application. The key model for soft computing is the human mind. The fuzzy logic, genetic algorithm, genetic

programming, and neural network can be accepted as the main techniques of soft computing. In the following neural network and genetic programming methods were alternatively used to derive two different prediction formulation of available rotation capacity of cold-formed RHS-SHS steel beams.

3.1.2 Gene expression programming (GEP)

Genetic programming (GP), proposed by (Koza, 1992) is essentially an application of genetic algorithms to computer programs. GP has been applied successfully to solve discrete, non-differentiable, combinatory, and general nonlinear engineering optimization problems (Goldberg, 1989). It is an evolutionary algorithm based the methodology inspired by biological evolution to find computer that performs a task defined by a user. Therefore, it is a machine learning technique used to construct a population of computer programs according to a fitness landscape determined by a program's ability to perform a given computational task. Similar to genetic algorithm (GA), the GP needs only the problem to be defined. Then, the program searches for a solution in a problem-independent manner (Koza, 1992).

Ferreira (2001) introduced Gene expression programming (GEP) and it can be considered as a natural development of genetic algorithms and genetic programming. GEP evolves computer programs of different sizes and shapes encoded in linear chromosomes of fixed-length. GEP algorithm begins with the random generation of the fixed-length chromosomes of each individual for the initial population. Then, the chromosomes are expressed and the fitness of each individual is evaluated based on the quality of the solution it represents.

The GEP may not take all of the input parameters for constructing the model. Because of the computational iterations, if a parameter has a negligible effect, it will not be included in the model derived.

To clarify the GEP basis it is convenient to draft the fundamentals of GP. The GP reproduces computer programs to solve problems by executing the following steps [8] (as described in Fig. 3.2):

(1) Generate an initial population of random compositions of the functions and terminals of the problem (computer programs).

(2) Execute each program in the population and assign it a fitness value according to how well it solves the problem.

(3) Create a new population of computer programs:

(i) Copy the best existing programs,

(ii) Create new computer programs by mutation,

(iii) Create new computer programs by crossover.

Differently from GP, the significant improvement of GEP is that it makes it possible to infer exactly the phenotype given the sequence of a gene, and vice versa, which is termed as Karva language. For example, a diagram can represent the following algebraic expression (Eq. 3.1), which is the expression tree as follows (Figure 3.1).

$$Y = \sqrt{\sqrt{\frac{d_3}{\sin d_2 + c_1 - \ln c_1}} \times d_1} \qquad (3.1)$$

Sub-ET 1
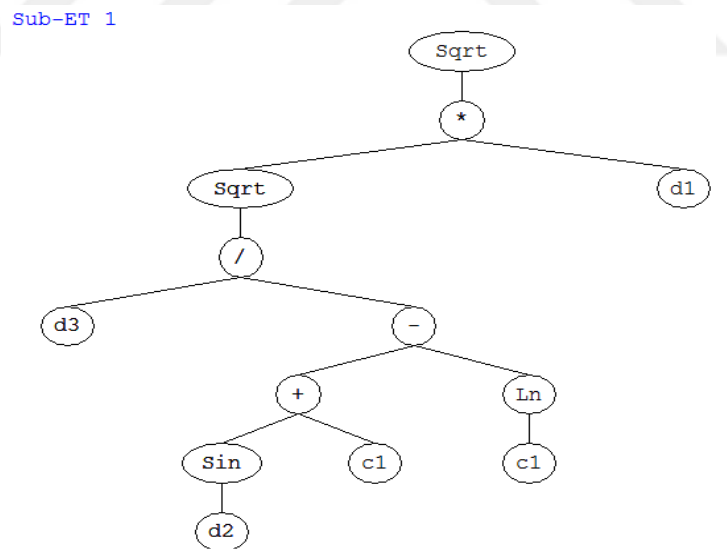
Figure 3.1 A sample sub-expression tree for a mathematical operation (Mermerdaş, 2013).

45

```
                    ┌──────────┐
                    │  Gen=0   │
                    └──────────┘
                         │
                         ▼
              ┌──────────────────────┐
              │  Create initial random│
              │      population       │
              └──────────────────────┘
                         │
                         ▼
         ┌──────────────────────┐  YES  ┌──────────────┐
    ┌───▶│  Termination criteron├──────▶│ Designate the│
    │    │      satisfied       │       │    result    │
    │    └──────────────────────┘       └──────────────┘
    │              │ NO                        │
    │              ▼                           ▼
    │    ┌──────────────────────┐        ┌──────────┐
    │    │ Evaluate fitness of each│      │   End    │
    │    │   individial in the   │       └──────────┘
    │    │      population       │
    │    └──────────────────────┘
    │              │
    │              ▼
    │    ┌──────────────────────┐
    │    │    Individiuals=0     │
    │    └──────────────────────┘
    │              │
    │              ▼
    │  ┌─────────┐ YES ┌──────────────────┐
    └──│Gen=Gen+1│◀────│  Individiuals=M? │◀──────────────────┐
       └─────────┘     └──────────────────┘                   │
                              │ NO                             │
                              ▼                                │
      Mutation   ┌──────────────────────┐  Reproduction       │
    ┌────────────│ Select genetic operation│──────────┐       │
    │            │    probabilistically  │            │       │
    │            └──────────────────────┘            │       │
    │                     │ Crossover                 │       │
    ▼                     ▼                           ▼       │
┌──────────────┐  ┌──────────────┐      ┌──────────────┐     │
│Select one    │  │Select two    │      │Select one    │     │
│individual    │  │individuals   │      │individual    │     │
│based on fitness│ │based on fitness│    │based on fitness│   │
└──────────────┘  └──────────────┘      └──────────────┘     │
    │                     │                     │             │
    ▼                     ▼                     ▼             │
┌──────────────┐  ┌──────────────┐      ┌──────────────┐     │
│Perform mutation│ │Perform crossover│   │Perform reproduction│ │
└──────────────┘  └──────────────┘      └──────────────┘     │
    │                     │                     │             │
    ▼                     ▼                     ▼             │
┌──────────────┐  ┌──────────────┐      ┌──────────────┐     │
│Insert mutant │  │Insert two offspring│ │Copy into new │     │
│into new      │  │into new population│  │population    │     │
│population    │  └──────────────┘      └──────────────┘     │
└──────────────┘          │                     │             │
    │                     ▼                     ▼             │
    ▼            ┌──────────────┐      ┌──────────────┐       │
┌──────────────┐ │Individuals=  │     │Individuals=  │       │
│Individuals=  │ │Individual+2  │     │Individual+1  │       │
│Individual+1  │ └──────────────┘     └──────────────┘       │
└──────────────┘        │                     │              │
    │                   │                     └──────────────┘
    └───────────────────┴────────────────────────────────────
```

Figure 3.2 Flowchart for the genetic programming paradigm (Zhao and Hancock, 2001)

3.1.3 Neural networks (NN)

An artificial neural network (NN) is an information-processing paradigm that is inspired by the way biological nervous systems, such as the brain, process information. The key element of this paradigm is the novel structure of the information processing system. It is composed of a large number of highly interconnected processing elements (neurons) working in unison to solve specific

problems. NNs, like people, learn by example. An NN is conf igured for a specific application, such as pattern recognition or data classification, through a learning process. Learning in biological systems involves adjustments to the synaptic connections that exist between the neurons.

The training of NNs by back propagation have three stages (Schalkoff, 1997): (i) the feed forward of the input training pattern, (ii) the calculation and back propagation of the associated error, and (iii) the adjustment of the weights. This process can be used with a number of different optimization strategies. The error between the output of the network and the target value is propagated backward during the backward pass and used to update the weights of the previous layers as shown in Fig.3.3
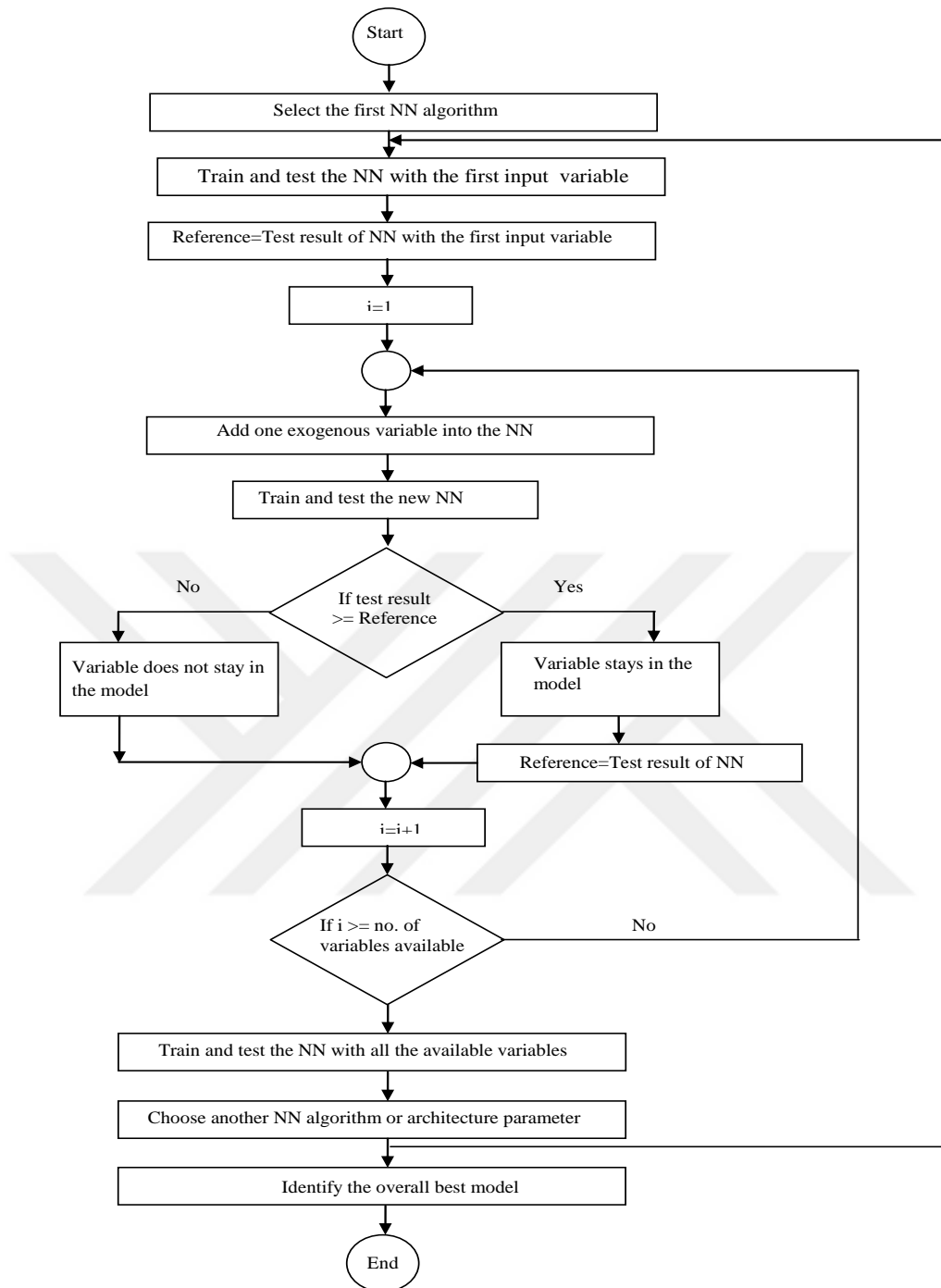
Figure 3.3. Forward strategy for selecting NN architecture and model (Susac, et al., 2005)

In this study, neural network fitting tool (nftool) provided as a soft-computing tool in MatlabV.R2012a was utilized to perform neural network modeling. In fitting problems, a neural network may be used to map between a data set of numeric

inputs and a set of numeric targets. The nftool helps create and train a network, and evaluate its performance using mean square error and regression analysis.

A two-layer feed-forward network with sigmoid hidden neurons and linear output neurons can fit multi-dimensional mapping problems arbitrarily well, given consistent data and enough neurons in its hidden layer. The network was trained with Levenberg-Marquardt back propagation algorithm.

An artificial neuron consists of three main components namely weights, bias, and an activation function. Each neuron receives inputs $I_1, I_2, \ldots, I_n$ attached with a weight w_i which shows the connection strength for that input for each connection. Each input is then multiplied by the corresponding weight of the neuron connection. A bias can be defined as a type of connection weight with a constant nonzero value added to the summation of weighted inputs, as given in Eq. 3.2. Generalized algebraic matrix operation was also given in Eq. 3.3. To clarify the mathematical operations in an artificial neuron.

$$U_k = Bias_k + \sum_{j=1}^{n} w_{k,j} \times I_j$$

(3.2)

$$U_k = \begin{bmatrix} w_{11} & w_{12} & . & . & . & w_{1n} \\ w_{21} & . & & & & . \\ . & & & & & \\ . & & . & & & . \\ . & & & . & & . \\ . & & & . & & . \\ w_{m1} & . & . & . & . & w_{mn} \end{bmatrix}_{m \times n} \begin{bmatrix} I_1 \\ I_2 \\ . \\ . \\ . \\ . \\ I_n \end{bmatrix}_{n \times 1} + \begin{bmatrix} Bias_1 \\ Bias_2 \\ . \\ . \\ . \\ . \\ Bias_m \end{bmatrix}_{m \times 1} = \begin{bmatrix} U_1 \\ U_2 \\ . \\ . \\ . \\ . \\ U_m \end{bmatrix}_{m \times 1}$$

(3.3)

Since nftool uses the normalized values in the range of [-1, 1], the input parameters were normalized by means of Eq. 3.4 in order to get the prediction results after execution of the training process of the NN. Moreover, the obtained results are also in the normalized form. Therefore, considering the Eq. 3.4 and the normalization coefficients a and b for outputs, de-normalization process is applied and the results are monitored.

$$\beta_{normalized} = a\beta + b$$

(3.4)

Where β is the actual input parameter or output values given in Table 2 and Table 6, respectively. $\beta_{normalized}$ is the normalized value of input parameters or outputs ranging between [-1, 1]. *a* and *b* are normalization coefficients given in the following equations (Eqs. 3.5-3.6).

$$a = \frac{2}{\beta_{max} - \beta_{min}}$$
(3.5)

$$b = -\frac{\beta_{max} + \beta_{min}}{\beta_{max} - \beta_{min}}$$
(3.6)

Where β_{max} and β_{min} are the maximum and minimum actual values of either inputs or outputs.

3.2 Description of the database used for derivation of the models

The proposed formulations of *S* for Shrinkage were derived using a set of 586 experimental data available in the technical literature [Zhang et al. (2003), Wongkeo et al. (2012), Yoo et al. (2012), Khatib et al. (2008) and (Khatri and Sirivivatnanon, 1995)] for training and testing the proposed models.

Table 3.1 summarizes the selected experimental data. In detail, the generated models for shrinkage following input parameters: *w/b* (water/binder), *SF* (silica fume) content in kg/m^3, *FA* (fly ash) content in kg/m^3, *C* (cement) content in kg/m^3, aggregate/binder ratio, f_c (compressive strength) in MPa, *type of shrinkage* for drying shrinkage 1, for Autogenous shrinkage 0, and *dry time* in days.

All data samples were put in an order to establish a consistent sequence of the inputs to be used for derivation of the models as shown in table 1,2,3,4 and 5 Appendix A. Thus, generally, eight inputs parameters were utilized for development of prediction models. The data set was randomly divided into two parts to obtain training and testing databases.

The GeneXproTools.4.0 and MatlabV.R2012a software's were used for derivation of the GEP and NN based mathematical models, respectively.

For clarity, sake, in the next Sections, where it is discussed the comparison between the experimental and predicted rotation capacity, the effectiveness of the correlation is evaluated by means of the correlation coefficient "R" (Eq. 3.7), which describes the fit of the models' output variable approximation curve to the actual test data output variable curve. Higher r coefficients indicate a model with better output approximation capability.

$$R = \frac{\sum (m_i - m')(p_i - p')}{\sqrt{(m_i - m')^2 (p_i - p')^2}}$$

(3.7)

where m' and p' are mean values of measured (m_i) and predicted (p_i) values, respectively

Table 3.1 Summary of experimental database

data source (586)	Input								Output
	X1	X2	X3	X4	X5	X6	X7	X8	Y
	w/b	SF	FA	cement	Agg/b.	f_c Mpc @28 days	Type Shrinkage	Dry Time	Shrinkage
Zhang et al (2003)	0.27-0.35	0-50	0	446-498	3.38-3.70	57.33-86.94	0-1	1-98	34-282
Wongkeo et al (2012)	0.49	0-42	0-269	269-538	2.64-2.75	29.05-69.05	1	7-91	93-1100
Yoo et al (2012)	0.30	0-88	0-175	408-583	2.68-2.57	54.8-69.8	0	1-49	39-400
Khatib et al (2008)	0.36	0	0-400	100-500	3.25-3.5	11-72.58	1	2-56	5-432
Khatri and Sirivivatnanon (1995)	0.34-0.36	0-46	0-100	282-425	4.15-4.30	65-94.99	1	7-400	267-895

3.3 Proposed Models

3.3.1 Proposed GEP model

The prediction model derived from GEP is presented in Eq. 3.8. The GEP parameters used for derivation of the mathematical models are given in Table 3.2. As it can be seen from Table 3.2, in order to provide an accurate model, various mathematical operations were used.

$$S = S_1 + S_2 + S_3 + S_4 + S_5 + S_6 + S_7 + S_8 + S_9 + S_{10} \tag{3.8}$$

Where $S_1, S_2\ S_3 \ldots\ldots\ldots S_{10}$ are sub expressions

$$S_1 = \cos\left[e^{\sqrt[3]{d_0}}\right] \tag{3.8 a}$$

$$S_2 = -4.88385 \tag{3.8 b}$$

$$S_3 = \cos\left[\sin\left(\tan\left(\ln 1.733399 + 10^{1.733399} - d_6 \times d_5 + 1.733399\right)\right)\right] \tag{3.8 c}$$

$$S_4 = d_0 \left[\frac{\left(\frac{\tan(d_5 \times d_4)}{d_5 + d_6}\right)}{\sqrt{d_0}}\right] \tag{3.8 d}$$

$$S_5 = \sqrt{e^{d_5 - (-3.03775)} \times (d_6) + \ln d_7} \tag{3.8 e}$$

$$S_6 = \left[\tan^{-1}\left(\sqrt[4]{(\cos d_3 \times d_2 + d_5)^3}\right)\right]^3 \tag{3.8 f}$$

$$S_7 = 10^{\left[\sin\left(\tan^{-1}(d_7 - \ln d_7) + d_5\right)\right]} - d_5 \tag{3.8 g}$$

$$S_8 = \sqrt[32]{\tan^{-1} d_2 \times (-5.326263 - d_4) \times d_1 + d_7} \tag{3.8 h}$$

$$S_9 = \cot(-5.326263 + d_4) \tag{3.8 i}$$

$$S_{10} = \sqrt[3]{d_0} \tag{3.8 j}$$

Table 3.2. GEP parameters used for proposed models.

Parameters		S for shrinkage
P1	Function Set	+, -, *, /, √, ^, ln, exp, sin, tan, inverse, Pow
P2	Number of generation	99521
P3	Choromosomes	30
P4	Head size	10
P5	Linking function	Addition
P6	Number of genes	10
P7	Mutation rate	0.044
P8	Inversion rate	0.1
P9	One-point recombination rate	0.3
P10	Two-point recombination rate	0.3
P11	Gene recombination rate	0.1
P12	Gene transposition rate	0.1

The models developed by the software in its native language can be automatically parsed into visually appealing expression trees, permitting a quicker and more complete comprehension of their mathematical/logical intricacies. Figure 3.4 demonstrates the expression tree for the terms used in the formulation of the GEP model.
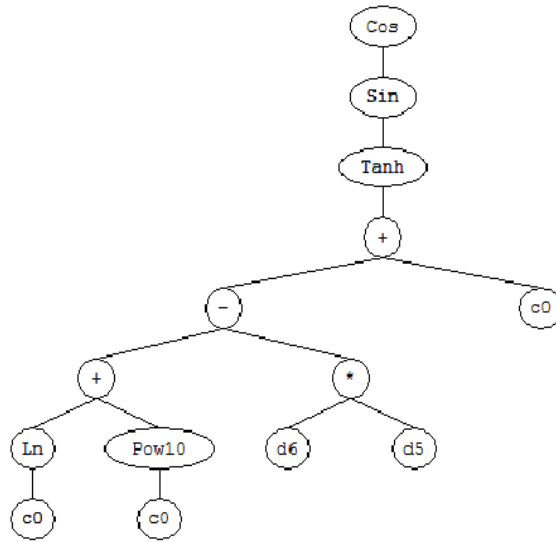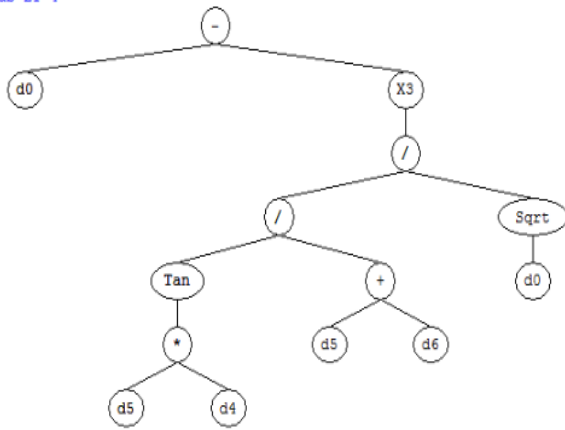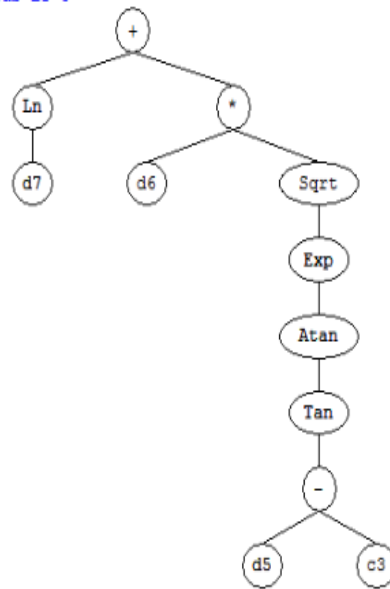
(a)
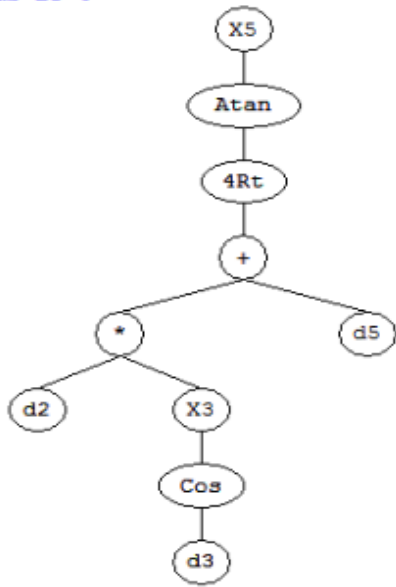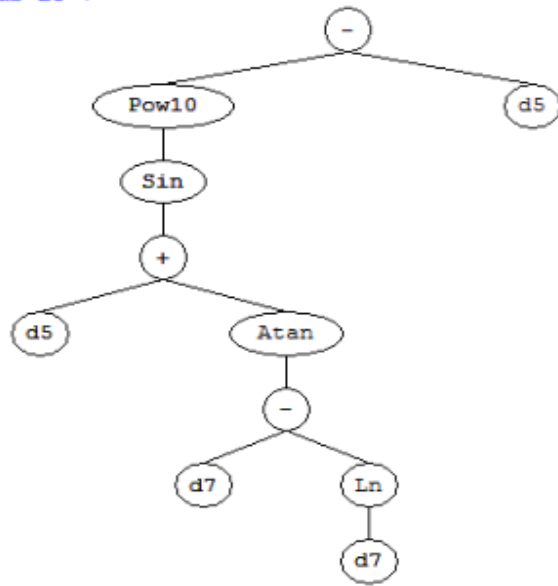
Sub-ET 6
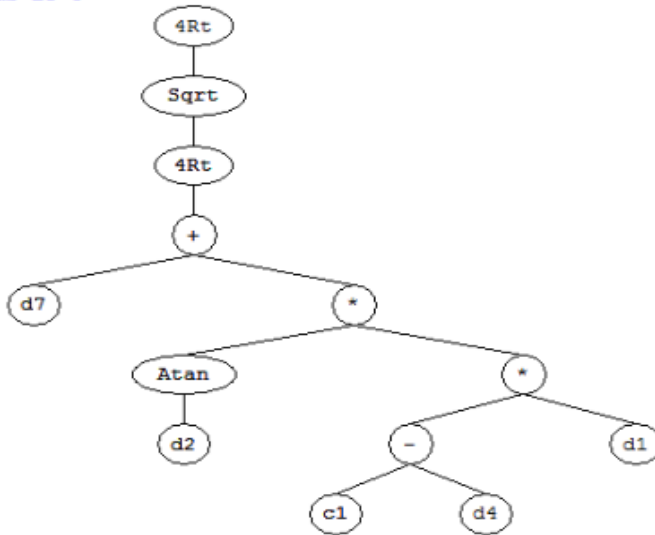
Sub-ET 7

Sub-ET 8

Sub-ET 9
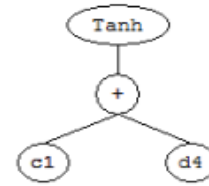
Sub-ET 10

·inkage: Where d0 = w/b
(water/binder); d1 = SF (silica fume); d2 = FA (fly ash); d3= C (cement); d4 =
(aggregate/binder); d5= fc (compressive strength); d6 = (type of shrinkage); d7=
(dry time), c0, c1, c2, c3 are constants/

The performance of the proposed GEP prediction model in Eq. 3.8 is graphically demonstrated in Fig. 3.5 for training and in Fig 3.6 for testing data sets. It seems that there is a far trend in the variation of the data between predicted and experimental

56

data. Correlation coefficients equal to 0.863 and 0.789 were calculated for training and testing databases, respectively, thus indicating not strong correlation between actual and predicted values. Moreover, close values of the correlation coefficients may be considered as an evidence for the consistency and good fitness of the proposed model.
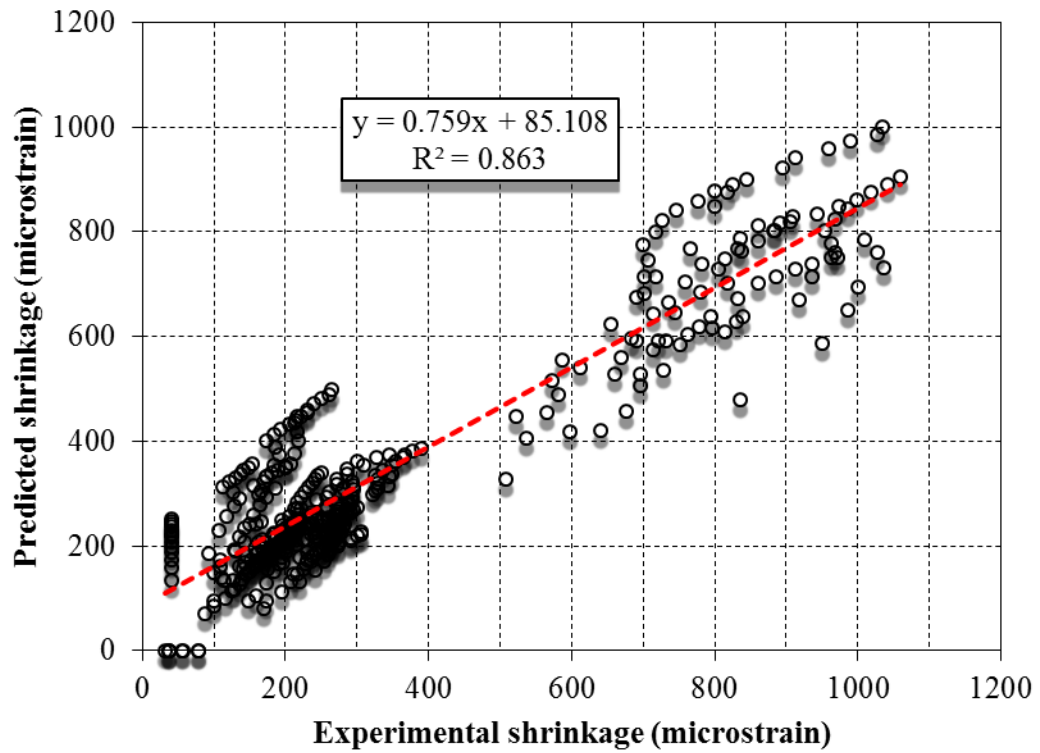
Figure 3.5 Predicted shrinkage values from GEP vs. experimental data for training
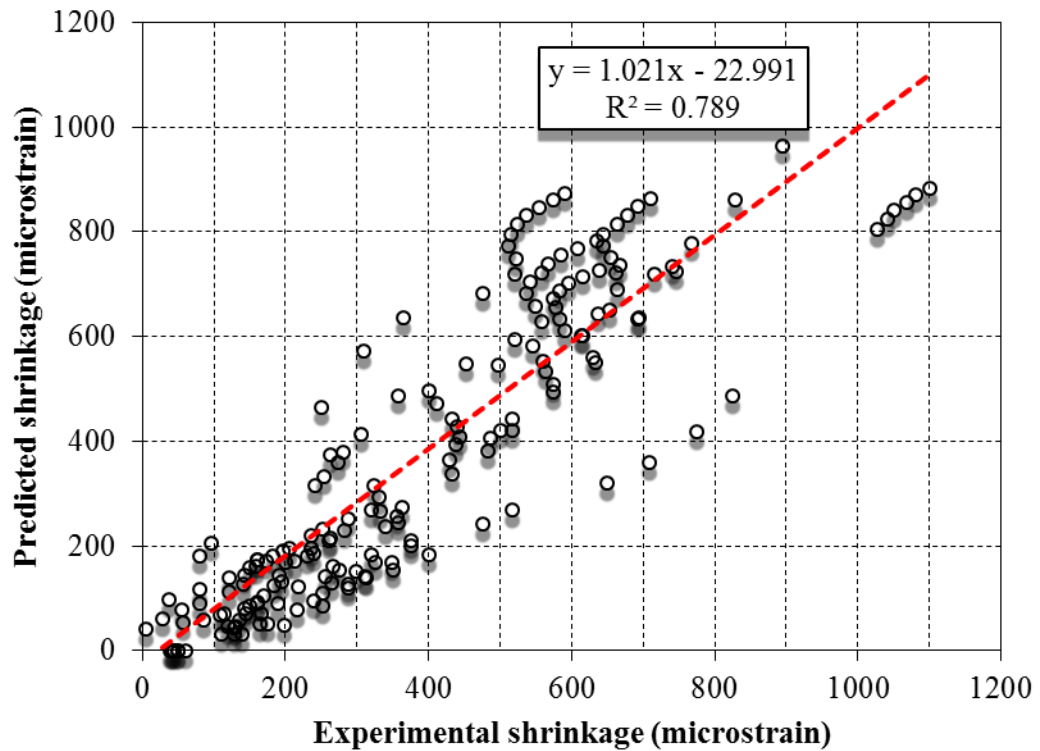
Figure 3.6 Predicted shrinkage values from GEP vs. experimental data for testing

3.3.2 Proposed NN model

A NN architecture, as shown in Fig. 3.7, was adopted to develop the NN model. That means there are eight nodes in the input layer, corresponding to eight factors from I_1 to I_8, 20 nodes in the hidden layer, and one in the output layer corresponding to the shrinkage. It should be noted that all numeric variables were normalized to a range of [-1, 1] before being introduced to the NN. Therefore, one must enter the normalized values in the mathematical operations given for NN model. Normalization of the data is achieved according to the mathematical operations given in Eqs. 3.4-3.6 It should also be noted that the final result obtained from Eq. 3.9 is also in the normalized form, which needs to be de-normalized according to Eq. 3.4 and normalization coefficients given in Table 3.3.
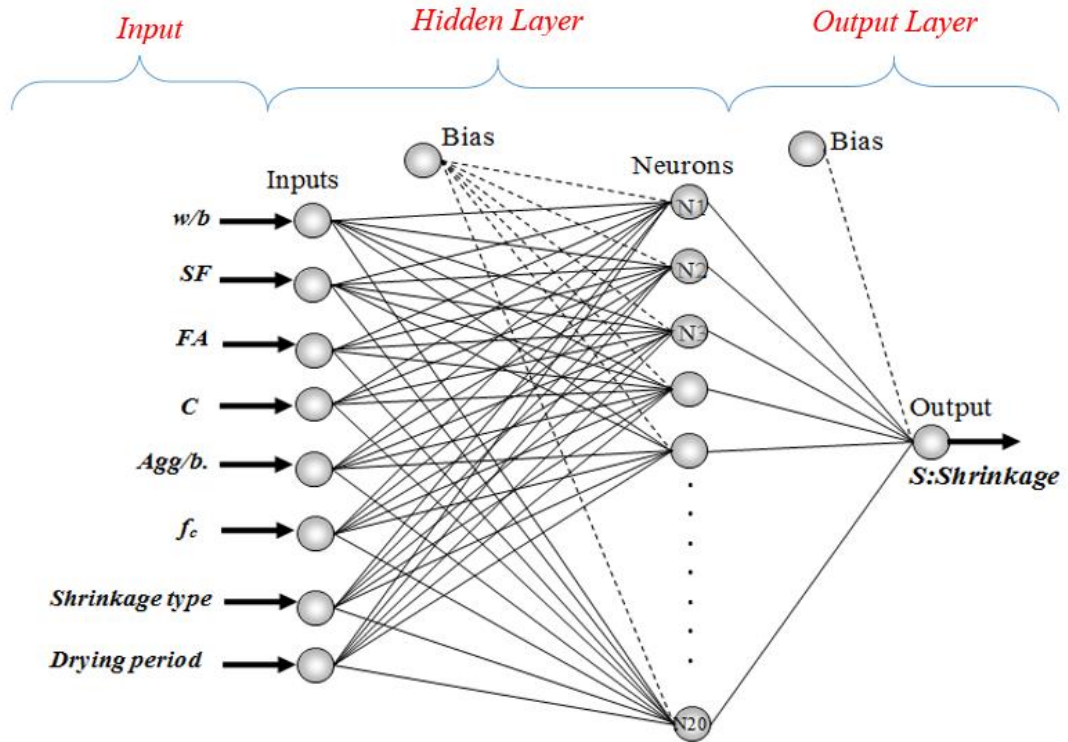
Figure 3.7 Architecture of neural network

$$Shrinkage = Bias_{output\,layer} + \sum_{k=1}^{m} LW_k f(U_k)$$

(3.9)

Where $Bias_{output\,layer} = -1.7249$ and $f(x)$ (Hyperbolic tangent) is the activation function given in Eq. 3.10, LW_k is layer weight matrix U_k numerical value of neurons

Calculation of U is shown in Eq. 3.11 LW_k matrix is also given in Eq 3.12

$$f(x) = \frac{2}{1 - e^{-2x}} - 1$$

(3.10)

$$U = \begin{bmatrix}
0.1908 & -1.803 & 0.0873 & 0.7623 & -0.1331 & -1.4559 & -0.3369 & -1.5765 \\
1.336 & -0.257 & 1.9303 & -0.796 & 0.851 & 2.4924 & 0.016 & -1.2352 \\
0.7413 & 0.3955 & 0.921 & -0.7256 & 0.2407 & 1.2586 & -2.3354 & 0.9309 \\
0.7555 & 0.3286 & -0.2206 & 1.2888 & -0.8885 & 1.0273 & 0.2604 & -2.3917 \\
0.5732 & 0.208 & 1.5959 & 1.44 & 0.1226 & 1.4484 & -0.4694 & -3.2405 \\
-1.2354 & 0.8284 & -0.5011 & -0.2014 & 1.9002 & 0.8489 & -0.9686 & 0.2244 \\
-0.3063 & -1.8275 & 0.2715 & 0.5259 & 1.3442 & -2.2712 & 0.367 & -0.6669 \\
0.1888 & 0.2276 & 0.4856 & 0.737 & 0.3709 & -0.06 & -5.3211 & -8.2235 \\
0.5043 & 0.4569 & 1.1168 & 1.4441 & 0.2978 & 0.3478 & -0.7296 & -2.9012 \\
1.0541 & -0.5796 & 0.5104 & -1.9961 & -0.4117 & 0.7198 & -1.5012 & -0.1507 \\
-1.1694 & -0.1551 & -0.1716 & -0.7359 & 0.232 & -7.6509 & 1.8679 & -0.2992 \\
0.067 & -1.6273 & -2.3283 & 0.6925 & 0.3623 & 1.2884 & 0.1942 & 0.1286 \\
-0.5885 & 1.4898 & 1.2218 & -0.7913 & -1.448 & 0.3074 & -0.3418 & 0.7812 \\
1.4778 & -2.7926 & 0.4601 & 0.4953 & 2.559 & 4.16 & 0.0882 & -0.3506 \\
-0.3467 & -0.2172 & 0.3685 & -1.542 & 1.2205 & 3.8501 & 1.0123 & 1.027 \\
-3.1121 & 1.1517 & -0.8458 & 0.3275 & 0.0566 & -8.3806 & -1.8627 & 0.583 \\
-1.0581 & 1.3466 & 0.2873 & 1.3621 & -3.031 & -2.0197 & -1.9895 & 1.0801 \\
-0.2626 & 0.6351 & 0.6929 & 1.748 & 0.069 & -6.0709 & -1.4018 & -0.2991 \\
0.8306 & -0.506 & -0.4179 & -1.1953 & -0.2531 & 1.1383 & -0.7668 & 0.2324 \\
0.3459 & 1.0081 & -1.0881 & 0.4976 & -1.1249 & -3.0761 & 0.8297 & -2.8866
\end{bmatrix}_{20\times8} \times \begin{bmatrix}
w/b \\
SF \\
FA \\
C \\
Agg/b \\
f_c \\
Shr.type \\
Time
\end{bmatrix}_{8\times1} + \begin{bmatrix}
2.5334 \\
-2.0022 \\
1.4367 \\
-2.16 \\
-3.7156 \\
1.5463 \\
-2.3974 \\
-3.9 \\
-2.4121 \\
1.1096 \\
-1.0209 \\
0.4657 \\
-0.4179 \\
1.161 \\
-0.2536 \\
1.1396 \\
-2.5899 \\
2.2622 \\
2.1491 \\
-4.3735
\end{bmatrix}_{20\times1} = \begin{bmatrix}
U_1 \\
U_2 \\
U_3 \\
U_4 \\
U_5 \\
U_6 \\
U_7 \\
U_8 \\
U_9 \\
U_{10} \\
U_{11} \\
U_{12} \\
U_{13} \\
U_{14} \\
U_{15} \\
U_{16} \\
U_{17} \\
U_{18} \\
U_{19} \\
U_{20}
\end{bmatrix}_{20\times1}$$

(3.11)

$$\text{Layerweights} = \begin{bmatrix} 1.6671 \\ 1.3796 \\ 2.892 \\ -0.65194 \\ -2.5559 \\ 1.0008 \\ 0.57559 \\ -3.9264 \\ 1.3711 \\ -1.5766 \\ -2.5045 \\ -3.1582 \\ -0.93087 \\ 1.2166 \\ 0.93796 \\ -2.2957 \\ 1.7001 \\ 5.1574 \\ -1.7862 \\ -0.55315 \end{bmatrix}_{20\times1} \qquad (3.12)$$

Table 3.3 Normalization coefficients

Normalization parameter	w/b ratio	SF	FA	C	Agg/b	f_c^* (Mpa) @28 days	Type of Shrinkage	Dry time (days)	Shrinkage strain
β_{max}	0.49	88	400	583	4.468	112.80	1	400	1100
β_{min}	0.27	0	0	100	2.57	11	0	1	5.4
a	9.296699	0.022727	0.005	0.004141	1.060519	0.019646	2	0.005012531	0.001827
b	-3.51011	-1	-1	-1.41408	-3.72861	-1.21611	-1	-1.005012531	-1.00987

The obtained results from the NN model are also plotted in Fig. 3.8 yielding 0.993 and 0.954 correlation coefficients for training and testing data sets, respectively, the estimated results have close tendency to the experimental values.
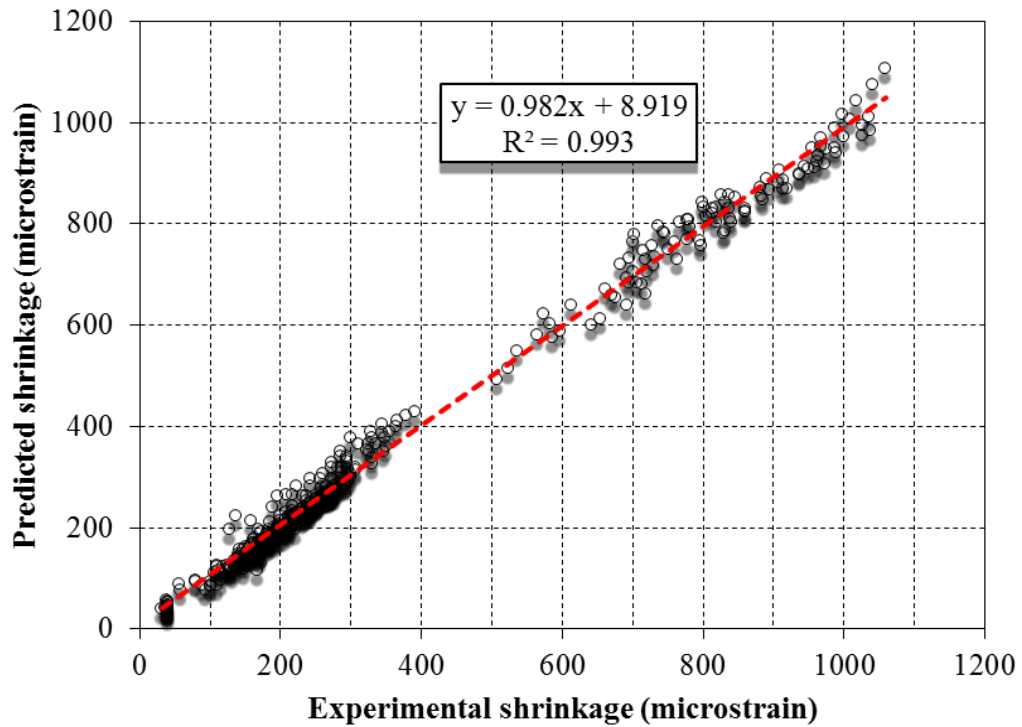
Figure 3.8 Predicted shrinkage values from NN vs. experimental data for training
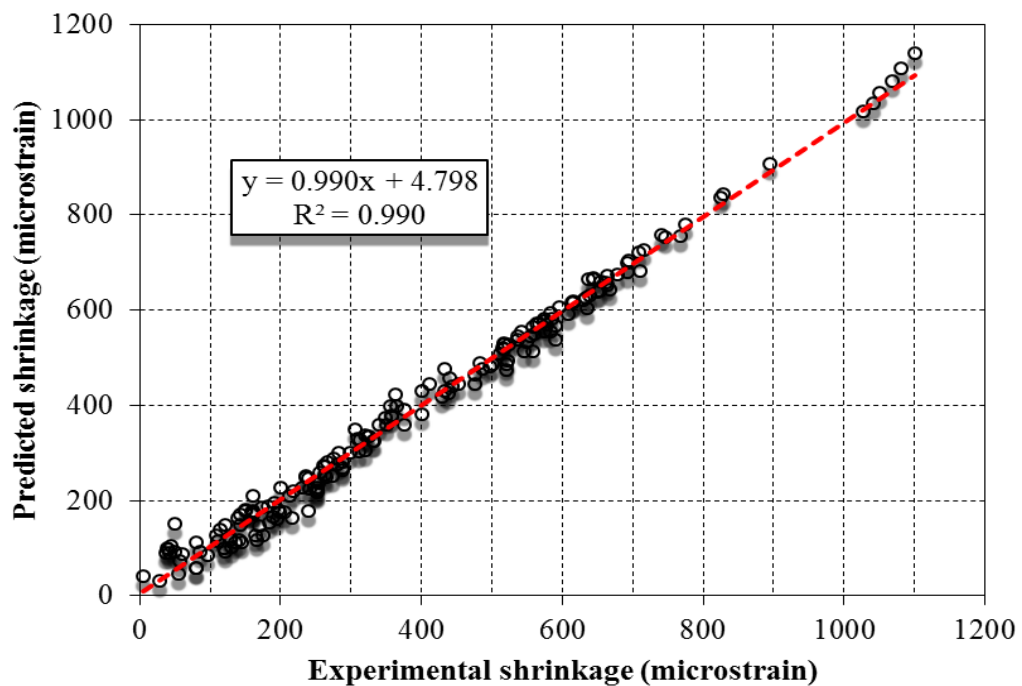
Figure 3.9 Predicted shrinkage values from NN vs. experimental data for testing

3.4 Comparison of the proposed models

In order to compare the prediction of the proposed models with experimental shrinkage, the figures 3.10-3.14 were plotted. Figure 3.10 includes the experimental and predicted autogenous shrinkage values, while the other figures contain drying shrinkage values.

Observing figure 3.10 it can be seen that prediction performance of GEP for autogenous shrinkage values between 0-100 microstrain is totally misleading. The GEP model yielded both invalid (0 microstrain) and extremely overestimated values. However, NN model performed well in this interval. Moreover, for the higher autogenous shrinkage values (**>** 100 microstrain), NN model demonstrated almost prefect estimation performance while GEP model mostly gave underestimated results.
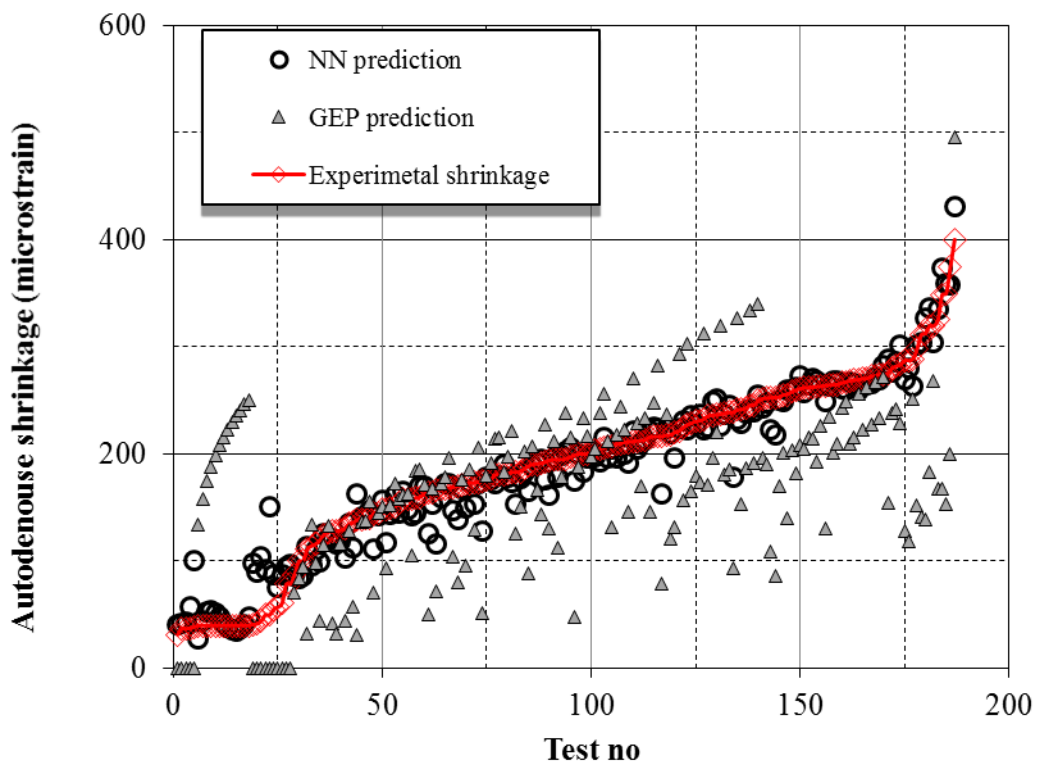
Figure 3.10 Comparison of experimental autogenous shrinkage values with those predicted by NN and GEP

For drying shrinkage values, GEP model had overestimated results between experimental values of 0-300 microstrain. However, as the experimental drying

shrinkage values increased the tendency of GEP estimation decreased. Especially for the drying shrinkage values of 900-1200 microstrain all of the GEP values were below the exprimental findings. On the other hand, NN model achived more prese and accurated prediction performance in all of the intervals.
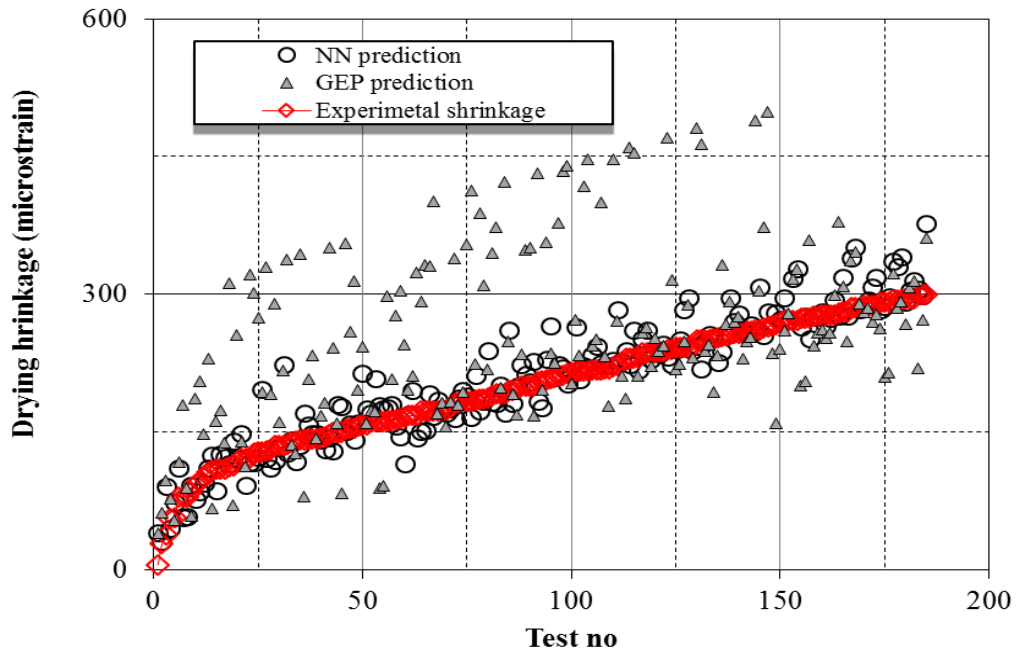
Figure 3.11 Comparison of experimental drying shrinkage values between 0-300 microstrain with those predicted by NN and GEP
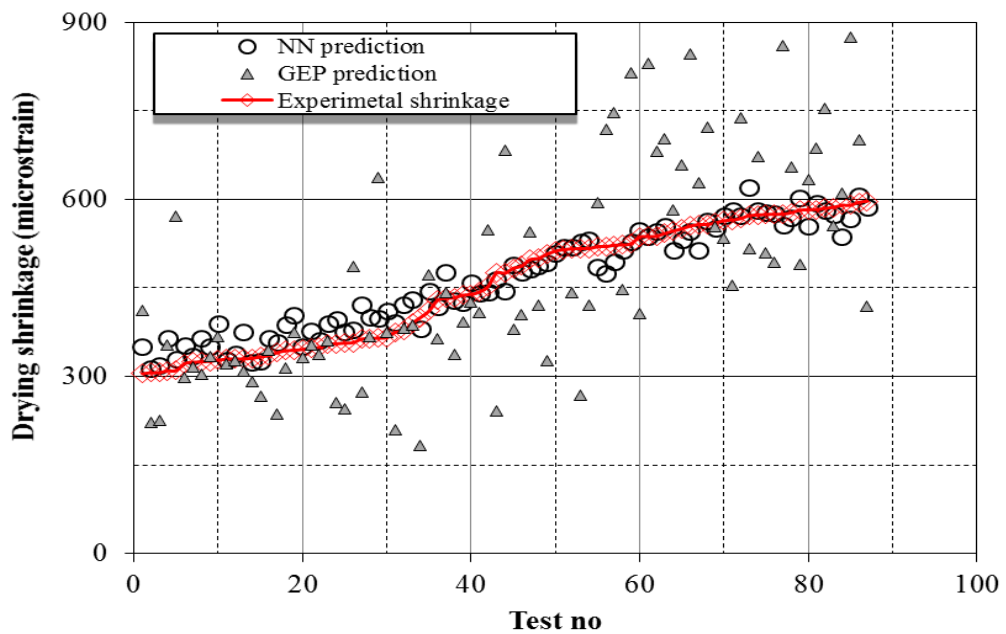
Figure 3.12 Comparison of experimental drying shrinkage values between 300-600 microstrain with those predicted by NN and GEP
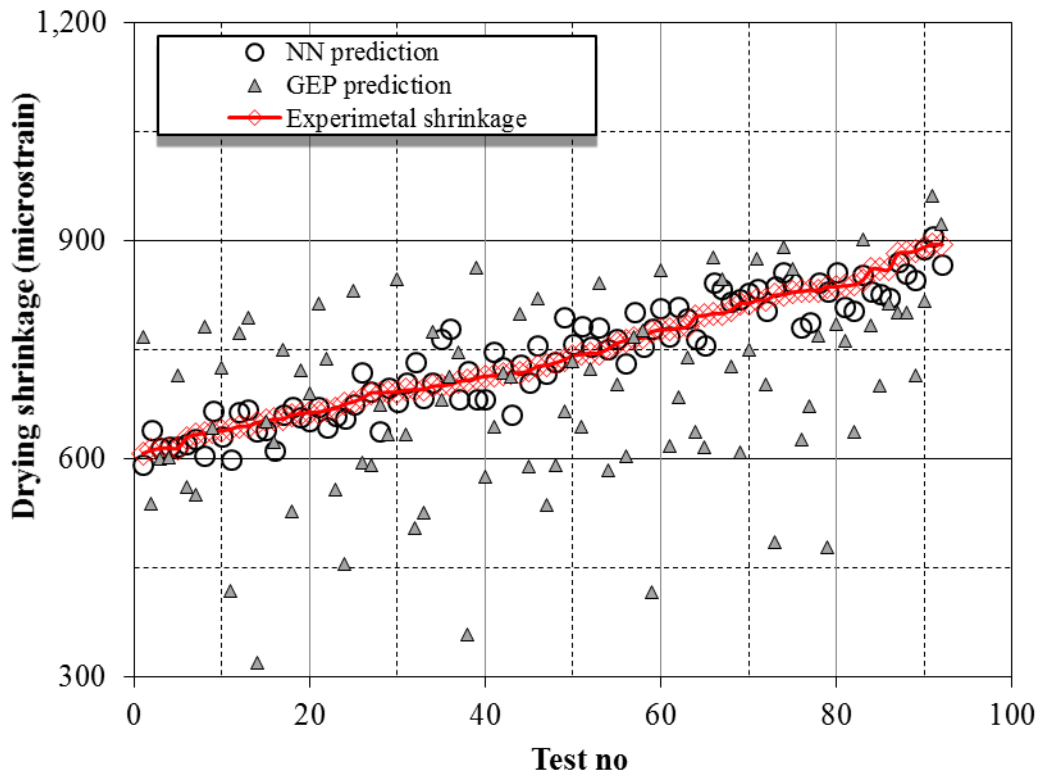
Figure 3.13 Comparison of experimental drying shrinkage values between 600-900 microstrain with those predicted by NN and GEP
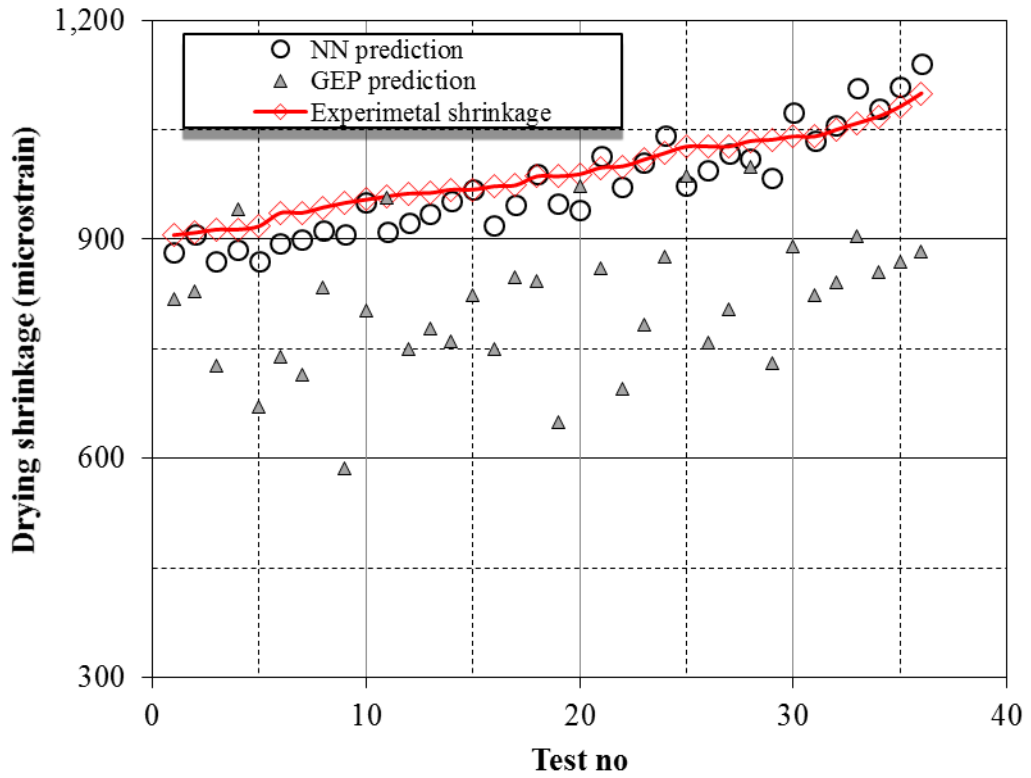
Figure 3.14 Comparison of experimental drying shrinkage values between 900-1200 microstrain with those predicted by NN and GEP

CHAPTER 4

EXPERIMENTAL VALIDATION OF THE MODELS

4.1 Details of experimental study

4.1.1 Introduction

In this stage, experiments are designed to characterize the compressive strength, and drying shrinkage properties of four mixes containing mineral admixtures. The hardened concretes tested for the compressive strength, Shrinkage accompanied by the water loss also monitored for a drying period of 40 days. The materials and procedures used for these experiments discussed in this chapter.

4.1.2 Materials

The details of materials used in this research are given below. The concrete production was done to test the shrinkage behaviour of concrete.

4.1.2.1 Cement

CEM I 42.5 R type Portland cement having specific gravity of 3.14 and Blaine fineness of 327 m^2/kg was utilized for preparing the concrete specimens used in determination of compressive strength and dry shrinkage. The chemical composition of the cement shown in Table 4.1

Table 4.1 Chemical composition of the cement

Chemical composition of the cement (%)								
CaO	SiO_2	Al_2O_3	Fe_2O_3	MgO	SO_3	K_2O	Na_2O	LOI
62.58	20.25	5.31	4.04	2.82	2.73	0.92	0.22	2.98

4.1.2.2 Fly ash

The fly ash (FA) used in this research was a class F type according to ASTM C 618 (2002) and obtained from Yumurtalik-Sugozu thermal power plant in the form of Commercial grade. It had a specific gravity of 2.25 and the Blaine fineness of 287 m^2/kg. The chemical analysis of FA shown in Table 4.2

Table 4.2 Chemical composition of the fly ash

Chemical composition of the fly ash (%)								
CaO	SiO$_2$	Al$_2$O$_3$	Fe$_2$O$_3$	MgO	SO$_3$	K$_2$O	Na$_2$O	LOI
4.24	56.2	20.17	6.69	1.92	0.49	1.89	0.58	1.78

4.1.2.3 Silica fume

A commercial grade silica fume (SF) obtained from Norway was utilized in this study. It had a specific gravity of 2.2 and the specific surface area (Nitrogen BET Surface Area) of 21080 m^2/kg. In Table 4.3, both the chemical analysis and physical properties of SF provided.

Table 4.3 Chemical composition of the silica fume

Chemical composition of the silica fume (%)								
CaO	SiO$_2$	Al$_2$O$_3$	Fe$_2$O$_3$	MgO	SO$_3$	K$_2$O	Na$_2$O	LOI
0.45	90.36	0.71	1.31	-	0.41	1.52	0.45	3.11

4.1.2.4 Aggregates.

Fine aggregate and coarse aggregates used for production of concrete is the mixture of crushed stone with specific gravities of 2.65, 2.66 respectively. In addition, the grading of the aggregates was kept constant for concrete production. Fig 4.1 demonstrates the gradation curves of the each aggregate and aggregate mix in comparison to reference curves (A16, B16, and C16). Moreover, fuller's parabola was also considered for grading. Fuller's parabola expressed by Eq. 3.1.

$$dp_i = 100 \times \sqrt{\frac{d_i}{d_{max}}}$$
(4.1)

Where

dp_i is percent passing from sieve size of "i"

d_i is sieve size

d_{max} is the maximum aggregate size (16 mm for this study)
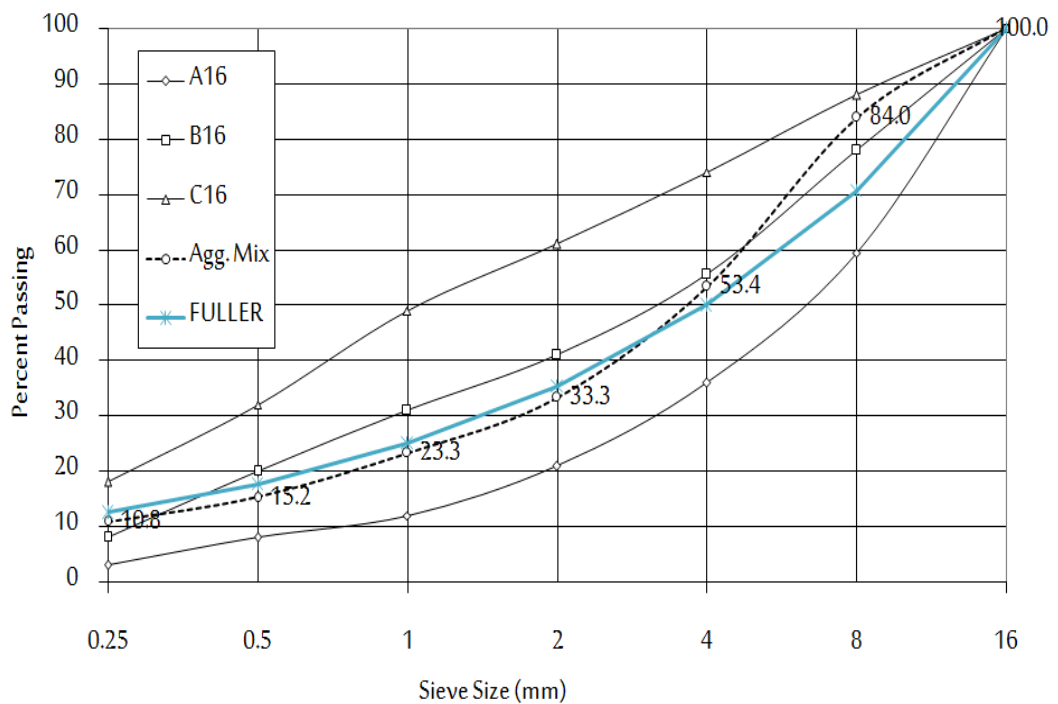
Figure 4.1. Gradation curves of aggregates

The particle size gradation obtained through the sieve analysis and physical properties of the fine and coarse aggregates are presented in Table 4.4

Table 4.4 Sieve analysis and physical properties of aggregate.

Sieve Analysis		
Sieve size (mm)	Passing %	
	Crushed limestone	Crushed sand
16	100	100
8	64.36	100
4	3.01	94.58
2	0.78	59.91
1	0.78	41.74
0.5	0.78	27.11
0.25	0.78	19.07
Pan	0	0
Spec. Grav.	2.65	2.65

4.1.2.5 Superplasticizer

A sulphonated naphthalene formaldehyde superplasticizer (SP) with a specific gravity of 1.19 was used in all mixtures. The properties of superplasticizer are given in Table 4.5 as reported by the local supplier.

Table 4.5 Properties of superplasticizer

Properties	Superplasticizer
Name	Daracem 200
Color tone	Dark brown
State	Liquid
Specific gravity	1.19
Chemical description	sulphonated naphthalene formaldehyde
Recommended dosage	% 1-2 (% binder content)

4.1.3 Mix proportions

As shown in Table 4.6 the four concrete mixes were designed

Table 4.6 Designation and composition properties of mixes

No.	Mix Designation	Cement (CEM I 42.5 R type)	Fly Ash	Silica fume
1	Plain F0S0	100 %	0 %	0 %
2	Binary F10S0	90 %	10%	0 %
3	Binary F0S15	85 %	0 %	15%
4	Ternary F15S10	75 %	15%	10%

The letter "FA" and "SF" were used to indicate replacement levels of fly ash and silica fume, respectively. The mixtures were designed at 0.45 water/binder ratios (w/b). In codification of concretes. The w/b ratio was 0.45 and the total cementitious materials content was 400 kg/m^3. In the production of the concretes.

The mixture S0F0 in Table 4.7 was designated as the control mixture which included only ordinary Portland cement as the binder while the remaining mixtures incorporated binary (PC+FA, PC+SF) ternary (PC+FA+ SF) cementitious blends in

which a proportion of portland cement was replaced with the mineral admixtures. The replacement ratios for both FA and SF were 10 and 15% by weight of the total binder. When preparing binary and ternary mixtures, FA and SF were replaced by cement according to the specified replacement.

Table 4.7 Mix proportions for concrete (kg/m³)

Mix Description	SF0FA0	SF0FA10	SF15FA0	SF15FA10
Cement	400	360	340	300
FA	0	40	0	40
SF	0	0	60	60
Water	180	180	180	180
Fine Aggregate	970.8	962.9	957.3	949.8
Coarse aggregate (Medium only)	812.7	806.0	801.3	795.1
Superplasticiser	4.4	3.2	8.0	6.4
Fresh unit weight (kg/m^3)	2367.9	2352.1	2346.7	2331.3

4.1.4 Specimen Preparation and Curing

All concretes were mixed in accordance with ASTM C192 standard in a power driven rotating pan mixer with a 50 l capacity. All samples were poured into the steel moulds in two layers, each of which being vibrated for a couple of seconds.

After casting the moulded specimens were protected with a plastic sheet and left in the casting room for 24 hr. Thereafter, the samples of compressive strength were demolded and cured in water until the testing ages.

4.1.4 Test methods

4.1.4.1 Compressive strength

For compressive strength measurement of concretes, 150x150x150 mm cubes was tested according to ASTM C39 (2012) by means of a 3000 kN capacity testing machine. The test was performed on the test specimens at the ages 28 days to monitor the compressive strength development. The compressive strength was computed from average of three specimens at each testing age.

4.1.4.2 Drying shrinkage and weight loss

Free shrinkage test specimens having a dimension of 70x70x280 mm for each mixture were cured for 24 h at 20 ^{o}C and 100% relative humidity and then were demoulded. After that, the specimens were exposed to drying in a humidity cabinet at 23 ± 2 ^{o}C and 50 ± 5% relative humidity, as per ASTM C157 for about 40 days. The length change was measured by means of a dial gage extensometer with a 200 mm gage length. The shape of the shrinkage specimens as well as the location of the reference pins are shown in Fig. 3.16. Measurements were carried out every 24 h for the first 3 weeks and then 3 times a week. At the same time, weight loss measurements were also performed on the same specimens. Variations in the free shrinkage strain and the weight loss were monitored during the 41-day drying period (at 23 ± 2 ^{o}C and 50 ± 5% relative humidity) and the average of three prism specimens were used for each property.
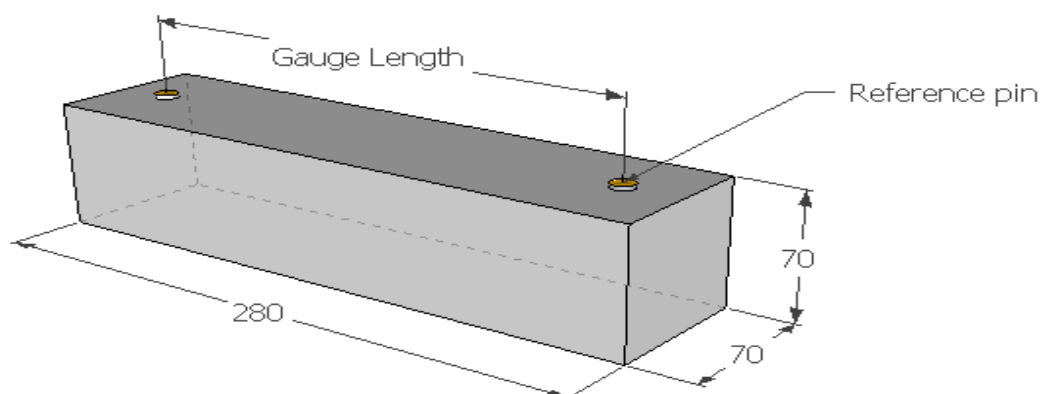
Figure 4.1 Free shrinkage specimens

4.2 Discussion of results

Free shrinkage strain developments of the concretes are depicted in Fig. 4.2; it can be observed that Mix containing SF15FA10 showed higher shrinkage than the other mixtures. The highest shrinkage in SF15FA10 mix in the age of 40 days is found 515 microstrain. The lowest shrinkage in SF0FA10 mix at the age 40 days is found to be lower than those in control mixture.
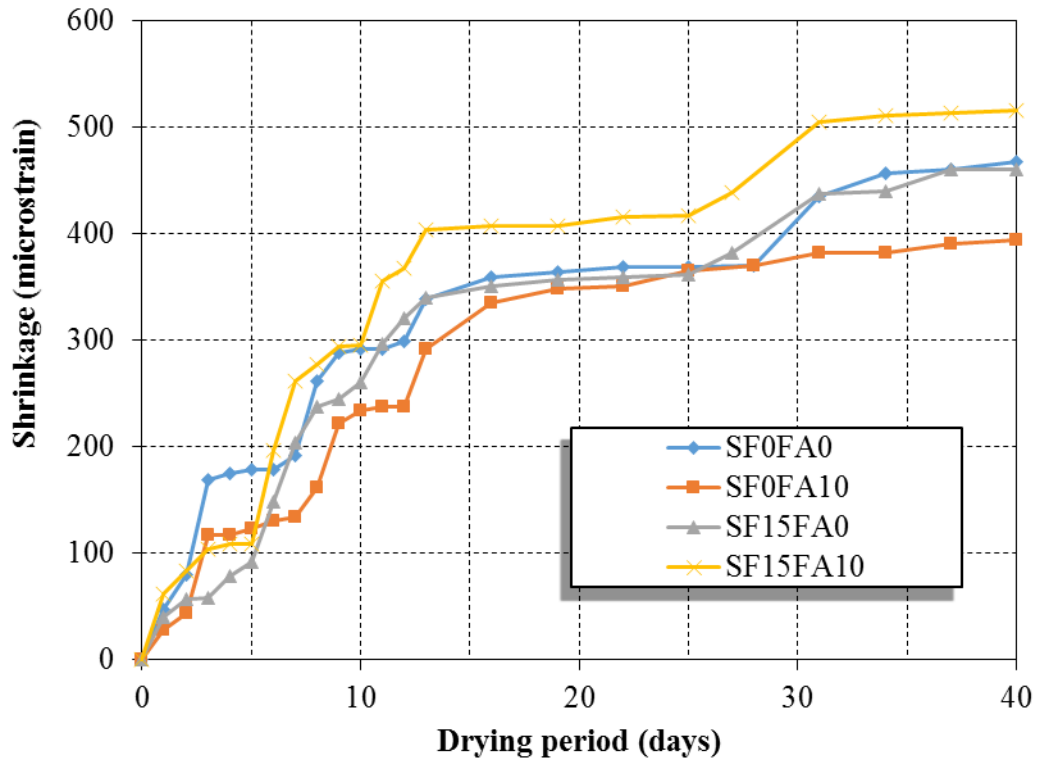
Figure 4.2 Shrinkage of concretes over 40 days of drying period

Weight losses of the concretes for 40 days of drying period are illustrated in Fig. 4.3. The maximum weight loss of 3.15 % was observed in SF15FA10 concrete while the minimum was observed at control concrete as 2.2.

73
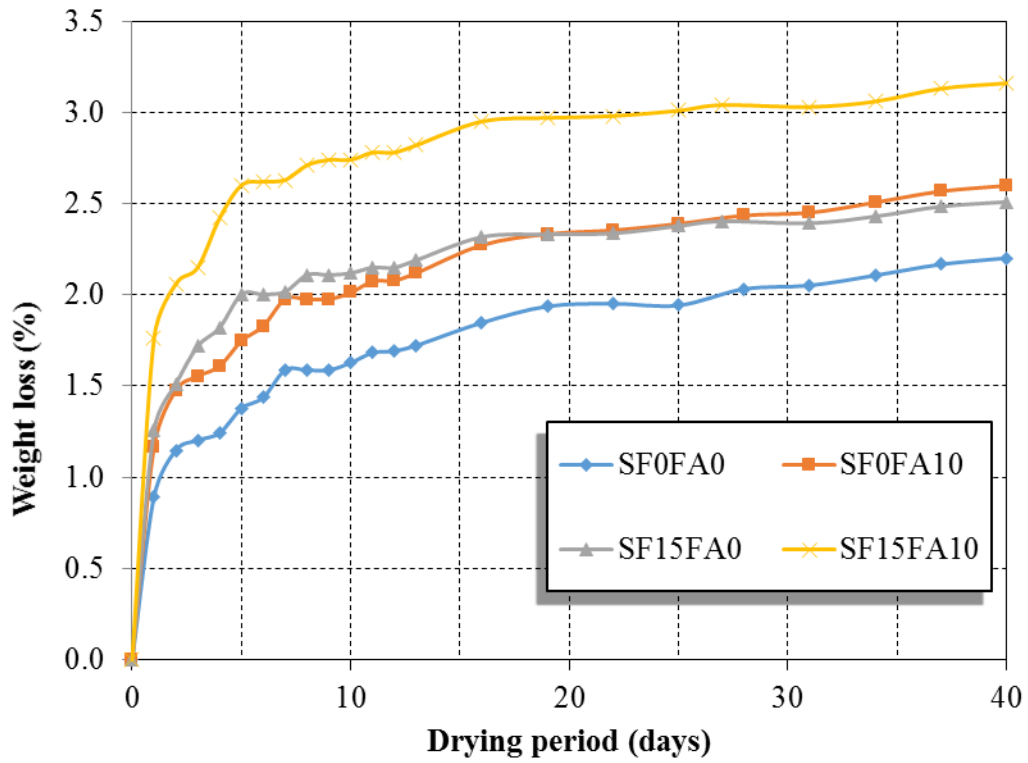
Figure 4.3 Weight loss of concrete

Fig. 4.4 shows the compressive strength values of concrete, the maximum value observed in FA0SF15 the figure indicated that there was an increase in compressive strength with the increase in SF content. While added FA to concrete mixes, compressive strength systematically decreases.
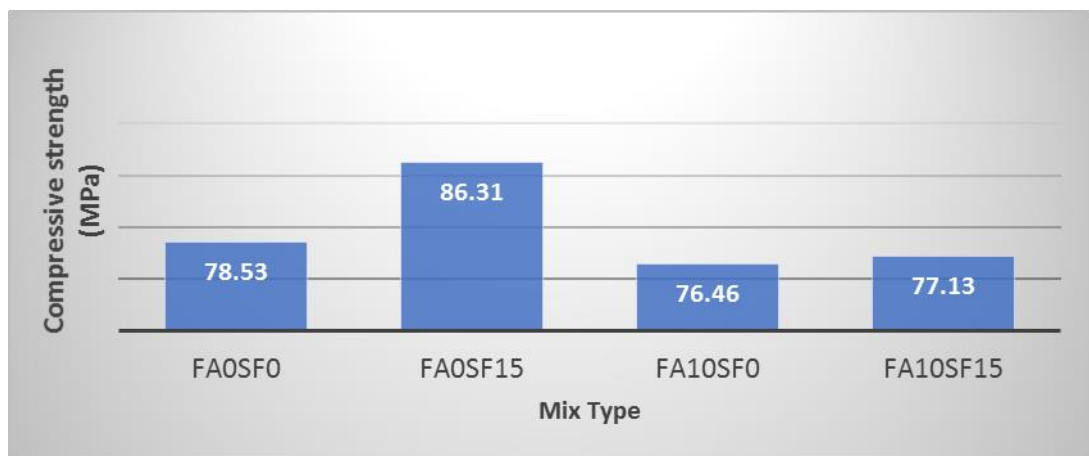
Figure 4.4 Compressive strength of concrete

Figure 4.5 shows the tendencies of the shrinkage values obtained from experimental study and proposed prediction models.
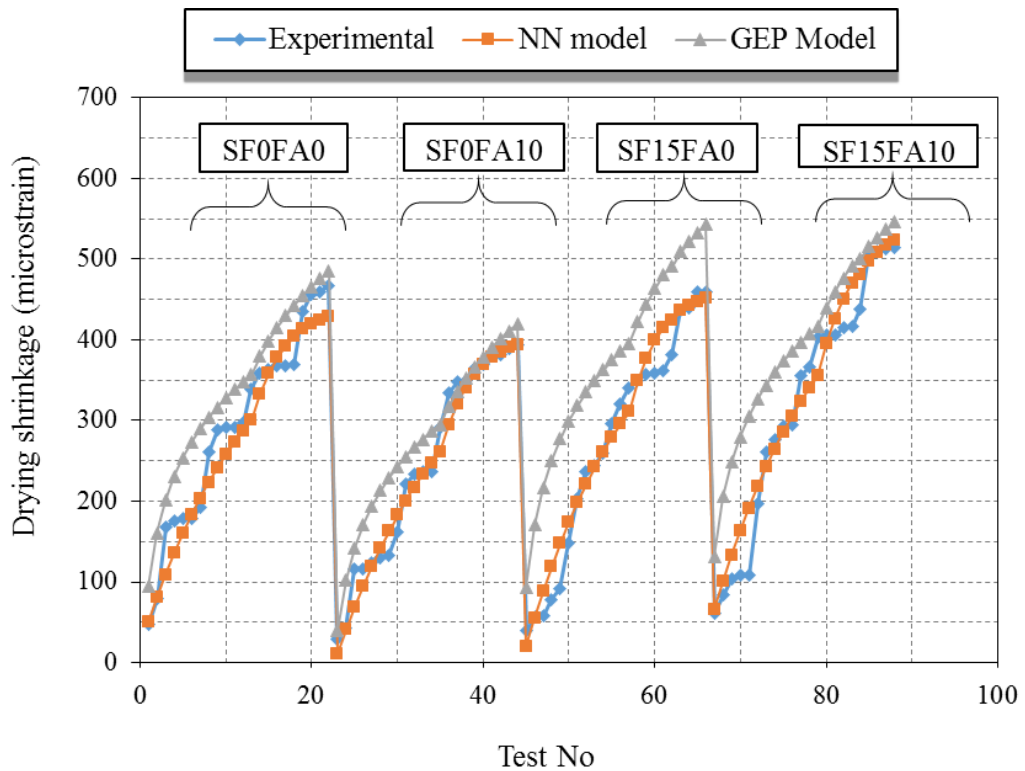
Figure 4.5 Comparison between proposed model and experimental drying shrinkage values

Although both of the models showed similar trends to that of experimental study, the best performance seemed to be obtained for SF0FA10 concrete. However, for SF15FA0 concrete GEP indicated a diverging trend. Similarly for SF15FA10 concrete group, GEP indicated clearly hier predication performance. Nevertheless, NN model illustrated almost prefect estimation capability for all four types of concrete

CHAPTER 5

CONCLUSIONS

Based on the mathematical modeling and experimental results reported in this thesis, the following conclusions can be drawn:

- Numerical modeling of shrinkage of concrete containing mineral admixtures was conducted using neural network (NN) and gene expression programming (GEP). To this aim, available experimental data presented in the existing literature were used to derive those models. In order to evaluate their efficiency and advantages, the performance of the proposed models was compared to that provided by the collected data in the previous studies.

- The prediction model for shrinkage estimation of the concretes produced with fly ash and silica fume can efficiently be constructed using NN. The constructed NN model showed a good performance on both training and testing data sets.

- A comparison with the existing analytical modeling for the collected data referred that the NN models provide better prediction results than the GEP model. The errors obtained from GEP model were very high especially for SF incorporated concrete

- The accuracy of the proposed models is found to be good enough to be utilized for prediction purposes.

- Experimental study indicated that utilization of mineral admixtures affected the shrinkage behaviors of concretes significantly. The highest shrinkage strain development was observed for SF15FA10 concrete. However, SF0FA10 concrete demonstrated the lowest trend. It could be due to the fact that FA has low pozzolanic reactivity, and hence autogenous shrinkage at early ages is low. Control concrete (0% FA, 0% SF) and SF15FA0 concrete indicated almost similar behaviour in shrinkage strain development.

- The .highest compressive strength value at the end of 28 days of curing was observed for FA0SF15 concrete. The improvement of concrete was due to high pozzolanic reaction of SF and its micro filling effect.

- The comparison of the shrinkage value obtained from the proposed models with the observed experimental results of this thesis proved that NN model can reliably be utilized for prediction purpose. However, GEP model yielded overestimated result for all four types of concrete

REFERENCES

Abbas, A., Abid, S., Abbas, J. (2013) Adaptation of Artificial Intelligence to Predict Concrete Strength, *Materials Science and Engineering*, **10**, 661-669

ASTM C 618. (2002). Standard Specification for Coal Fly Ash and Raw or Calcined Natural Pozzolan for Use in Concrete

ASTM C192 Standard Practice for Making and Curing Concrete Test Specimens in the Laboratory"

Bal, L., and Bodin, F. (2013) Artificial neural network for predicting drying shrinkage of concrete, *Construction and Building Materials*, **38**, 248–254

Baykasoglu, A., Oztas, A., Özbay, E. (2009) Prediction and multi-objective optimization of high-strength concrete parameters via soft computing approaches, *Expert Systems with Applications*, **36**, 6145–6155

Bouzoubaâ, N., Bilodeau, A., Sivasundaram, V., Fournier, B. (2002). Development of Ternary Blends for High-Performance Concrete, *Materials technology laboratory*.

Castelli, M., Vanneschi, L., Silva, S. (2013) Prediction of high performance concrete strength using Genetic Programming with geometric semantic genetic operators, *Expert Systems with Applications,* **40**, 6856–6862

Cevik, A., Atmaca, N., Ekmekyapar, T., Guzelbey, I. (2009). Flexural buckling load prediction of aluminium alloy columns using soft computing techniques, *Expert Systems with Applications*, **36**, 6332–6342

Chandwani V., Agrawal V., Nagar R. (2013) Applications of Soft Computing in Civil Engineering: A Review, *International Journal of Computer Applications*,**81**,0975 – 888

Charniak E. and McDermott D. (1985) Introduction to Artificial Intelligence. Addison-Wesley, Reading, MA

Chaturvedi, D.K. (2008). Soft Computing Techniques and its applications in Electrical Engineering, Studies in Computational Intelligence, **103**, 1-10.

Coppin, B. (2004) Artificial intelligence illuminated, -1sted, ISBN 0-7637-3230-3, book

Dantas, A., Leite, L., Nagahama, K. (2013) Prediction of compressive strength of concrete containing construction and demolition waste using artificial neural networks, *Construction and Building Materials*, **38**, 717–722

Deng, Y., Wang, P., (2010). Predicting the shrinkage of thermal insulation mortar by probabilistic neural networks, *Applied Physics & Engineering*, **3**, 212-222

Erdem, T., Kırca, O. (2008). Use of binary and ternary blends in high strength concrete, *Construction and Building Materials*, **22**, 1477–1483

Farzadnia, N., Ali, A., Demirboga, R., (2011). Incorporation of Mineral Admixtures in Sustainable High Performance Concrete. *International Journal of Sustainable Construction Engineering & Technology*, **2**, Issue 1.

Ferreira C., (2001) Gene expression programming: a new adaptive algorithm for solving problems. *Complex Systems*, **13**, (2): 87-129.

Goldberg D. (1989) Genetic Algorithms in search, optimization and machine learning. MA: Addison-Welsley, book

Guler, K., Demir, F., Pakdamar, F., (2012). Stress–strain modelling of high strength concrete by fuzzy logic approach, *Construction and Building Materials*, **37**, 680–684

Gulley, N. (1995). Fuzzy Logic Toolbox for Use with MATLAB, book

Guneyisi, E., Gesoglu, M., Karaoglu, S., Mermerdas, K., (2012). Strength, permeability and shrinkage cracking of silica fume and metakaolin concretes. *Construction and Building Materials*, **34**, 120-130

Guneyisi, E., Gesoglu, M., Özbay, E., (2010). Strength and drying shrinkage properties of self-compacting concretes incorporating multi-system blended mineral admixtures, *Construction and Building Materials*, **24**, 1878–1887

Haugeland, J. (1985) Artificial Intelligence: The Very Idea, book

Holt E. (2001) Early Age Autogenous Shrinkage of Concrete, *Technical Research Center of Finland-ESPOO*, VTT PUBLICATIONS, 446

Holt E., (2005) Contribution of Mixture Design to Chemical and Autogenous Shrinkage of Concrete at Early Ages, *Cement and Concrete Research*, **35**(3), 464-472

Hou, Q. (2013) Setting behavior and shrinkage of high performance pavement concrete: Effect of supplementary cementitious materials, chemical admixtures and temperature, master thesis.

J. Koza, (1992) Genetic Programming: On the Programming of Computers By *Means of Natural Selection*, MIT Press, Cambridge, Mass, USA

Justnes H., Van Gernert A., Verb oven F., and Sellevold E.1., *Total and External Chemical Shrinkage of Low W/C Ratio Cement Pastes,* Advances in Cement Research, **8**(31), 121-126, 1996.

Karthikeyan, J., Upadhyay, A., Bhandari, N., (2007). Artificial neural network for prediction creep and shrinkage of high performance concrete, *Advances concrete technology,* **6**, 135-142

Khairallah (2009) Analysis of autogenous and drying Shrinkage of concrete, thesis

Khatib J., (2008) Performance of self-compacting concrete containing fly ash *Construction and Building Materials*, **22**, 1963–1971

Khatri R. and Sirivivatnanon V. (1995) Effect of different supplementary cementitious materials on mechanical properties of high performance concrete *cement and concrete research*, **25**, 209-220.

Konar, A., (2000). Artificial Intelligence and Soft Computing Behavioral and Cognitive Modeling of the Human Brain, *book*

Kose, M., Kayadelen, C., (2010). Modeling of transfer length of prestressing strands using genetic programming and neuro-fuzzy, *Advances in Engineering Software*, **41**, 315–322

Koza, J. (1992) Genetic Programming on the Programming of Computers by Means of Natural Selection, London, England, book

Lee, S.C. and Han, S.W. (2002). Neural-network-based models for generating artificial earthquakes and response spectra. *Computers and Structures* **80**, 1627–1638.

Li 1., and Yao Y, *A study on creep and drying shrinkage of high performance concrete,* Cement and Concrete Research, **31**(8), 1203-1206,2001.

Lu, P., Chen, S., Zheng, Y. (2012) Artificial Intelligence in Civil Engineering*, Mathematical Problems in Engineering*, **10**, 1155-145974

Luger, G., Stubblefield, W. (1993) artificial intelligence structures and strategies for complex problem solving, book

Lura P., Jensen O. M., and Van B. K.,(2003) *Autogenous Shrinkage in High-Shrinkage Cement Paste: An evaluation of Basic Mechanisms,* Cement and Concrete Research, **33**(2), 223- 232,2003.

Mala, K., Mullick, A., Jain, K., Singh, P., (2013). Effect of Relative Levels of Mineral Admixtures on Strength of Concrete with Ternary Cement Blend. *International Journal of Concrete Structures and Materials*, **3**, 239–249

Maruyama, Teramoto, A. (2013) Temperature dependence of autogenous shrinkage of silica fume cement pastes with a very low water–binder ratio, *Cement and Concrete Research*, **50**, 41–50

Mauro Castelli, M., Vanneschi, L., Silva, S. (2013) Prediction of high performance concrete strength using Genetic Programming with geometric semantic genetic operators, *Expert Systems with Applications*, **40**, 6856–6862

Meddah, M., Lmbachiya, M., Dhir, R., (2014). Potential use of binary and composite limestone cements in concrete production, *Construction and Building Materials*, **58**, 193–205

Mehta P.K., and Meterio P.1., (2006) *Concrete Microstructure, Properties, and Materials,* Third Edition, New York, McGraw-Hill Companies

Mermerdaş, K. (2013). Characterization and Utilization of Calcined Turkish Kaolins for Improving Strength and Durability Aspects of Concrete. *Ph. D. Thesis*, Gaziantep University, Gaziantep.

Nazari, A., Torgal, F. (2013) Predicting compressive strength of different geopolymers by artificial neural networks, *Ceramics International*, **39**, 2247–2257

Nedushan, B., (2012). Prediction of elastic modulus of normal and high strength concrete using ANFIS and optimal nonlinear regression models, *Construction and Building Materials*, **36**, 665–673

Newman, J., Choo, B. (2003) Advanced Concrete Technology Concrete Properties, Elsevier Ltd, book

Omar W., Makhtar A.M., Lai T.P., Omar R., and Kwong N.M. (2008) Creep, Shrinkage and Elastic Modulus of Malaysian Concrete*, Final Report-Project*, No: LPIPMlCREAMiUPP *02-02-06-09-23, .*

Özbay, E. (2007) Effects of Mineral Admixtures on the Fresh and Hardened Properties of Self Compacting Concretes: Binary, Ternary, and Quaternary Systems, PhD Thesis

Ozcan, F., Atis, C., Karahan, O., Uncuoglu, E., Tanyildizi, H. (2009) Comparison of artificial neural network and fuzzy logic models for prediction of long term compressive strength of silica fume concrete, *Advances in Engineering Software*, **40**, 856–863

Pedrycz, W., Aliev, R. (2009). Logic-oriented neural networks for fuzzy neurocomputing. *Neurocomputing*, **73**, 10–23

Radocea A., *A study on the Mechanisms of Plastic Shrinkage of Cement-Based Materials,* PhD Thesis, CTH Goteborg, Sweden, 1992.

Rich E. & Knight K. (1991). Artificial Intelligence. MacGraw-Hill, New York

Rowe, N. (1988) Artificial Intelligence through Prolog, Prentice-Hall, 1988, ISBN 0-13-048679-5, book

Russell, S., Norvig, P. (1995) Artificial Intelligence A Modern Approach, Prentice-Hall, Inc., New Jersey 07632

Saridemir, M. (2009) Prediction of compressive strength of concretes containing metakaolin and silica fume by artificial neural networks, *Advances in Engineering Software*, **40**, 350–355.

Sarıdemir, M. (2014) Effect of specimen size and shape on compressive strength of concrete containing fly ash: Application of genetic programming for design, *Materials and Design*, **56**, 297-304

Schalkoff .J. (1997) Artificial Neural Networks. McGraw-Hill, New York

Sgambi, L. (2008) Artificial Intelligence: Historical Development and Applications in Civil Engineering Field, Taylor & Francis Group, London, ISBN 978-0-415-46844-2

Shaeles, C.A., and Hover, K.C. (1988) Influence of mix proportion and construction operations on plastic shrinkage cracking in thin slabs, *ACI Materials Journal*, **85**, 495-504.

Shahin, M.A., Maier, H.R. and Jaksa, M.B. (2002). Predicting settlement of Shallow Foundations using Neural Networks, Journal of Geotechnical and Geoenvironmental Engineering, **128**(9), 785-793.

Silva, W., Stemberk, P. (2012). Predicting self-compacting concrete shrinkage based on a modified fuzzy logic model, *18thInternational Conference*, 1173–1181

Susac MZ, Sarlija N, Bensic M (2005) Selecting neural network architecture for investment profitability predictions. *Journal of information and organizational sciences*, **29** (2):83-95

Tangtermsirikul, S. (1995) Class C Fly Ash as a Shrinkage Reducer for Cement Paste, ASTM Special Publication, American Society for Testing and Materials, Volume 153

Tazawa E. (1999), Autogenous Shrinkage of Concrete*, London*, E. & FN Spon, book

Tazawa E., and Miyazawa S., *Influence of Cement and Admixtures on Autogenous Shrinkage of Cement Paste,* Cement and Concrete Research, **25**(2), 281-287, 1995.

Thomas, M., Shehata, M., Shashiprakash, S., Hopkins, D., Cail, K. (1999). Use of ternary cementitious systems containing silica fume and fly ash in concrete, *Cement and Concrete Research*, **29**, 1207–1214

Tia M. et al (2005) Modulus of elasticity, creep and shrinkage of concrete. Gainesville: Department of Civil & Coastal Engineering, College of Engineering

Topc, I., Sarıdemir, M. (2008) Prediction of compressive strength of concrete containing fly ash using artificial neural networks and fuzzy logic, *Computational Materials* Science, **41**, 305–311.

Tsai, H., Lin, Y., (2011). Modular neural network programming with genetic optimization, *Expert Systems with Applications,* **38**, 11032–11039

Uysal, M., Tanyildizi, H., (2012). Estimation of compressive strength of self-compacting concrete containing polypropylene fiber and mineral additives exposed to high temperature using artificial neural network

Vanluchene, R.D. and Sun, R. (1990). Neural Networks in Structural Engineering, Computer-Aided Civil and Infrastructure Engineering, **5**(3), 207-215.

Wang, X., Bektas, F., Taylor, P., Wang, K., Tikalsky, P., (2011). Drying shrinkage behavior of mortars made with ternary blends, *Transportation Research Board*.

Wongkeo, W., Thongsanitgarn, P., Chaipanich, A., (2012). Compressive Strength of Binary and Ternary Blended Cement Mortars Containing Fly Ash and Silica Fume Under Autoclaved Curing TIChE International Conference 2011, Hatyai, Songkhla THAILAND

Yang, E. H., Yang, Y. and Li, V. C. (2007). Use of high volumes of fly ash to improve ECC mechanical properties and material greenness. *ACI Materials Journal*, **104** (6), 620-628.

Yoo S, Kwon S, Jung S (2012) Analysis technique for autogenous shrinkage in high performance concrete with mineral and chemical admixtures *Construction and Building Materials*, **34**, 1–10

Zade, L. (1994) soft computing and fuzzy logic, IEEE Software, University of California at Berkeley

Zarandi, M., Alaeddini, A., Turksen, I. (2008) A hybrid fuzzy adaptive sampling – Run rules for Shewhart control charts, *Information Sciences*, **178**, 1152–1170

Zarandi, M., urksen, I., Sobhani, J., Ramezanianpour, A. (2008) Fuzzy polynomial neural networks for approximation of the compressive strength of concrete, *Applied Soft Computing Journal*, **8**, 488–498

Zhang M. H., Tam C.T., and Leow M.P., (2003) Effect of Water-to-Cementitious Materials Ratio and Silica Fume on the Autogenous Shrinkage of Concrete, *Cement and Concrete Research*, **33**, 1687–1694

Zhao XL, Hancock GJ. (1991) Tests to determine plate slenderness limits for cold-formed rectangular hollow sections of grade C450. Steel Construct J Aust Inst Steel Construct **25**(4):2–16.

APPENDIX
Appendix A
Input and output databases

Table A.1 database from Zhang et al

Data Source	Number	INPUT								OUTPUT
		X1	X2	X3	X4	X5	X6	X7	X8	Y
		w/b	SF (Kg/m3)	FA (Kg/m3)	cement (kg/m3)	Aggregate/ Binder	fc Mpa (28Day) 150 x150	Auto : 0 dry or free :1	Dry Time (DAYS)	Shrinkage
Zhang et al (2003)	1	0.27	0	0	496	3.70	77.94	0	1	37
	2	0.27	0	0	496	3.70	77.94	0	7	100
	3	0.27	0	0	496	3.70	77.94	0	14	129
	4	0.27	0	0	496	3.70	77.94	0	21	139
	5	0.27	0	0	496	3.70	77.94	0	28	148
	6	0.27	0	0	496	3.70	77.94	0	35	157
	7	0.27	0	0	496	3.70	77.94	0	42	163
	8	0.27	0	0	496	3.70	77.94	0	49	168
	9	0.27	0	0	496	3.70	77.94	0	56	173
	10	0.27	0	0	496	3.70	77.94	0	63	177
	11	0.27	0	0	496	3.70	77.94	0	70	181
	12	0.27	0	0	496	3.70	77.94	0	77	186
	13	0.27	0	0	496	3.70	77.94	0	84	190
	14	0.27	0	0	496	3.70	77.94	0	91	195
	15	0.27	0	0	496	3.70	77.94	0	98	197
	16	0.27	25	0	471	3.64	82.08	0	1	79
	17	0.27	25	0	471	3.64	82.08	0	7	170
	18	0.27	25	0	471	3.64	82.08	0	14	195
	19	0.27	25	0	471	3.64	82.08	0	21	207
	20	0.27	25	0	471	3.64	82.08	0	28	216
	21	0.27	25	0	471	3.64	82.08	0	35	224
	22	0.27	25	0	471	3.64	82.08	0	42	229
	23	0.27	25	0	471	3.64	82.08	0	49	231
	24	0.27	25	0	471	3.64	82.08	0	56	238
	25	0.27	25	0	471	3.64	82.08	0	63	243
	26	0.27	25	0	471	3.64	82.08	0	70	246
	27	0.27	25	0	471	3.64	82.08	0	77	252

Data Source	Number	INPUT								OUTPUT
		X1	X2	X3	X4	X5	X6	X7	X8	Y
		w/b	SF (Kg/m3)	FA (Kg/m3)	cement (kg/m3)	Aggregate/ Binder	fc Mpa (28Day) 150 x150	Auto : 0 dry or free :1	Dry Time (DAYS)	Shrinkage
	28	0.27	25	0	471	3.64	82.08	0	84	255
	29	0.27	25	0	471	3.64	82.08	0	91	262
	30	0.27	25	0	471	3.64	82.08	0	98	265
	31	0.27	50	0	446	3.62	86.94	0	1	79
	32	0.27	50	0	446	3.62	86.94	0	7	172
	33	0.27	50	0	446	3.62	86.94	0	14	220
	34	0.27	50	0	446	3.62	86.94	0	21	241
	35	0.27	50	0	446	3.62	86.94	0	28	253
	36	0.27	50	0	446	3.62	86.94	0	35	260
	37	0.27	50	0	446	3.62	86.94	0	42	263
	38	0.27	50	0	446	3.62	86.94	0	49	264
	39	0.27	50	0	446	3.62	86.94	0	56	268
	40	0.27	50	0	446	3.62	86.94	0	63	269
	41	0.27	50	0	446	3.62	86.94	0	70	270
	42	0.27	50	0	446	3.62	86.94	0	77	272
Zhang et al (2003)	43	0.27	50	0	446	3.62	86.94	0	84	274
	44	0.27	50	0	446	3.62	86.94	0	91	280
	45	0.27	50	0	446	3.62	86.94	0	98	282
	46	0.3	0	0	497	3.60	63.09	0	1	38
	47	0.3	0	0	497	3.60	63.09	0	7	88
	48	0.3	0	0	497	3.60	63.09	0	14	116
	49	0.3	0	0	497	3.60	63.09	0	21	124
	50	0.3	0	0	497	3.60	63.09	0	28	135
	51	0.3	0	0	497	3.60	63.09	0	35	140
	52	0.3	0	0	497	3.60	63.09	0	42	145
	53	0.3	0	0	497	3.60	63.09	0	49	150
	54	0.3	0	0	497	3.60	63.09	0	56	154
	55	0.3	0	0	497	3.60	63.09	0	63	158
	56	0.3	0	0	497	3.60	63.09	0	70	164
	57	0.3	0	0	497	3.60	63.09	0	77	167
	58	0.3	0	0	497	3.60	63.09	0	84	171
	59	0.3	0	0	497	3.60	63.09	0	91	177
	60	0.3	0	0	497	3.60	63.09	0	98	181

Data Source	Number	INPUT								OUTPUT
		X1	X2	X3	X4	X5	X6	X7	X8	Y
		w/b	SF (Kg/m3)	FA (Kg/m3)	cement (kg/m3)	Aggregate/ Binder	fc Mpa (28Day) 150 x150	Auto : 0 dry or free :1	Dry Time (DAYS)	Shrinkage
	61	0.3	25	0	472	3.54	75.33	0	1	57
	62	0.3	25	0	472	3.54	75.33	0	7	148
	63	0.3	25	0	472	3.54	75.33	0	14	173
	64	0.3	25	0	472	3.54	75.33	0	21	184
	65	0.3	25	0	472	3.54	75.33	0	28	191
	66	0.3	25	0	472	3.54	75.33	0	35	195
	67	0.3	25	0	472	3.54	75.33	0	42	200
	68	0.3	25	0	472	3.54	75.33	0	49	202
	69	0.3	25	0	472	3.54	75.33	0	56	204
	70	0.3	25	0	472	3.54	75.33	0	63	207
	71	0.3	25	0	472	3.54	75.33	0	70	209
	72	0.3	25	0	472	3.54	75.33	0	77	211
	73	0.3	25	0	472	3.54	75.33	0	84	212
	74	0.3	25	0	472	3.54	75.33	0	91	213
	75	0.3	25	0	472	3.54	75.33	0	98	217
Zhang et al (2003)	76	0.3	50	0	447	3.52	81.99	0	1	55
	77	0.3	50	0	447	3.52	81.99	0	7	158
	78	0.3	50	0	447	3.52	81.99	0	14	211
	79	0.3	50	0	447	3.52	81.99	0	21	236
	80	0.3	50	0	447	3.52	81.99	0	28	252
	81	0.3	50	0	447	3.52	81.99	0	35	258
	82	0.3	50	0	447	3.52	81.99	0	42	262
	83	0.3	50	0	447	3.52	81.99	0	49	263
	84	0.3	50	0	447	3.52	81.99	0	56	264
	85	0.3	50	0	447	3.52	81.99	0	63	266
	86	0.3	50	0	447	3.52	81.99	0	70	267
	87	0.3	50	0	447	3.52	81.99	0	77	269
	88	0.3	50	0	447	3.52	81.99	0	84	270
	89	0.3	50	0	447	3.52	81.99	0	91	272
	90	0.3	50	0	447	3.52	81.99	0	98	274
	91	0.35	0	0	498	3.50	57.33	0	14	40
	92	0.35	0	0	498	3.50	57.33	0	21	40
	93	0.35	0	0	498	3.50	57.33	0	28	40

Data Source	Number	INPUT								OUTPUT
		X1	X2	X3	X4	X5	X6	X7	X8	Y
		w/b	SF (Kg/m3)	FA (Kg/m3)	cement (kg/m3)	Aggregate/ Binder	fc Mpa (28Day) 150 x150	Auto : 0 dry or free :1	Dry Time (DAYS)	Shrinkage
	94	0.35	0	0	498	3.50	57.33	0	35	40
	95	0.35	0	0	498	3.50	57.33	0	42	40
	96	0.35	0	0	498	3.50	57.33	0	49	40
	97	0.35	0	0	498	3.50	57.33	0	56	40
	98	0.35	0	0	498	3.50	57.33	0	63	40
	99	0.35	0	0	498	3.50	57.33	0	70	40
	100	0.35	0	0	498	3.50	57.33	0	77	40
	101	0.35	0	0	498	3.50	57.33	0	84	40
	102	0.35	0	0	498	3.50	57.33	0	91	40
	103	0.35	0	0	498	3.50	57.33	0	98	40
	104	0.35	25	0	473	3.40	63.27	0	1	37
	105	0.35	25	0	473	3.40	63.27	0	7	100
	106	0.35	25	0	473	3.40	63.27	0	14	127
	107	0.35	25	0	473	3.40	63.27	0	21	140
	108	0.35	25	0	473	3.40	63.27	0	28	151
	109	0.35	25	0	473	3.40	63.27	0	35	160
Zhang et al (2003)	110	0.35	25	0	473	3.40	63.27	0	42	168
	111	0.35	25	0	473	3.40	63.27	0	49	174
	112	0.35	25	0	473	3.40	63.27	0	56	180
	113	0.35	25	0	473	3.40	63.27	0	63	183
	114	0.35	25	0	473	3.40	63.27	0	70	192
	115	0.35	25	0	473	3.40	63.27	0	77	200
	116	0.35	25	0	473	3.40	63.27	0	84	205
	117	0.35	25	0	473	3.40	63.27	0	91	210
	118	0.35	25	0	473	3.40	63.27	0	98	216
	119	0.35	50	0	447	3.38	67.68	0	1	32
	120	0.35	50	0	447	3.38	67.68	0	7	114
	121	0.35	50	0	447	3.38	67.68	0	14	159
	122	0.35	50	0	447	3.38	67.68	0	21	180
	123	0.35	50	0	447	3.38	67.68	0	28	196
	124	0.35	50	0	447	3.38	67.68	0	35	206
	125	0.35	50	0	447	3.38	67.68	0	42	212
	126	0.35	50	0	447	3.38	67.68	0	49	216

Data Source	Number	INPUT								OUTPUT
		X1	X2	X3	X4	X5	X6	X7	X8	Y
		w/b	SF (Kg/m3)	FA (Kg/m3)	cement (kg/m3)	Aggregate/ Binder	fc Mpa (28Day) 150 x150	Auto :0 dry or free :1	Dry Time (DAYS)	Shrinkage
	127	0.35	50	0	447	3.38	67.68	0	56	221
	128	0.35	50	0	447	3.38	67.68	0	63	227
	129	0.35	50	0	447	3.38	67.68	0	70	233
	130	0.35	50	0	447	3.38	67.68	0	77	237
	131	0.35	50	0	447	3.38	67.68	0	84	241
	132	0.35	50	0	447	3.38	67.68	0	91	246
	133	0.35	50	0	447	3.38	67.68	0	98	250
	134	0.27	0	0	496	3.70	77.94	1	14	100
	135	0.27	0	0	496	3.70	77.94	1	21	144
	136	0.27	0	0	496	3.70	77.94	1	28	174
	137	0.27	0	0	496	3.70	77.94	1	35	184
	138	0.27	0	0	496	3.70	77.94	1	42	215
	139	0.27	0	0	496	3.70	77.94	1	49	226
	140	0.27	0	0	496	3.70	77.94	1	56	242
Zhang et al (2003)	141	0.27	0	0	496	3.70	77.94	1	63	242
	142	0.27	0	0	496	3.70	77.94	1	70	258
	143	0.27	0	0	496	3.70	77.94	1	77	266
	144	0.27	0	0	496	3.70	77.94	1	84	269
	145	0.27	0	0	496	3.70	77.94	1	91	276
	146	0.27	0	0	496	3.70	77.94	1	98	281
	147	0.27	25	0	471	3.64	82.08	1	14	109
	148	0.27	25	0	471	3.64	82.08	1	21	145
	149	0.27	25	0	471	3.64	82.08	1	28	156
	150	0.27	25	0	471	3.64	82.08	1	35	163
	151	0.27	25	0	471	3.64	82.08	1	42	200
	152	0.27	25	0	471	3.64	82.08	1	49	209
	153	0.27	25	0	471	3.64	82.08	1	56	219
	154	0.27	25	0	471	3.64	82.08	1	63	238
	155	0.27	25	0	471	3.64	82.08	1	70	238
	156	0.27	25	0	471	3.64	82.08	1	77	259
	157	0.27	25	0	471	3.64	82.08	1	84	260
	158	0.27	25	0	471	3.64	82.08	1	91	277
	159	0.27	25	0	471	3.64	82.08	1	98	277

Data Source	Number	INPUT								OUTPUT
		X1	X2	X3	X4	X5	X6	X7	X8	Y
		w/b	SF (Kg/m3)	FA (Kg/m3)	cement (kg/m3)	Aggregate/ Binder	fc Mpa (28Day) 150 x150	Auto :0 dry or free :1	Dry Time (DAYS)	Shrinkage
	160	0.27	50	0	446	3.62	86.94	1	14	136
	161	0.27	50	0	446	3.62	86.94	1	21	177
	162	0.27	50	0	446	3.62	86.94	1	28	192
	163	0.27	50	0	446	3.62	86.94	1	35	231
	164	0.27	50	0	446	3.62	86.94	1	42	236
	165	0.27	50	0	446	3.62	86.94	1	49	243
	166	0.27	50	0	446	3.62	86.94	1	56	251
	167	0.27	50	0	446	3.62	86.94	1	63	251
	168	0.27	50	0	446	3.62	86.94	1	70	277
	169	0.27	50	0	446	3.62	86.94	1	77	277
	170	0.27	50	0	446	3.62	86.94	1	84	292
	171	0.27	50	0	446	3.62	86.94	1	91	295
	172	0.27	50	0	446	3.62	86.94	1	98	300
	173	0.3	0	0	497	3.60	63.09	1	14	110
	174	0.3	0	0	497	3.60	63.09	1	21	174
	175	0.3	0	0	497	3.60	63.09	1	28	197
	176	0.3	0	0	497	3.60	63.09	1	35	219
	177	0.3	0	0	497	3.60	63.09	1	42	231
Zhang et al (2003)	178	0.3	0	0	497	3.60	63.09	1	49	252
	179	0.3	0	0	497	3.60	63.09	1	56	274
	180	0.3	0	0	497	3.60	63.09	1	63	274
	181	0.3	0	0	497	3.60	63.09	1	70	292
	182	0.3	0	0	497	3.60	63.09	1	77	292
	183	0.3	0	0	497	3.60	63.09	1	84	300
	184	0.3	0	0	497	3.60	63.09	1	91	306
	185	0.3	0	0	497	3.60	63.09	1	98	306
	186	0.3	25	0	472	3.54	75.33	1	14	109
	187	0.3	25	0	472	3.54	75.33	1	21	168
	188	0.3	25	0	472	3.54	75.33	1	28	168
	189	0.3	25	0	472	3.54	75.33	1	35	184
	190	0.3	25	0	472	3.54	75.33	1	42	200
	191	0.3	25	0	472	3.54	75.33	1	49	217
	192	0.3	25	0	472	3.54	75.33	1	56	217

| Data Source | Number | INPUT | | | | | | | | OUTPUT |
| | | X1 | X2 | X3 | X4 | X5 | X6 | X7 | X8 | Y |
		w/b	SF (Kg/m3)	FA (Kg/m3)	cement (kg/m3)	Aggregate/ Binder	fc Mpa (28Day) 150 x150	Auto : 0 dry or free :1	Dry Time (DAYS)	Shrinkage
	193	0.3	25	0	472	3.54	75.33	1	63	236
	194	0.3	25	0	472	3.54	75.33	1	70	236
	195	0.3	25	0	472	3.54	75.33	1	77	258
	196	0.3	25	0	472	3.54	75.33	1	84	258
	197	0.3	25	0	472	3.54	75.33	1	91	288
	198	0.3	25	0	472	3.54	75.33	1	98	288
	199	0.3	50	0	447	3.52	81.99	1	14	143
	200	0.3	50	0	447	3.52	81.99	1	21	216
	201	0.3	50	0	447	3.52	81.99	1	28	237
	202	0.3	50	0	447	3.52	81.99	1	35	256
	203	0.3	50	0	447	3.52	81.99	1	42	272
	204	0.3	50	0	447	3.52	81.99	1	49	286
	205	0.3	50	0	447	3.52	81.99	1	56	277
	206	0.3	50	0	447	3.52	81.99	1	63	295
Zhang et al (2003)	207	0.3	50	0	447	3.52	81.99	1	70	295
	208	0.3	50	0	447	3.52	81.99	1	77	330
	209	0.3	50	0	447	3.52	81.99	1	84	330
	210	0.3	50	0	447	3.52	81.99	1	91	346
	211	0.3	50	0	447	3.52	81.99	1	98	349
	212	0.35	0	0	498	3.50	57.33	1	14	158
	213	0.35	0	0	498	3.50	57.33	1	21	216
	214	0.35	0	0	498	3.50	57.33	1	28	256
	215	0.35	0	0	498	3.50	57.33	1	35	281
	216	0.35	0	0	498	3.50	57.33	1	42	294
	217	0.35	0	0	498	3.50	57.33	1	49	326
	218	0.35	0	0	498	3.50	57.33	1	56	335
	219	0.35	0	0	498	3.50	57.33	1	63	348
	220	0.35	0	0	498	3.50	57.33	1	70	355
	221	0.35	0	0	498	3.50	57.33	1	77	365
	222	0.35	0	0	498	3.50	57.33	1	84	366
	223	0.35	0	0	498	3.50	57.33	1	91	377
	224	0.35	0	0	498	3.50	57.33	1	98	390
	225	0.35	25	0	473	3.40	63.27	1	14	128

| Data Source | Number | INPUT | | | | | | | | OUTPUT |
| | | X1 | X2 | X3 | X4 | X5 | X6 | X7 | X8 | Y |
		w/b	SF (Kg/m3)	FA (Kg/m3)	cement (kg/m3)	Aggregate/ Binder	fc Mpa (28Day) 150 x150	Auto : 0 dry or free :1	Dry Time (DAYS)	Shrinkage
	226	0.35	25	0	473	3.40	63.27	1	21	188
	227	0.35	25	0	473	3.40	63.27	1	28	208
	228	0.35	25	0	473	3.40	63.27	1	35	242
	229	0.35	25	0	473	3.40	63.27	1	42	272
	230	0.35	25	0	473	3.40	63.27	1	49	288
	231	0.35	25	0	473	3.40	63.27	1	56	288
	232	0.35	25	0	473	3.40	63.27	1	63	294
	233	0.35	25	0	473	3.40	63.27	1	70	294
	234	0.35	25	0	473	3.40	63.27	1	77	322
	235	0.35	25	0	473	3.40	63.27	1	84	325
	236	0.35	25	0	473	3.40	63.27	1	91	330
Zhang et al (2003)	237	0.35	25	0	473	3.40	63.27	1	98	344
	238	0.35	50	0	447	3.38	67.68	1	14	136
	239	0.35	50	0	447	3.38	67.68	1	21	195
	240	0.35	50	0	447	3.38	67.68	1	28	222
	241	0.35	50	0	447	3.38	67.68	1	35	243
	242	0.35	50	0	447	3.38	67.68	1	42	261
	243	0.35	50	0	447	3.38	67.68	1	49	272
	244	0.35	50	0	447	3.38	67.68	1	56	272
	245	0.35	50	0	447	3.38	67.68	1	63	285
	246	0.35	50	0	447	3.38	67.68	1	70	285
	247	0.35	50	0	447	3.38	67.68	1	77	310
	248	0.35	50	0	447	3.38	67.68	1	84	300
	249	0.35	50	0	447	3.38	67.68	1	91	328
	250	0.35	50	0	447	3.38	67.68	1	98	344

Table A.2 database from Wongkeo et al

| Data Source | Number | INPUT | | | | | | | | OUTPUT |
| | | X1 | X2 | X3 | X4 | X5 | X6 | X7 | X8 | Y |
		w/b	SF (Kg/m3)	FA (Kg/m3)	cement (kg/m3)	Aggregate/ Binder	fc Mpa (28Day) 150 x150	Auto : 0 dry or free :1	Dry Time DAYS	Shrinkage
	1	0.49	0	0	538	2.75	50.45	1	7	167
	2	0.49	0	0	538	2.75	50.45	1	14	187
	3	0.49	0	0	538	2.75	50.45	1	21	200
	4	0.49	0	0	538	2.75	50.45	1	28	212
	5	0.49	0	0	538	2.75	50.45	1	35	218
	6	0.49	0	0	538	2.75	50.45	1	42	217
	7	0.49	0	0	538	2.75	50.45	1	49	212
	8	0.49	0	0	538	2.75	50.45	1	56	217
	9	0.49	0	0	538	2.75	50.45	1	63	231
	10	0.49	0	0	538	2.75	50.45	1	70	240
	11	0.49	0	0	538	2.75	50.45	1	77	250
	12	0.49	0	0	538	2.75	50.45	1	84	261
	13	0.49	0	0	538	2.75	50.45	1	91	265
	14	0.49	0	269	269	2.64	29.05	1	7	93
	15	0.49	0	269	269	2.64	29.05	1	14	106
	16	0.49	0	269	269	2.64	29.05	1	21	118
	17	0.49	0	269	269	2.64	29.05	1	28	128
Wongkeo et al (2012)	18	0.49	0	269	269	2.64	29.05	1	35	136
	19	0.49	0	269	269	2.64	29.05	1	42	127
	20	0.49	0	269	269	2.64	29.05	1	49	112
	21	0.49	0	269	269	2.64	29.05	1	56	122
	22	0.49	0	269	269	2.64	29.05	1	63	130
	23	0.49	0	269	269	2.64	29.05	1	70	137
	24	0.49	0	269	269	2.64	29.05	1	77	142
	25	0.49	0	269	269	2.64	29.05	1	84	148
	26	0.49	0	269	269	2.64	29.05	1	91	153
	27	0.49	27	242	269	2.64	37.25	1	7	131
	28	0.49	27	242	269	2.64	37.25	1	14	143
	29	0.49	27	242	269	2.64	37.25	1	21	155
	30	0.49	27	242	269	2.64	37.25	1	28	164
	31	0.49	27	242	269	2.64	37.25	1	35	173
	32	0.49	27	242	269	2.64	37.25	1	42	165
	33	0.49	27	242	269	2.64	37.25	1	49	155

94

Data Source	Number	INPUT								OUTPUT
		X1	X2	X3	X4	X5	X6	X7	X8	Y
		w/b	SF (Kg/m3)	FA (Kg/m3)	cement (kg/m3)	Aggregate / Binder	fc Mpa (28Day) 150 x150	Auto : 0 dry or free :1	Dry Time DAYS	Shrinkage
	34	0.49	27	242	269	2.64	37.25	1	56	169
	35	0.49	27	242	269	2.64	37.25	1	63	173
	36	0.49	27	242	269	2.64	37.25	1	70	181
	37	0.49	27	242	269	2.64	37.25	1	77	190
	38	0.49	27	242	269	2.64	37.25	1	84	200
	39	0.49	27	242	269	2.64	37.25	1	91	208
	40	0.49	54	215	269	2.64	44.05	1	7	150
	41	0.49	54	215	269	2.64	44.05	1	14	162
	42	0.49	54	215	269	2.64	44.05	1	21	173
	43	0.49	54	215	269	2.64	44.05	1	28	184
	44	0.49	54	215	269	2.64	44.05	1	35	192
	45	0.49	54	215	269	2.64	44.05	1	42	186
	46	0.49	54	215	269	2.64	44.05	1	49	173
Wongkeo et al (2012)	47	0.49	54	215	269	2.64	44.05	1	56	184
	48	0.49	54	215	269	2.64	44.05	1	63	192
	49	0.49	54	215	269	2.64	44.05	1	70	205
	50	0.49	54	215	269	2.64	44.05	1	77	214
	51	0.49	54	215	269	2.64	44.05	1	84	221
	52	0.49	54	215	269	2.64	44.05	1	91	231
	53	0.49	0	0	538	2.75	56.84	1	7	597
	54	0.49	0	0	538	2.75	56.84	1	14	661
	55	0.49	0	0	538	2.75	56.84	1	21	683
	56	0.49	0	0	538	2.75	56.84	1	28	714
	57	0.49	0	0	538	2.75	56.84	1	35	701
	58	0.49	0	0	538	2.75	56.84	1	42	702
	59	0.49	0	0	538	2.75	56.84	1	49	782
	60	0.49	0	0	538	2.75	56.84	1	56	838
	61	0.49	0	0	538	2.75	56.84	1	63	861
	62	0.49	0	0	538	2.75	56.84	1	70	883
	63	0.49	0	0	538	2.75	56.84	1	77	906
	64	0.49	0	0	538	2.75	56.84	1	84	944
	65	0.49	0	0	538	2.75	56.84	1	91	974
	66	0.49	0	269	269	2.64	35.13	1	7	507

Data Source	Number	INPUT								OUTPUT
		X1	X2	X3	X4	X5	X6	X7	X8	Y
		w/b	SF (Kg/m3)	FA (Kg/m3)	cement (kg/m3)	Aggregate/ Binder	fc Mpa (28Day) 150 x150	Auto : 0 dry or free :1	Dry Time DAYS	Shrinkage
	67	0.49	0	269	269	2.64	35.13	1	14	536
	68	0.49	0	269	269	2.64	35.13	1	21	565
	69	0.49	0	269	269	2.64	35.13	1	28	582
	70	0.49	0	269	269	2.64	35.13	1	35	573
	71	0.49	0	269	269	2.64	35.13	1	42	612
	72	0.49	0	269	269	2.64	35.13	1	49	670
	73	0.49	0	269	269	2.64	35.13	1	56	714
	74	0.49	0	269	269	2.64	35.13	1	63	721
	75	0.49	0	269	269	2.64	35.13	1	70	763
	76	0.49	0	269	269	2.64	35.13	1	77	797
	77	0.49	0	269	269	2.64	35.13	1	84	830
	78	0.49	0	269	269	2.64	35.13	1	91	839
	79	0.49	27	242	269	2.64	48.55	1	7	676
	80	0.49	27	242	269	2.64	48.55	1	14	729
Wongkeo et al (2012)	81	0.49	27	242	269	2.64	48.55	1	21	751
	82	0.49	27	242	269	2.64	48.55	1	28	778
	83	0.49	27	242	269	2.64	48.55	1	35	744
	84	0.49	27	242	269	2.64	48.55	1	42	736
	85	0.49	27	242	269	2.64	48.55	1	49	779
	86	0.49	27	242	269	2.64	48.55	1	56	861
	87	0.49	27	242	269	2.64	48.55	1	63	886
	88	0.49	27	242	269	2.64	48.55	1	70	914
	89	0.49	27	242	269	2.64	48.55	1	77	936
	90	0.49	27	242	269	2.64	48.55	1	84	963
	91	0.49	27	242	269	2.64	48.55	1	91	968
	92	0.49	54	215	269	2.64	57.98	1	7	691
	93	0.49	54	215	269	2.64	57.98	1	14	759
	94	0.49	54	215	269	2.64	57.98	1	21	767
	95	0.49	54	215	269	2.64	57.98	1	28	861
	96	0.49	54	215	269	2.64	57.98	1	35	800
	97	0.49	54	215	269	2.64	57.98	1	42	800
	98	0.49	54	215	269	2.64	57.98	1	49	845
	99	0.49	54	215	269	2.64	57.98	1	56	895

Data Source	Number	INPUT								OUTPUT
		X1	X2	X3	X4	X5	X6	X7	X8	Y
		w/b	SF (Kg/m3)	FA (Kg/m3)	cement (kg/m3)	Aggregate/ Binder	fc Mpa (28Day) 150 x150	Auto :0 dry or free :1	Dry Time DAYS	Shrinkage
	100	0.49	54	215	269	2.64	57.98	1	63	914
	101	0.49	54	215	269	2.64	57.98	1	70	959
	102	0.49	54	215	269	2.64	57.98	1	77	989
	103	0.49	54	215	269	2.64	57.98	1	84	1027
	104	0.49	54	215	269	2.64	57.98	1	91	1035
	105	0.49	0	0	538	2.75	58.13	1	7	695
	106	0.49	0	0	538	2.75	58.13	1	14	814
	107	0.49	0	0	538	2.75	58.13	1	21	918
	108	0.49	0	0	538	2.75	58.13	1	28	936
	109	0.49	0	0	538	2.75	58.13	1	35	973
	110	0.49	0	0	538	2.75	58.13	1	42	964
	111	0.49	0	0	538	2.75	58.13	1	49	955
	112	0.49	0	0	538	2.75	58.13	1	56	968
	113	0.49	0	0	538	2.75	58.13	1	63	986
	114	0.49	0	0	538	2.75	58.13	1	70	998
Wongkeo et al (2012)	115	0.49	0	0	538	2.75	58.13	1	77	1018
	116	0.49	0	0	538	2.75	58.13	1	84	1041
	117	0.49	0	0	538	2.75	58.13	1	91	1059
	118	0.49	0	269	269	2.64	37.5	1	7	523
	119	0.49	0	269	269	2.64	37.5	1	14	586
	120	0.49	0	269	269	2.64	37.5	1	21	655
	121	0.49	0	269	269	2.64	37.5	1	28	691
	122	0.49	0	269	269	2.64	37.5	1	35	718
	123	0.49	0	269	269	2.64	37.5	1	42	706
	124	0.49	0	269	269	2.64	37.5	1	49	700
	125	0.49	0	269	269	2.64	37.5	1	56	718
	126	0.49	0	269	269	2.64	37.5	1	63	727
	127	0.49	0	269	269	2.64	37.5	1	70	746
	128	0.49	0	269	269	2.64	37.5	1	77	777
	129	0.49	0	269	269	2.64	37.5	1	84	818
	130	0.49	0	269	269	2.64	37.5	1	91	826
	131	0.49	27	242	269	2.64	55.63	1	7	641
	132	0.49	27	242	269	2.64	55.63	1	14	695

Table A.2 (continued)

| Data Source | Number | INPUT | | | | | | | | OUTPUT |
| | | X1 | X2 | X3 | X4 | X5 | X6 | X7 | X8 | Y |
		w/b	SF (Kg/m3)	FA (Kg/m3)	cement (kg/m3)	Aggregate/ Binder	fc Mpa (28Day) 150 x150	Auto :0 dry or free :1	Dry Time DAYS	Shrinkage
	133	0.49	27	242	269	2.64	55.63	1	21	732
	134	0.49	27	242	269	2.64	55.63	1	28	795
	135	0.49	27	242	269	2.64	55.63	1	35	832
	136	0.49	27	242	269	2.64	55.63	1	42	818
	137	0.49	27	242	269	2.64	55.63	1	49	805
	138	0.49	27	242	269	2.64	55.63	1	56	814
	139	0.49	27	242	269	2.64	55.63	1	63	832
	140	0.49	27	242	269	2.64	55.63	1	70	837
	141	0.49	27	242	269	2.64	55.63	1	77	882
	142	0.49	27	242	269	2.64	55.63	1	84	891
	143	0.49	27	242	269	2.64	55.63	1	91	909
	144	0.49	54	215	269	2.64	60	1	7	836
	145	0.49	54	215	269	2.64	60	1	14	950
	146	0.49	54	215	269	2.64	60	1	21	986
Wongkeo et al (2012)	147	0.49	54	215	269	2.64	60	1	28	1000
	148	0.49	54	215	269	2.64	60	1	35	1036
	149	0.49	54	215	269	2.64	60	1	42	1027
	150	0.49	54	215	269	2.64	60	1	49	1009
	151	0.49	54	215	269	2.64	60	1	56	1027
	152	0.49	54	215	269	2.64	60	1	63	1041
	153	0.49	54	215	269	2.64	60	1	70	1050
	154	0.49	54	215	269	2.64	60	1	77	1068
	155	0.49	54	215	269	2.64	60	1	84	1082
	156	0.49	54	215	269	2.64	60	1	91	1100
	157	0.49	0	0	538	2.75	65.95	1	7	500
	158	0.49	0	0	538	2.75	65.95	1	14	564
	159	0.49	0	0	538	2.75	65.95	1	21	615
	160	0.49	0	0	538	2.75	65.95	1	28	653
	161	0.49	0	0	538	2.75	65.95	1	35	664
	162	0.49	0	0	538	2.75	65.95	1	42	662
	163	0.49	0	0	538	2.75	65.95	1	49	655
	164	0.49	0	0	538	2.75	65.95	1	56	645
	165	0.49	0	0	538	2.75	65.95	1	63	645

Table A.2 (continued)

Data Source	Number	INPUT								OUTPUT
		X1	X2	X3	X4	X5	X6	X7	X8	Y
		w/b	SF (Kg/m3)	FA (Kg/m3)	cement (kg/m3)	Aggregate/ Binder	fc Mpa (28Day) 150 x150	Auto : 0 dry or free :1	Dry Time DAYS	Shrinkage
Wongkeo et al (2012)	166	0.49	0	0	538	2.75	65.95	1	70	664
	167	0.49	0	0	538	2.75	65.95	1	77	679
	168	0.49	0	0	538	2.75	65.95	1	84	692
	169	0.49	0	0	538	2.75	65.95	1	91	711
	170	0.49	0	269	269	2.64	48.57	1	7	305
	171	0.49	0	269	269	2.64	48.57	1	14	400
	172	0.49	0	269	269	2.64	48.57	1	21	498
	173	0.49	0	269	269	2.64	48.57	1	28	547
	174	0.49	0	269	269	2.64	48.57	1	35	590
	175	0.49	0	269	269	2.64	48.57	1	42	583
	176	0.49	0	269	269	2.64	48.57	1	49	578
	177	0.49	0	269	269	2.64	48.57	1	56	574
	178	0.49	0	269	269	2.64	48.57	1	63	583
	179	0.49	0	269	269	2.64	48.57	1	70	595
	180	0.49	0	269	269	2.64	48.57	1	77	615
	181	0.49	0	269	269	2.64	48.57	1	84	639
	182	0.49	0	269	269	2.64	48.57	1	91	668
	183	0.49	27	242	269	2.64	61.43	1	7	280
	184	0.49	27	242	269	2.64	61.43	1	14	358
	185	0.49	27	242	269	2.64	61.43	1	21	453
	186	0.49	27	242	269	2.64	61.43	1	28	520
	187	0.49	27	242	269	2.64	61.43	1	35	558
	188	0.49	27	242	269	2.64	61.43	1	42	550
	189	0.49	27	242	269	2.64	61.43	1	49	538
	190	0.49	27	242	269	2.64	61.43	1	56	543
	191	0.49	27	242	269	2.64	61.43	1	63	558
	192	0.49	27	242	269	2.64	61.43	1	70	568
	193	0.49	27	242	269	2.64	61.43	1	77	585
	194	0.49	27	242	269	2.64	61.43	1	84	608
	195	0.49	27	242	269	2.64	61.43	1	91	635
	196	0.49	54	215	269	2.64	69.05	1	7	250
	197	0.49	54	215	269	2.64	69.05	1	14	310
	198	0.49	54	215	269	2.64	69.05	1	21	365

99

Table A.2 (continued)

Data Source	Number	INPUT								OUTPUT
		X1	X2	X3	X4	X5	X6	X7	X8	Y
		w/b	SF (Kg/m3)	FA (Kg/m3)	cement (kg/m3)	Aggregate/ Binder	fc Mpa (28Day) 150 x150	Auto :0 dry or free :1	Dry Time DAYS	Shrinkage
	199	0.49	54	215	269	2.64	69.05	1	28	475
	200	0.49	54	215	269	2.64	69.05	1	35	520
	201	0.49	54	215	269	2.64	69.05	1	42	523
Wongkeo et al (2012)	202	0.49	54	215	269	2.64	69.05	1	49	513
	203	0.49	54	215	269	2.64	69.05	1	56	515
	204	0.49	54	215	269	2.64	69.05	1	63	525
	205	0.49	54	215	269	2.64	69.05	1	70	537
	206	0.49	54	215	269	2.64	69.05	1	77	555
	207	0.49	54	215	269	2.64	69.05	1	84	575
	208	0.49	54	215	269	2.64	69.05	1	91	590

Table A.3 database from Yoo et al

Data Source	Number	INPUT								OUTPUT
		X1	**X2**	**X3**	**X4**	**X5**	**X6**	**X7**	**X8**	**Y**
		w/b	SF (Kg/m3)	FA (Kg/m3)	cement (kg/m3)	Aggregate/ Binder	fc Mpa (28Day) 150 x150	Auto :0 dry or free :1	Dry Time DAYS	Shrinkage
Yoo et al (2012)	1	0.30	0	0	583	2.68	58.32	0	1	41
	2	0.30	0	0	583	2.68	58.32	0	3	128
	3	0.30	0	0	583	2.68	58.32	0	7	217
	4	0.30	0	0	583	2.68	58.32	0	14	253
	5	0.30	0	0	583	2.68	58.32	0	21	287
	6	0.30	0	0	583	2.68	58.32	0	28	311
	7	0.30	0	0	583	2.68	58.32	0	49	348
	8	0.30	0	88	496	2.62	55.9	0	1	44
	9	0.30	0	88	496	2.62	55.9	0	2	128
	10	0.30	0	88	496	2.62	55.9	0	3	164
	11	0.30	0	88	496	2.62	55.9	0	7	189
	12	0.30	0	88	496	2.62	55.9	0	14	218
	13	0.30	0	88	496	2.62	55.9	0	21	255
	14	0.30	0	88	496	2.62	55.9	0	28	275
	15	0.30	0	88	496	2.62	55.9	0	49	319
	16	0.30	0	175	408	2.57	54.8	0	1	50
	17	0.30	0	175	408	2.57	54.8	0	3	136
	18	0.30	0	175	408	2.57	54.8	0	7	169
	19	0.30	0	175	408	2.57	54.8	0	14	191
	20	0.30	0	175	408	2.57	54.8	0	21	200
	21	0.30	0	175	408	2.57	54.8	0	28	239
	22	0.30	0	175	408	2.57	54.8	0	49	237
	23	0.30	44	0	540	2.65	66	0	1	39
	24	0.30	44	0	540	2.65	66	0	2	111
	25	0.30	44	0	540	2.65	66	0	3	175
	26	0.30	44	0	540	2.65	66	0	7	239
	27	0.30	44	0	540	2.65	66	0	14	264
	28	0.30	44	0	540	2.65	66	0	21	298
	29	0.30	44	0	540	2.65	66	0	28	325
	30	0.30	44	0	540	2.65	66	0	49	375
	31	0.30	88	0	496	2.62	69.2	0	1	50
	32	0.30	88	0	496	2.62	69.2	0	2	139
	33	0.30	88	0	496	2.62	69.2	0	3	199

Data Source	Number	INPUT								OUTPUT
		X1	X2	X3	X4	X5	X6	X7	X8	Y
		w/b	SF (Kg/m3)	FA (Kg/m3)	cement (kg/m3)	Aggregate/ Binder	fc Mpa (28Day) 150 x150	Auto : 0 dry or free :1	Dry Time DAYS	Shrinkage
	34	0.30	88	0	496	2.62	69.2	0	7	253
	35	0.30	88	0	496	2.62	69.2	0	14	287
	36	0.30	88	0	496	2.62	69.2	0	21	312
	37	0.30	88	0	496	2.62	69.2	0	28	350
	38	0.30	88	0	496	2.62	69.2	0	49	400
	39	0.30	29	58	496	2.63	67.4	0	1	61
	40	0.30	29	58	496	2.63	67.4	0	2	119
	41	0.30	29	58	496	2.63	67.4	0	3	145
	42	0.30	29	58	496	2.63	67.4	0	7	183
Yoo et al (2012)	43	0.30	29	58	496	2.63	67.4	0	14	212
	44	0.30	29	58	496	2.63	67.4	0	21	236
	45	0.30	29	58	496	2.63	67.4	0	28	262
	46	0.30	29	58	496	2.63	67.4	0	49	289
	47	0.30	58	117	408	2.57	69.8	0	1	42
	48	0.30	58	117	408	2.57	69.8	0	2	130
	49	0.30	58	117	408	2.57	69.8	0	3	166
	50	0.30	58	117	408	2.57	69.8	0	7	194
	51	0.30	58	117	408	2.57	69.8	0	14	230
	52	0.30	58	117	408	2.57	69.8	0	21	261
	53	0.30	58	117	408	2.57	69.8	0	28	283
	54	0.30	58	117	408	2.57	69.8	0	49	319

Table A.4 database from Khatib et al

Data Source	Number	INPUT								OUTPUT
		X1	X2	X3	X4	X5	X6	X7	X8	Y
		w/b	SF (Kg/m3)	FA (Kg/m3)	cement (kg/m3)	Aggregate/ Binder	fc Mpa (28Day) 150 x150	Auto :0 dry or free :1	Dry Time DAYS	Shrinkage
Khatib et al (2008)	1	0.36	0	0	500	3.50	72.58	1	2	122
	2	0.36	0	0	500	3.50	72.58	1	3	161
	3	0.36	0	0	500	3.50	72.58	1	6	253
	4	0.36	0	0	500	3.50	72.58	1	15	324
	5	0.36	0	0	500	3.50	72.58	1	34	438
	6	0.36	0	0	500	3.50	72.58	1	40	443
	7	0.36	0	0	500	3.50	72.58	1	48	439
	8	0.36	0	0	500	3.50	72.58	1	56	432
	9	0.36	0	100	400	3.44	54.31	1	2	38
	10	0.36	0	100	400	3.44	54.31	1	3	80
	11	0.36	0	100	400	3.44	54.31	1	7	150
	12	0.36	0	100	400	3.44	54.31	1	9	161
	13	0.36	0	100	400	3.44	54.31	1	29	341
	14	0.36	0	100	400	3.44	54.31	1	34	357
	15	0.36	0	100	400	3.44	54.31	1	42	355
	16	0.36	0	100	400	3.44	54.31	1	56	364
	17	0.36	0	200	300	3.38	56.89	1	5	80
	18	0.36	0	200	300	3.38	56.89	1	7	96
	19	0.36	0	200	300	3.38	56.89	1	28	241
	20	0.36	0	200	300	3.38	56.89	1	34	254
	21	0.36	0	200	300	3.38	56.89	1	47	274
	22	0.36	0	200	300	3.38	56.89	1	56	264
	23	0.36	0	300	200	3.32	32.58	1	2	28
	24	0.36	0	300	200	3.32	32.58	1	3	55
	25	0.36	0	300	200	3.32	32.58	1	4	80
	26	0.36	0	300	200	3.32	32.58	1	7	122
	27	0.36	0	300	200	3.32	32.58	1	10	141
	28	0.36	0	300	200	3.32	32.58	1	15	143
	29	0.36	0	300	200	3.32	32.58	1	23	158
	30	0.36	0	300	200	3.32	32.58	1	30	173
	31	0.36	0	300	200	3.32	32.58	1	38	182
	32	0.36	0	300	200	3.32	32.58	1	50	196
	33	0.36	0	300	200	3.32	32.58	1	56	205

Table A.4 (continued)

| Data Source | Number | INPUT | | | | | | | | OUTPUT |
| | | X1 | X2 | X3 | X4 | X5 | X6 | X7 | X8 | Y |
		w/b	SF (Kg/m3)	FA (Kg/m3)	cement (kg/m3)	Aggregate/ Binder	fc Mpa (28Day) 150 x150	Auto : 0 dry or free :1	Dry Time DAYS	Shrinkage
Khatib et al (2008)	34	0.36	0	400	100	3.25	11	1	2	5
	35	0.36	0	400	100	3.25	11	1	5	57
	36	0.36	0	400	100	3.25	11	1	7	85
	37	0.36	0	400	100	3.25	11	1	12	108
	38	0.36	0	400	100	3.25	11	1	15	114
	39	0.36	0	400	100	3.25	11	1	27	142
	40	0.36	0	400	100	3.25	11	1	35	150
	41	0.36	0	400	100	3.25	11	1	47	161
	42	0.36	0	400	100	3.25	11	1	56	161

Table A.5 database from Khatri and Sirivivatnanon

| Data Source | Number | INPUT | | | | | | | | OUTPUT |
| | | X1 | X2 | X3 | X4 | X5 | X6 | X7 | X8 | Y |
		w/b	SF (Kg/m3)	FA (Kg/m3)	cement (kg/m3)	Aggregate/ Binder	fc Mpa (28Day) 150 x150	Auto : 0 dry or free :1	Dry Time DAYS	Shrinkage
	1	0.35	0	0	425	4.30	77.19	1	7	267
	2	0.35	0	0	425	4.30	77.19	1	14	375
	3	0.35	0	0	425	4.30	77.19	1	21	475
	4	0.35	0	0	425	4.30	77.19	1	30	517
	5	0.35	0	0	425	4.30	77.19	1	57	650
	6	0.35	0	0	425	4.30	77.19	1	93	708
	7	0.35	0	0	425	4.30	77.19	1	183	775
	8	0.35	0	0	425	4.30	77.19	1	400	825
	9	0.34	45	0	384	4.27	112.80	1	7	333
	10	0.34	45	0	384	4.27	112.80	1	14	433
	11	0.34	45	0	384	4.27	112.80	1	21	483
	12	0.34	45	0	384	4.27	112.80	1	30	517
Khatri and Sirivivatnanon (1995)	13	0.34	45	0	384	4.27	112.80	1	57	575
	14	0.34	45	0	384	4.27	112.80	1	93	633
	15	0.34	45	0	384	4.27	112.80	1	183	692
	16	0.34	45	0	384	4.27	112.80	1	400	742
	17	0.34	45	65	320	4.20	91.02	1	7	331
	18	0.34	45	65	320	4.20	91.02	1	14	429
	19	0.34	45	65	320	4.20	91.02	1	21	487
	20	0.34	45	65	320	4.20	91.02	1	30	516
	21	0.34	45	65	320	4.20	91.02	1	57	574
	22	0.34	45	65	320	4.20	91.02	1	93	629
	23	0.34	45	65	320	4.20	91.02	1	183	695
	24	0.34	45	65	320	4.20	91.02	1	400	745
	25	0.36	46	106	282	4.15	89.63	1	7	411
	26	0.36	46	106	282	4.15	89.63	1	14	560
	27	0.36	46	106	282	4.15	89.63	1	21	615
	28	0.36	46	106	282	4.15	89.63	1	30	636
	29	0.36	46	106	282	4.15	89.63	1	57	716
	30	0.36	46	106	282	4.15	89.63	1	93	767
	31	0.36	46	106	282	4.15	89.63	1	183	829
	32	0.36	46	106	282	4.15	89.63	1	400	895

Appendix B

Photographic views

Figure B 1 Photographic view during concrete production

Figure B 2 Photographic view of molded specimens

Figure B 3 Photographic view of demoulded specimens

Figure B 4 Photographic view of shrinkage specimens and curing room (controlled temperature and humidity)

Figure B 5 Photographic view of shrinkage reading by dial comparator

Figure B 6 Photographic view of compressive strength testing